

**POLITECNICO DI TORINO**

**SOLID-STATE WELDING OF LIGHT ALLOY  
COMPONENTS  
FRICTION STIR WELDING**



**SUPERVISORS**

Prof. Franco Lombardi  
Prof. Pasquale Russo Spena  
Prof. Manuela DeMaddis

**CANDIDATE**

Tataranni Angelo

Academic Year 2020 - 2021

This work is subject to the Creative Commons Licence

All Rights Reserved

## ABSTRACT

The thesis is about new solid-state welding process called Friction Stir Welding.

The first part consists of a brief explanation of how it works, what are the main properties of the tool used and what are the parameters needed to be set in order to get a good welded joint.

Then, after a deep research into literature, reading books and various papers, the design of some welding tools with a special pin and shoulder and their own proper adapter has been performed in order to be able to weld Aluminium Alloys sheets with different thickness (1.5 mm and 2.5 mm) and arranged so that butt and lap joint could be obtained.

The tool adapter must fit the dimensions of the tool holder provided by the machine produced by "STIRTEC" and located in "Eurodies" company in Rivoli (TO).

The welding tools and the tool adapter designed have been verified against static failure.

No fatigue analysis has been done since the components are not subjected to variable loads.

Then, a detailed drawing of the tool adapter with all the shape and dimensional tolerances needed has been done, so that the component could be ready to be produced and machined.

After understanding the production operations useful to create the tool adapter, an overview about turning and milling, explaining the main parameters and cutting tools has been written.

The last chapter consists of an explanation of the G-code used to drive the machining passages in a CNC machine. A G-code for the turning process needed to machine the Tool Adapter has been written using the software "CNCSimulator".

# TABLE OF CONTENTS

LIST OF FIGURES .....	5
LIST OF TABLES .....	7
1. Friction Stir Welding .....	10
1.1 Process.....	11
1.2 Types of joints .....	12
1.3 Microstructure .....	14
1.3.1 Grain size.....	15
1.3.2 Microstructural defects.....	16
1.4 Rotating tool.....	18
1.4.1 Shoulder.....	19
1.4.2 Pin.....	19
1.5 Process parameters .....	20
1.6 Comparison of Friction Stir Welding with fusion welding processes .....	21
2. Aluminium alloys .....	23
2.1 Properties and characteristics of the Aluminium.....	23
2.2 Aluminium alloy series .....	24
3. Experimental procedure.....	27
3.1 STIRTEC Friction Stir Welding machine .....	27
3.2 Tool adapter.....	30
3.2.1 Tool adapter design verification.....	34
3.2.1.1 Static verification section A .....	35
3.2.1.2 Static verification section B.....	37
3.2.1.3 Static verification section C.....	39
3.2.1.4 Static verification section D .....	41
3.3 Analysis of tolerances .....	42
3.4 Case study 1: Lap Joint .....	45
3.4.1 Tool Design: Suggested solution.....	48
3.5 Case Study 2: Butt Joint .....	50
3.5.1 Tool Design: Suggested solution.....	52
3.6 Case Study 3: Butt Joint .....	54
3.6.1 Tool Design: Suggested solution.....	55
3.7 Static analysis of welding tool.....	58
3.7.1 Welding Tool-Section A.....	59
3.7.2 Welding Tool-Section B:.....	60

3.7.3 Welding Tool Section C .....	62
3.8 Deflection deformation of Welding Tool .....	63
3.9 Verification of M16 x 1,5 stud .....	64
3.10 Verification of M5 stud .....	64
4. Turning operation: overview .....	66
4.1 Lathe machine structure .....	67
4.2 Operations .....	68
4.3 Cutting parameters .....	69
4.3.1 Cutting speed and depth of cut .....	69
4.4 Cutting Tools.....	72
4.4.1 Cutting tool's materials .....	74
5. Milling operation: overview .....	76
5.1 Milling machine .....	76
5.2 Operations .....	77
5.3 Milling parameters .....	79
5.4 Milling Tools.....	80
6. G-code .....	83
7. Conclusion .....	87
8. List of attachments.....	89
1. Tool holder. 2D drawing .....	89
2. Tool adapter, 2D drawing.....	90
3. Welding Tool Case Study 1, 2D drawing.....	91
4. Welding Tool Case Study 2, 2D drawing.....	92
5. Welding Tool Case Study 3, 2D drawing.....	93
Bibliography and Sitography .....	94

# LIST OF FIGURES

Figure 1 - FSW Market Revenue and Growth, 2016-2026 [13].....	10
Figure 2 - Evolution of worldwide article citations and patent application related to Friction Stir Welding process since 1995 [14]. .....	11
Figure 3 - FSW process [1]. .....	12
Figure 4 - Different types of joints [1]. .....	13
Figure 5 - Example of fixture design of butt joint [2]. .....	13
Figure 6 - Lap Joint [23].....	14
Figure 7 - Microstructural zones of FSW done on 7075Al-T651 aluminium alloy [1]. .....	15
Figure 8 - Effect of processing parameters on nugget shape in FSP A356: (a) 300rpm, 51 mm/min and (b) 900 rpm, 203 mm/min (standard threaded pin) [1]. .....	15
Figure 9 - Grain size variation in different region of the nugget zone of 7050Al [1]. .....	16
Figure 10 - Hook defect [7]. .....	17
Figure 11 - Material flow produced by conventional threaded tool with rotation speed 1200 rpm and traverse speed 150 mm/min [16]. .....	17
Figure 12 - Hook and cold lap defect: (a) effective lap width (ELW); (b) hook height on advancing side (D1); (c) cold lap defect and hook height on retreating side (D2) [16]. .....	18
Figure 13 - Rotating tool [1]. .....	18
Figure 14 - Tool shoulder geometries [18]. .....	19
Figure 15 - Whorl™ and MX Triflute™ tools developed by The Welding Institute (TWI) [1]. .....	20
Figure 16 - Comparison of the distortion caused by FSW and by arc welding on aluminium sheets of 5 mm thickness [14]. .....	22
Figure 17 - Aluminium Alloy Designation System [3]. .....	25
Figure 18 - Comparison between different groups of alloys [3]. .....	26
Figure 19 - STIRTEC Machine main dimensions. ....	29
Figure 20 - STIRTEC Friction Stir Welding Machine. ....	29
Figure 21 - STIRTEC tool holder dimensions. ....	30
Figure 22 - STIRTEC Tool holder_ hole for fixture welding tool. ....	31
Figure 23 - STIRTEC Tool Holder. ....	31
Figure 24 - STIRTEC Tool holder upper part. ....	32
Figure 25 - Tool Adapter, 3D drawing. ....	33
Figure 26 - Tool Adapter 2D Drawing. ....	33
Figure 27 - Sections chosen for static analysis. ....	35
Figure 28 - Section A of the tool adapter. ....	35
Figure 29 - Section B of the tool adapter. ....	37
Figure 30 - Stress concentration factor $K_t$ for shaft in torsion. ....	38
Figure 31 - Section C of the tool adapter. ....	39
Figure 32 - Stress concentration factor $K_t$ for shaft in torsion. ....	40
Figure 33 - Section D of the tool adapter. ....	41
Figure 34 - Tool Adapter 2D Drawing. ....	42
Figure 35 - Tool Holder and Tool Adapter tolerances. ....	43
Figure 36 - General tolerances ISO 2768 [34]. ....	44
Figure 37 - Friction Stir LAP welding [7]. .....	45
Figure 38 - Features and geometry of four welding tools [7]. .....	46
Figure 39 - Hooking height (HH) and lower plate effective thickness (ET) for the different tools [7]. .....	46
Figure 40 - Hook slope for the different tools [7]. .....	47

Figure 41 - Results of tensile test, 600 rpm rotational speed [7].	47
Figure 42 - Lap joint Welding Tool's 2D drawing.	48
Figure 43 - Lap joint Welding Tool's 3D drawing.	49
Figure 44 - Different tool shoulder geometries. Dimension in mm [6].	50
Figure 45 - Welding surface by Tool $T_{FC}$ [6].	50
Figure 46 - Nominal contact surfaces between shoulder and specimens [6].	51
Figure 47 - Horizontal microhardness. "A" means advancing side, "R" retreating side [6].	51
Figure 48 - Focus on shoulder and pin features.	52
Figure 49 - Butt joint Welding tool's 3D drawing.	53
Figure 50 - Butt joint welding Tool's 2D drawing.	53
Figure 51 - Three different tools used [9].	54
Figure 52 - Tensile properties with tool with shoulder diameter 18 mm [9].	54
Figure 53 - Butt joint Welding tool's 3D drawing.	55
Figure 54 - Butt joint Welding Tool's 2D drawing.	56
Figure 55 - Spiral channel for Tool Case Study 3	57
Figure 56 - Sections chosen for static analysis.	58
Figure 57 - Section A of the welding tool.	59
Figure 58 - Section B for welding tool.	60
Figure 59 - Stress concentration factor $K_t$ for shaft in torsion.	61
Figure 60 - Section C of the welding tool.	62
Figure 61 - Turning operation [25].	66
Figure 62 - Lathe machine [24].	67
Figure 63 - Turning operation [27].	68
Figure 64 - Grooving operation [27].	68
Figure 65 - Drilling operation [27].	69
Figure 66 - Constant values for Taylor's equation [26].	69
Figure 67 - Effect of cutting speed, feed rate, depth of cut, nose radius and work piece hardness on the surface roughness [30].	71
Figure 68 - Single point cutting tool [31].	72
Figure 69 - Different types of insert [33].	72
Figure 70 - Different types of Turning tools' insert [32].	73
Figure 71 - Relation between hardness and toughness of the main materials used for cutting tools [28].	74
Figure 72 - Hardness vs Temperature graph for different cutting tools' materials [29].	75
Figure 73 - Horizontal and Vertical Milling machine [35].	76
Figure 74 - Plain Milling Operation [36].	77
Figure 75 - Face Milling Operation [36].	78
Figure 76 - Straddle Milling Operation [36].	78
Figure 77 - Angular Milling [36].	79
Figure 78 - Suggested Cutting speed [m/min] used in milling operations [40].	80
Figure 79 - End Mill Tool [38].	81
Figure 80 - Slab Mill Tool [39].	81
Figure 81 - Roughing End Mill Tool [38].	82
Figure 82 - Thread Mill Tool [38].	82
Figure 83 - Types of Milling Cutters [39].	83
Figure 84 - G-code commands [41].	84
Figure 85 - Starting workpiece: Cylinder with 90 mm of length and 40 mm of diameter.	85
Figure 86 - Cylinder after first turning operation.	85

Figure 87 - Starting cylinder workpiece for machining the bottom part .....	86
Figure 88 - Hole machining.....	86
Figure 89 - Attachment 1: Tool holder.....	89
Figure 90 - Attachment 2: Tool Adapter.....	90
Figure 91 - Attachment 3: Welding Tool, case study 1.....	91
Figure 92 - Attachment 4: Welding Tool, case study 2.....	92
Figure 93 - Attachment 5: Welding Tool, case study 3.....	93

## LIST OF TABLES

Table 1 - FSW process variables [2].....	21
Table 2 - Friction Stir Welding pros. ....	22
Table 3 - Aluminium properties [21].....	23
Table 4 - Overall machine dimensions.....	27
Table 5 - Working parameters.....	28
Table 6 - H13, material properties.....	34
Table 7 - Data used for the computation of the stress concentration factor. ....	38
Table 8 - Data used for the computation of the stress concentration factor. ....	40
Table 9 - Tool Adapter - Welding Tool tolerances. ....	44
Table 10 - Dimensions of tool 1 for butt joint.....	52
Table 11 - Dimensions of tool 2 for butt joint.....	55
Table 12 - Data used for the computation of the stress concentration factor. ....	61
Table 13 - Cutting parameters.....	70
Table 14 - Optimization parameters [30]. ....	71

# Introduction

The thesis work has been done in collaboration with 'Eurodies', company leader in process key bodywork components intended for prototypes and small series in the automotive field and with J-Tech Lab of Politecnico, a research center for advanced joining technologies.

It has the aim of improving the knowledge about Friction Stir Welding solid-state joining technique and design a Tool Adapter and various Welding Tools in order to be able to weld Aluminium Alloy with 1.5 mm of thickness.

The thesis work is the first step towards future experimental activities with the aim of improving the Friction Stir Welding's applications.

Friction Stir Welding is growing up continuously, as could be confirmed by the increasing trend of scientific papers citations and new patents that have been registered in the last 10 years (nearly 4400).

The machine used to accomplish this task is a STIRTEC machine, located in Eurodies company, Rivoli (TO).

The main characteristics of the machine consists of a maximum vertical force of 100kN, a maximum transversal and lateral force of 40kN, a maximum spindle torque of 600 Nm and a maximum spindle speed of around 1500 rpm.

After a deep research into literature's scientific papers, since the dimension of the tool's shoulder necessary to weld Aluminium Alloy with 1.5 mm of thickness were too small with respect to the dimension of the tool holder provided by the company, it has been decided to create a tool adapter able to accommodate the various tools.

The tool adapter presents on the bottom side, four threaded holes for M5 studs that allow the connection with the welding tool.

This type of connection has been thought so that, at the beginning the welding tool fills the entire hole and is fixed by means the two upper threaded holes, then, after the welding tool's pin has worn out, it could be re-machined and re-used, fixing the tool adapter and the welding tool by means of the two bottom holes and inserting on the empty space left, a disk able to withstand the vertical force produced in working conditions.

The welding tools designed are three and present, obviously the same upper part, that must match with the tool adapter, and three different bottom parts.

The case study one's tool is characterized by a flat shoulder and a stepped conical threaded pin, the welding tool belonging to case study two presents a simple cylindrical pin and a concave shoulder that allows better material keeping and, finally, the case study three's tool shows a tapered squared pin and a scroll shoulder, a spiral groove cut that guarantees better material vertical flow and higher plastic work and heat production because of the higher contact surface. All these tasks have been accomplished in the various chapters described briefly here below:

1. CHAPTER 1: In the chapter 1 there is a deep description of Friction Stir Welding process as a whole and, in particular, there is a focus on welding tools' shoulder and pin possible designs, the microstructure obtained at the end of the process, the possible type of joints that could be created and a comparison between FSW and the common fusion welding processes (TIG, MIG, MAG).
2. CHAPTER 2: The chapter 2 consists of a brief description of the main characteristics of the Aluminium and its alloys.

3. CHAPTER 3: The chapter 3 presents the experimental procedure. It consists of the description of the main steps done to design and verify statically the tool adapter and various welding tools.
4. CHAPTER 4: The chapter 4 presents a description of the turning operation, analysing the lathe machine structure, the various cutting parameters and cutting tools.
5. CHAPTER 5: The chapter 5 consists of a milling operation description, its main parameters, cutting tools and the various machines that could be used.
6. CHAPTER 6: The chapter 6 presents an explanation of the GCode useful to drive the machining operations. For the production of the tool adapter a Gcode has been written by using the “CNCSimulator” software.
7. CHAPTER 7: In chapter 7 a brief conclusion has been reported analysing the future challenges of Friction Stir Welding.

# 1. Friction Stir Welding

FRICTION STIR WELDING (FSW) is a new solid-state joining technique invented at The Welding Institute (TWI) in 1991 and is considered one of the most important discovery in metal joining process.

It is defined a green technology due to its energy efficiency, environment friendliness and versatility [1].

In fact, compared to the other most used fusion welding processes, it is characterized by no using of any cover gasses or flux, the energy consumption is very low and different kind of materials can be welded.

The welding process is widely diffused in the industrial world: it has been evaluated that the joining process represents the 4.5% of the gross energy consumption of the Europe Union, while according to the EU Regulation 2019/1784 of the European Commission, the final annual energy consumption connected to the welds should exceed 6 TWh in 2030, equal to 2.4 million tons of CO<sub>2</sub> equivalent [12].

The application of the Friction Stir Welding technique is increasing continuously even in the aeronautical field where its replacement of traditional bolting joint helps to reach the lightening goal and allows to overcome drawbacks related to the use of heterogeneous junctions (bolts, screws, studs) like additional mass contribution, stress concentration near the holes decreasing the fatigue resistance.

Therefore, Friction Stir Welding is used in many aeronautic companies such as Boeing, Lockheed Martin or Marshall Space Flight Center [14].

Recently, the FSW technique is being applied not only to weld different workpieces, but it is also performed to a single piece of metal in order to increase its own strength and fatigue properties changing the microstructure.

In Figure 1, it is possible to understand how the CAGR (Compound Annual Growth Rate) of Global friction stir welding is increasing continuously, up to 6.9% during the forecast period 2018 - 2026 [13].



Figure 1 - FSW Market Revenue and Growth, 2016-2026 [13].

To further underline how Friction Stir welding technique is growing up, as written in the article by D. Jacquin et al. [14], nearly 4400 patent families have been registered in the last 10 years and they are widely increasing over the past years of almost 70% between 2005 and 2018 according to Scopus (2019), Figure 2b.

Furthermore, the citations in scientific papers of about this new technique is raising up by a factor 4, passing from nearly 350 to 1500 in the same period of time, Figure 2a ,and these data demonstrate how the engineering world is getting more and more interested.

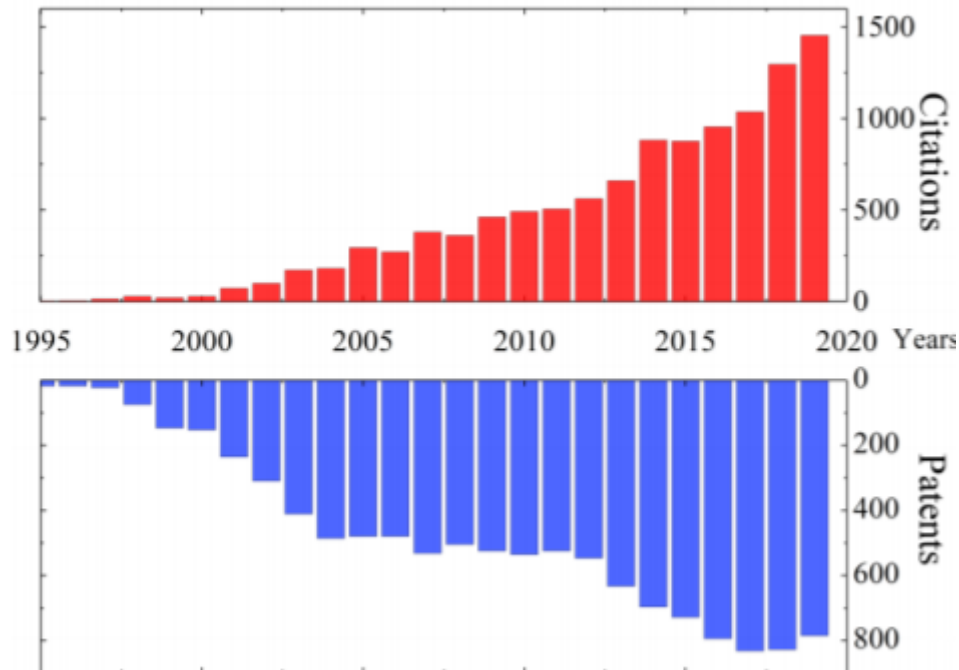


Figure 2 - Evolution of worldwide article citations and patent application related to Friction Stir Welding process since 1995 [14].

## 1.1 Process

The joining process, shown in the Figure 3, consists of a non-consumable rotating tool, with a specially designed pin and shoulder, that is plunged where the welding needs to be done, so in the interface line of the two components.

Friction Stir Welding is a solid-state process because the required heating to perform the joining of the two pieces, comes only from the friction between tool and workpieces and the plastic work produced by the action of the shoulder and the pin.

This type of process, characterized by no reaching of melting temperature, leads to have important benefits in the final properties of the welded piece, deeper explained in paragraph 1.5 in which also a comparison between FSW and common fusion welding processes is performed. During FSW process, the material in the welding zone undergoes strong plastic deformation and elevated temperature, so that fine and equiaxed re-crystallized grains are created. This type of microstructure leads to an increase of base metal mechanical properties, fatigue properties, enhanced formability, and exceptional super plasticity.

The Friction Stir Welding process consists of three main phases [2]:

1. *The plunge phase*: the welding process starts by inserting the non-consumable rotating tool inside the joint line between the two workpieces (in case of butt joint).
2. *The main phase*: the weld is made, thanks to the heat produced by friction and plastic work, moving the tool along the joint line. In some cases, with particular types of materials that present a higher melting temperature like copper, there could be a delay, called dwell time, in which the tool remains in the plunge location until the workpieces and the tool itself reach the right temperature to perform the process.
3. *The termination phase*: the welding tool is withdrawn from the workpiece, leaving a hole that must be cut. Sometimes an additional plate is placed at the end of the joining line, so that the tool can finish its stroke there, avoiding the creation of the hole in the workpieces.

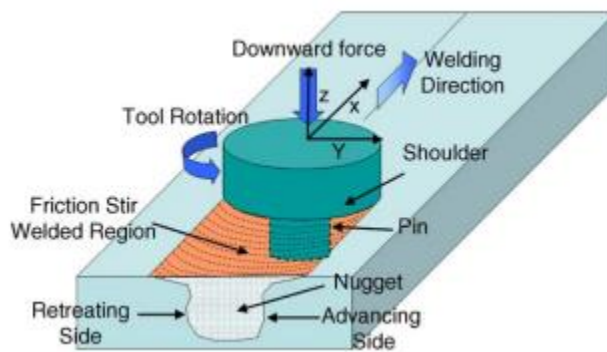


Figure 3 - FSW process [1].

## 1.2 Types of joints

The FSW can be used to produce different types of joints that are highlighted in Figure 4. They are named:

- a) square butt.
- b) edge butt.
- c) T butt joint.
- d) lap joint.
- e) multiple lap joint.
- f) T lap joint.
- g) fillet joint.

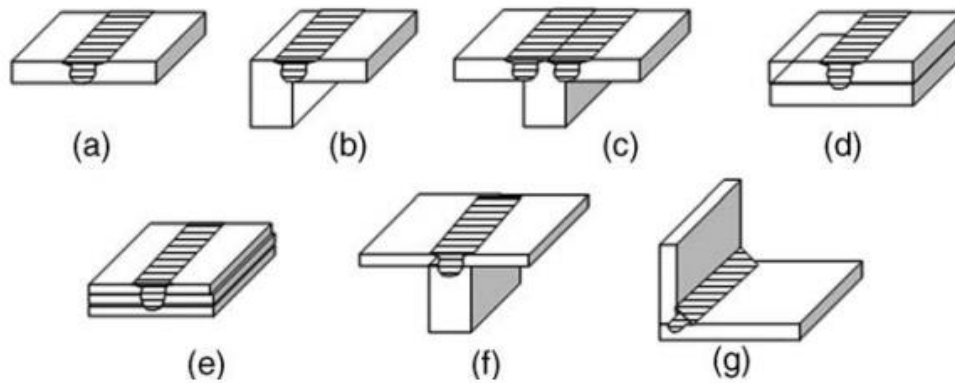


Figure 4 - Different types of joints [1].

In each of these types of welding configurations, the joining line appears smooth and as strong as the base material.

Since the most used joint configurations for FSW are butt and lap joint, they are going to be better explained in the following.

The *Butt joint* consists of having two plates or sheets with the same thickness in contact along one side and clamped on the working table ensuring that, during the plunge phase in which the tool is inserted in the joining line, the large forces developed do not separate them [1].

There could be the use of a removable anvil insert placed on the bottom side that reacts to the load produced by the rotating tool and avoids the movements of the two workpieces, Figure 5. It can be replaced in case of damage due to contact with the tool pin and, since the anvil is located on the bottom side of the region where the welding takes place, its mass and material must face good diffusion properties [2].

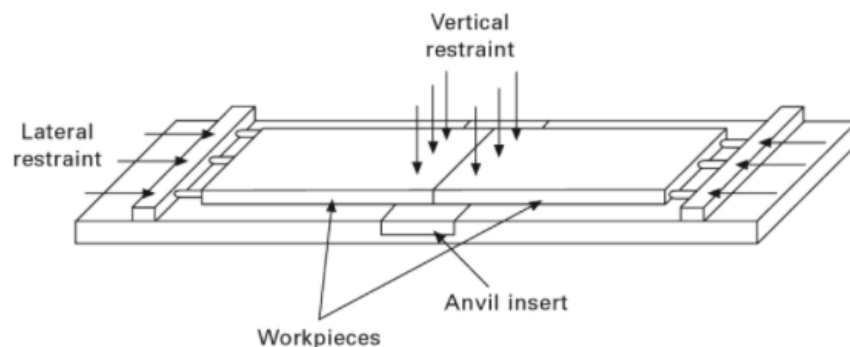


Figure 5 - Example of fixture design of butt joint [2].

On the other hand, the *Lap joint*, Figure 3e and 6, consists of having two or more lapped plates or sheets, that could have the same or different thickness. Even in this configuration, clamping is a fundamental aspect to avoid any sliding or bending of the pieces involved.

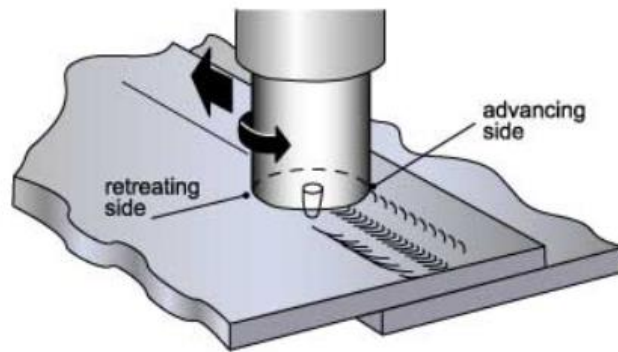


Figure 6 - Lap Joint [23].

## 1.3 Microstructure

Another point important to highlight in this first chapter is the different microstructural zones that it is possible to find after the application of the FSW process. There are five different regions, each characterized by their own properties (Figure 7):

- A. *Unaffected material or parent metal*: although it experiences elevated temperature during the welding process, it is not affected by the heat in terms of microstructures and mechanical properties. Its own properties remain the same.
- B. *Heat-affected zone (HAZ)*: this region reaches a temperature high enough so that affects its own properties (strength, ductility, corrosion susceptibility and toughness) but there is no plastic deformation of the original grain structure.
- C. *Thermomechanical affected zone (TMAZ)*: it undergoes plastic deformation and the heat from the welding process changes the properties of the material. No recrystallization occurs due to low deformation strain.
- D. *Nugget zone*: it exerts an intense plastic deformation and high temperature that generate a fully recrystallized area, called, also, stir zone.

The stir zone is the region that shows the highest hardness due to the presence of fine grains. It is located where the tool's pin acts, and its size is slightly greater than the pin diameter.

This region can be basin-shaped that grows going up to the surface or elliptical depending on the processing parameters, tool geometry, temperature of the workpiece and thermal conductivity of the material.

Recent conducted studies have established that low tool rotation rate of 300-500 rpm leads having the basin-shaped nugget zone, Figure 8a, while the elliptical nugget zone is shown increasing the rotational speed up to 700 rpm, Figure 8b [1].



Figure 7 - Microstructural zones of FSW done on 7075Al-T651 aluminium alloy [1].

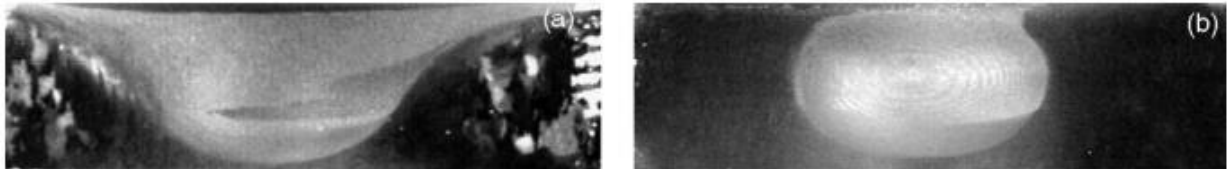


Figure 8 - Effect of processing parameters on nugget shape in FSP A356: (a) 300rpm, 51 mm/min and (b) 900 rpm, 203 mm/min (standard threaded pin) [1].

### 1.3.1 Grain size

The grain size is the driver of the mechanical properties in the nugget zone. Since in that region the recrystallization takes place, a simultaneous growth of the grains allows them to be finer, gaining, therefore, in better mechanical properties.

The grain size depends on various process parameters.

As explained in the article written by R.S. Mishra et al. [1], in which studies performed by other scientists are reported, the recrystallized grain size can be reduced by decreasing the tool rotational rate at constant tool traverse speed.

For example, considering an alloy 1050Al, a constant tool travel speed and three different tool rotation rates of 560, 980, 1840 rpm, the resulting grain size was about 0.5, 1-2 and 3-4  $\mu\text{m}$  respectively [1].

Furthermore, it has been shown that an increase of rotational tool speed or an increase of the ratio between rotational and traverse speed leads to touch higher level of deformation and higher peak of temperature. Both factors affect the grain size growth.

As it is known, the higher degree of deformation, the finer recrystallized grains size, but the increase of the peak temperature leads to a remarkable grain growth. Subsequent studies have established that the grain size present in the nuggets zone where the recrystallization takes place is dominated by the peak of temperature [1]. The higher the temperature, the higher the grain growth.

Other studies conducted by Mahoney et al. [15] focus the attention about how the grain size change in different parts of the nugget zone and why.

The results reported in Figure 9, studying 6.35 mm thick FSP 7050Al, demonstrates that the grain size increases from retreating to advancing side and from the bottom to the top because of a different temperature reached. On the bottom side the pieces are in touch with the working table that for sure is at a lower temperature with respect to the weld zone and furthermore has a good heat dissipation property.

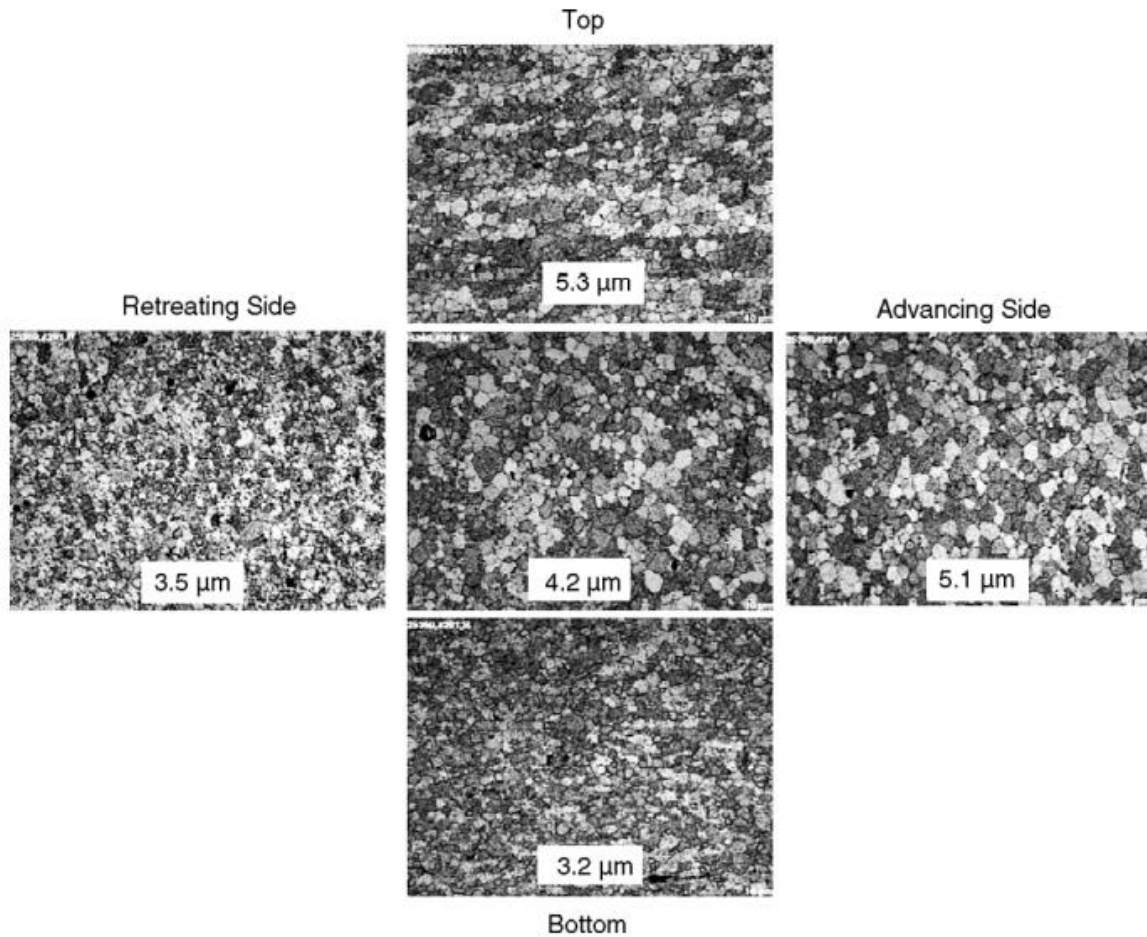


Figure 9 - Grain size variation in different region of the nugget zone of 7050Al [1].

### 1.3.2 Microstructural defects

One of the worst and most common defects that could appear during a Lap friction stir welding is called Hook that could form at the separating surface of the two Aluminium Alloy sheets. Emad Salari et al. [7] describe and experimentally study this defect doing a FSW of AA5456, with two different tempers, T321 and O and different thickness, 5mm and 2.5mm. An example of the hook phenomena is reported in Figure 10.

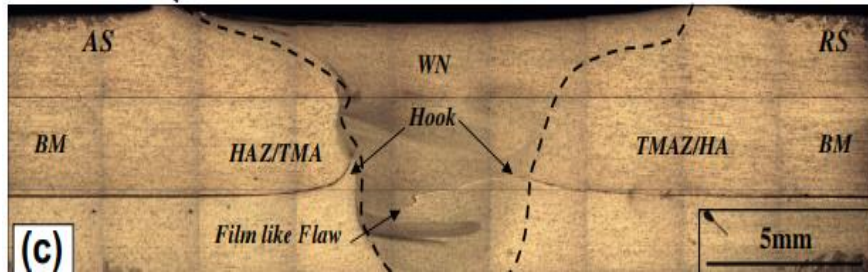


Figure 10 - Hook defect [7].

The defect is observed in TMAZ and NZ zone. Its presence in the TMAZ zone is due to the upward material flow, while it forms in the nuggets zone because of changes in material flow direction, from downward to upward.

The hooking average height and the lower plate effective thickness  $ET$ , defined as the distance between the middle point of the hook and the surface between the two sheets, are strictly connected to the type of tool designed.

They must be kept as low as possible because they negatively affect the mechanical properties. Where the hook is present, the failure occurs [7].

Another important defect needed to be underline is called Cold Lap. It is studied in the article written by Egoitz Aldanondo et al. [16] in which a lap joint between AA2099-T83 and AA2060-T8E30 aluminium alloys is performed. It forms since, during the welding process, at the advancing side and at the retreating side is present an upward material flow, flow 1 and 2 in Figure 11. Both flows are responsible for the creation of the hooks, defect described before. Then the flow moves toward the bottom side to fill the vacancy created by the shoulder and flow 3 is created. The cold lap defect is created by the third flow because of the not perfect mixture of the material on the faying surface, Figure 12.

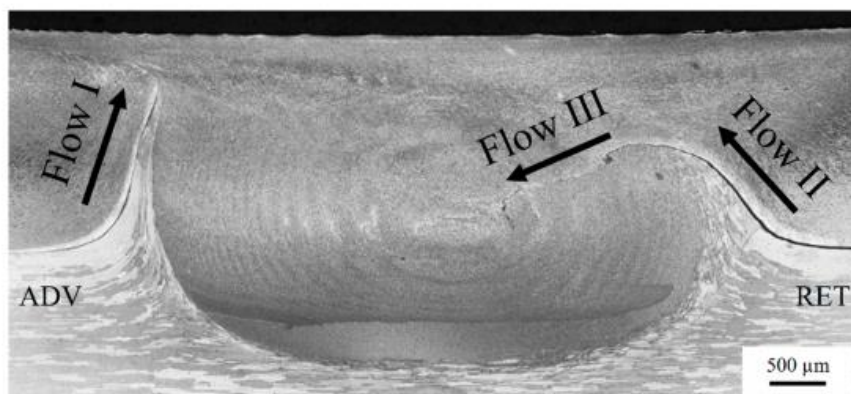


Figure 11 - Material flow produced by conventional threaded tool with rotation speed 1200 rpm and traverse speed 150 mm/min [16].

The consequence of the presence of hook and cold lap defect is a sheet thinning and in a reduction of the effective lap width (ELW).

The latter must be as large as possible in order to avoid the presence of a simple way for crack to propagate, so that optimum mechanical properties and fatigue strength are guaranteed.

The height of the hook and the length of the ELW can be managed by means the rotational speed and depends also on the type of tool used [16].

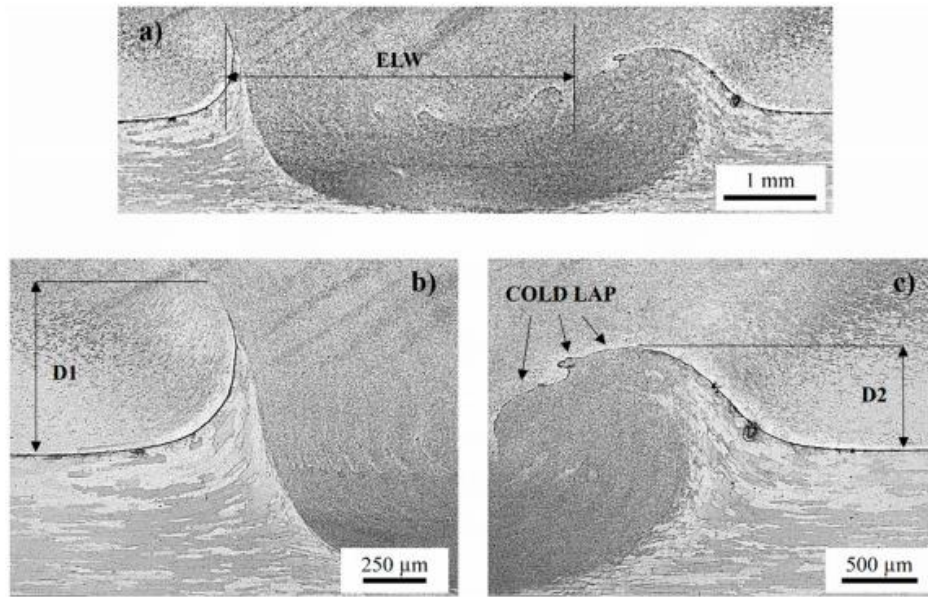


Figure 12 - Hook and cold lap defect: (a) effective lap width (ELW); (b) hook height on advancing side (D1); (c) cold lap defect and hook height on retreating side (D2) [16].

## 1.4 Rotating tool

One of the most crucial aspect of the Friction Stir Welding process is the design of the welding tool.

The tool has the function of heating the workpiece and leading the movement of the material making it soft in order to produce the joint. It is plunged at the pieces' interface and then, it moves along the weld seam.

In Figure 13, it is shown a schematical representation of the rotating tool and an example of some specific designs such as a scrolled shoulder and a threaded pin without and with flutes [1]. It's important to perform a detailed study of the different designs of pin and shoulder, because, depending on them, it is possible to improve many aspects of the final component such as the joint strength, the weld quality, the workpieces thickness and so on.

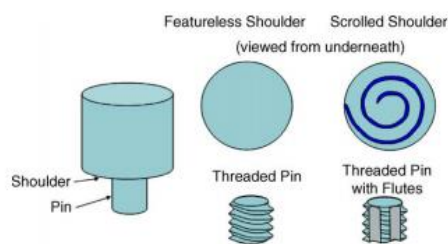


Figure 13 - Rotating tool [1].

## 1.4.1 Shoulder

The shoulder has an important role in terms of temperature, energy and torque production. The shoulder's diameter is a key parameter because its value determines the highest amount of heat produced (70 – 80% [17]), and its pressure over the upper surface drives the materials flow field.

The shoulder must keep the material in the joining region, avoiding its dispersion (stirring and moving the material). For this reason, a concave or scroll feature are usually adopted.

In order to use the Friction Stir Welding to different materials like copper, titanium, aluminium, magnesium, lead, steel and as much as possible working conditions (rotating tool rate, advancing tool speed, thickness of the workpieces), The Welding Institute (TWI) designed various types of shoulder profiles.

Some examples of them are reported in Figure 14.

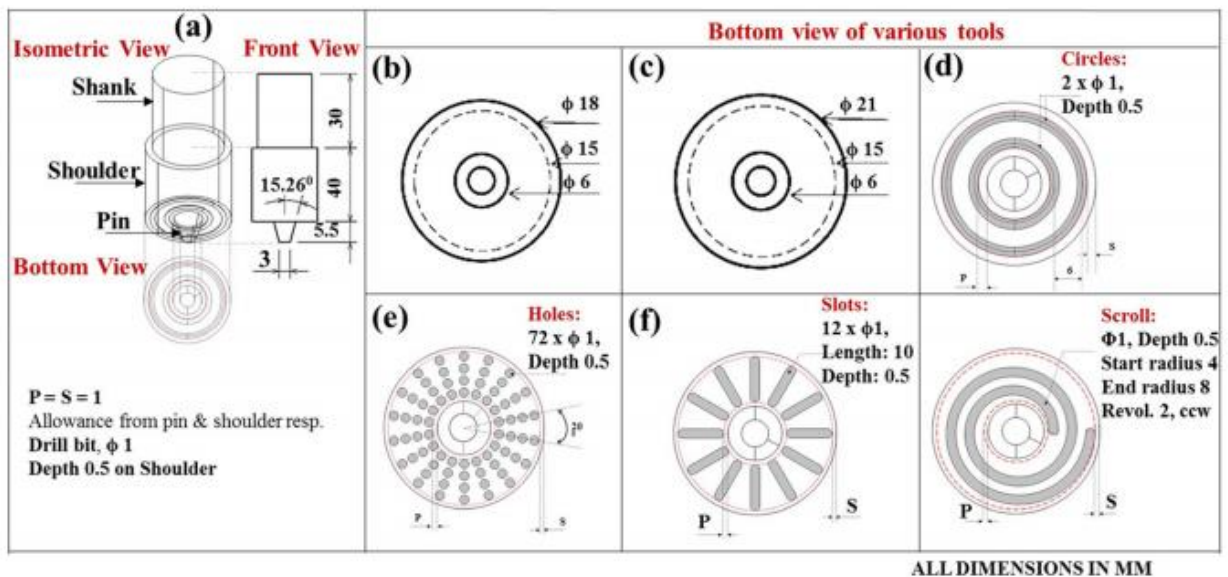


Figure 14 - Tool shoulder geometries [18].

## 1.4.2 Pin

The main role of the pin is heating the atoms that diffuse around it, penetrating the material till the shoulder touches the workpieces. Consequently, the metals become softer and deformed.

The amount of heat generated just by the action of the pin is around 15-20 % of the total heat required to perform the joining [17].

Furthermore, the pin diameter determines how big will be the nugget zone, where the recrystallization will take place.

Some of the most recent developments of TWI about the pin's profile are called Whorl™ and MX Triflute™, reported in Figure 14.

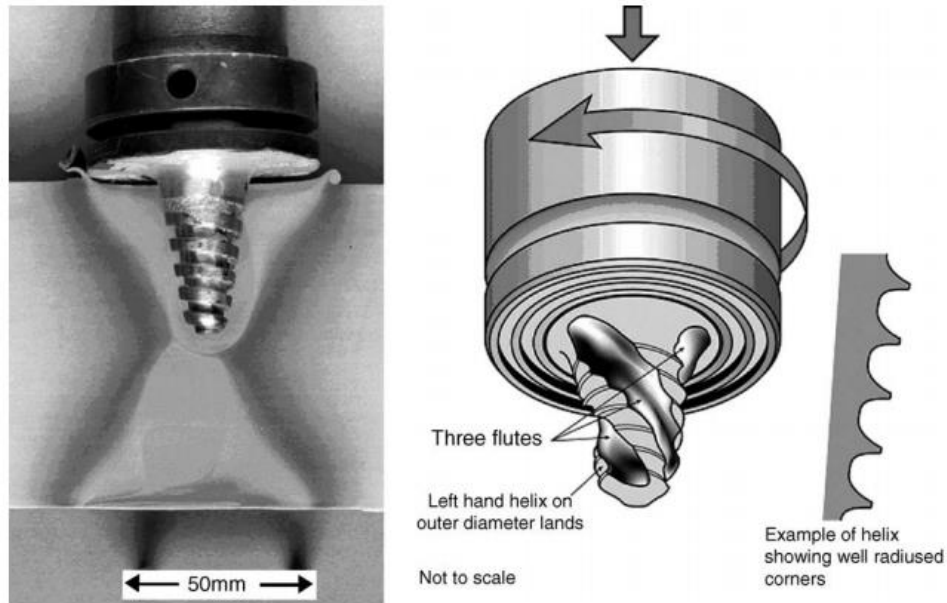


Figure 15 - Whorl™ and MX Triflute™ tools developed by The Welding Institute (TWI) [1].

As studied by Thomas et al. [19], all the positive aspects by using these types of pin profiles with respect to the conventional cylindrical one are:

1. Displacement of less material volume (60% less the Whorl™ and 70% less the MX Triflute™).
2. Reduction of welding force.
3. Easier flow of the plasticized material.
4. More contact surface between pin and material that leads to more heat generated.
5. Higher dynamic to static volume ratio (1.1:1 cylindrical pin, 1.8:1 for Whorl™ and 2.6 for the MX Triflute™, welding a 25mm thick plate).

## 1.5 Process parameters

The process parameters related to the tool design or the machine have to be well defined because they affect the joint properties, such as mechanical properties static and dynamic, fatigue strength, corrosion resistance, toughness and so on [2].

From them, it's possible to affect the heat generation, material flow, defect formation, grain size and the welding force produced.

Most of the variables to be aware of are summed in the Table 1 below, and the effect of them are explained in the following chapters.

Tool design variables	Machine variables	Other variables
Shoulder and pin materials	Welding speed	Anvil material
Shoulder diameter	Spindle speed	Anvil size
Pin diameter	Plunge force or depth	Workpiece size
Pin length	Tool tilt angle	Workpiece properties
Thread pitch		
Feature geometry		

*Table 1 - FSW process variables [2].*

## 1.6 Comparison of Friction Stir Welding with fusion welding processes

Everyone, in 2021, must be interested and attentive about the future of the entire world and so about the global warming, the continuous and irreversible increase of the average world temperature caused by mostly human activities since the 18<sup>th</sup> century.

One of the first aspect that caught my attention when I approached to Friction stir welding was that compared to the others fusion welding processes, it is, as written briefly in the introduction, a green technology due to its energy efficiency (30-40 % lower than fusion welding [12]), environment friendliness (no use of cover gas or flux) and versatility [1].

The most used fusion welding process for aluminium needed to be compared to the Friction Stir Welding are:

- TIG welding (Tungsten Inert Gas): a non-consumable tungsten electrode is used to make an arc between the electrode and the plates. The welding takes place in an inert environment created by a shielding gas. This process is characterized by the use of a consumable filler material that must be very similar to the two base plates.
- MAG (Metal Active Gas) or MIG (Metal Inert Gas): the welding is gained by means of an electric arc formed between a consumable wire electrode and the workpieces. The protection from the environment is guaranteed by an active gas, that participates to the welding like CO<sub>2</sub> in MAG, while on the other end by an inert gas like Argon in MIG.

By describing the two main fusion welding processes used to join aluminium it's possible to understand that they are all characterized by the use of consumable material that could be an electrode, a filler metals and shielding gases.

Therefore, if there is no use of any filler metals, all the aluminium alloys can be joined without concerning for the compatibility of composition (un-matches), which is an issue in fusion welding.

Furthermore, as described in the paper [10] in which the mechanical properties and the microstructure of component welded by FSW, TIG and MIG are compared, the heat input in

FSW is always lower than the one used in TIG and MIG and the better mechanical properties are showed by the components welded by FSW because of the finer grains produced.

Another important aspect is that in FSW the materials that are going to be welded do not reach the melting temperature but only a temperature high enough to make them viscous.

In case of industrial aluminium alloys, the temperature usually does not exceed 500 °C, which corresponds to approximately 75% of the melting temperature [14].

So, as a consequence, the reduced temperature reached makes lower distortion (no volumetric change), final deformation on welded piece, as shown in Figure 16, and residual stress, so that the fatigue performance is improved and allows to not face problems like weld porosities, segregation phenomena, gas inclusion and possible hot cracking coming from the solidification process.

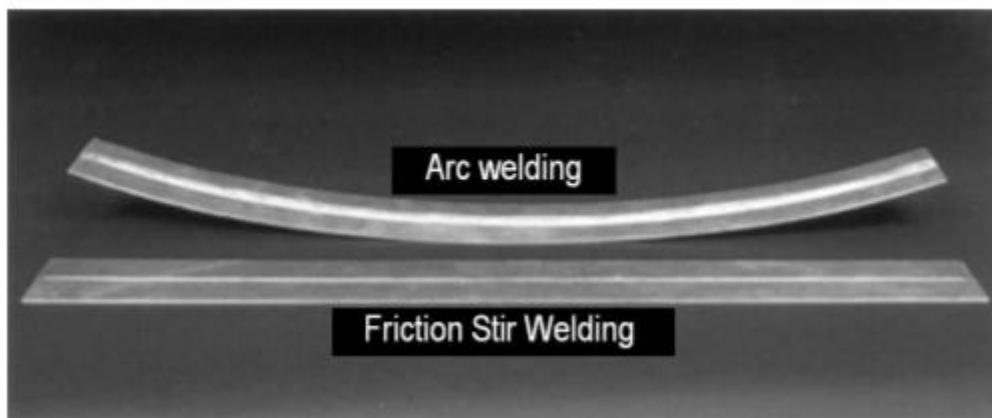


Figure 16 - Comparison of the distortion caused by FSW and by arc welding on aluminium sheets of 5 mm thickness [14].

Since the Friction Stir Welding is a full automated process, this leads to an increase of the equipment costs with respect to arc welding technique and a reduced operator’s skills requirement [2].

FSW can be used in every orientation without taking care of the gravitational effects on the process.

Here below, in Table 2, all the positive aspects that come from the use of Friction Stir Welding are summarized [11]:

Positive aspects of Friction Stir welding	
✓ No need for filler wire or shielding gas	✓ Expanded types of welds
✓ Improved safety due to the absence of toxic fumes and molten splatter	✓ Lower setup costs and less training
✓ Great weld appearance and minimal under/over matching	✓ Operate in all positions and orientations
✓ Reduced distortion compared to conventional welding	✓ Welds with similar mechanical and physical properties as the base metal
✓ Low environmental impact	✓ No cooldown period boosts efficiency and reduces costs

Table 2 - Friction Stir Welding pros.

## 2. Aluminium alloys

### 2.1 Properties and characteristics of the Aluminium

In the second chapter, the main characteristics and properties of the aluminium and its alloys are explained, since they are the materials going to be welded by Friction Stir Welding in the thesis work.

The aluminium is a metal which in its pure form is relatively soft, light, and abundant. With 8.07% it is the third element of the Earth's crust after oxygen and silicon [20].

The pure aluminium contains low level of impurities, less than 1%, and is produced by means of an electrolytic cell process [20].

Its density,  $2.7 \text{ g/cm}^3$  is almost one third of that of the steel,  $7.9 \text{ g/cm}^3$ .

Furthermore, from the corrosion point of view, its behaviour is defined active/passive: when it is exposed in the ambient atmosphere, it oxidizes very fast and then, it covers and protects itself with a film of oxide of about  $10 \text{ }\mu\text{m}$ , gaining high corrosion resistance properties.

Furthermore, it presents a good ductility (ability to be permanently stretched under tension) even at low temperatures due to FCC crystal structure. It can be hot rolled or cold rolled down to thickness of 6-7 micrometres and it can be extruded down to wall thicknesses of 0.5 mm and because of its not toxicity can be used for food storage and preparation.

Other Aluminium's properties important to underline are listed in the Table 3 below:

Property	Value
Atomic Number	13
Atomic Weight (g/mol)	26.98
Valency	3
Crystal Structure	FCC
Melting Point ( $^{\circ}\text{C}$ )	660.2
Boiling Point ( $^{\circ}\text{C}$ )	2480
Mean Specific Heat (0-100 $^{\circ}\text{C}$ ) (cal/g. $^{\circ}\text{C}$ )	0.219
Thermal Conductivity (0-100 $^{\circ}\text{C}$ ) (cal/cms. $^{\circ}\text{C}$ )	0.57
Co-Efficient of Linear Expansion (0-100 $^{\circ}\text{C}$ ) ( $\times 10^{-6}/^{\circ}\text{C}$ )	23.5
Electrical Resistivity at 20 $^{\circ}\text{C}$ ( $\Omega\cdot\text{cm}$ )	2.69
Density ( $\text{g/cm}^3$ )	2.6898
Modulus of Elasticity (GPa)	68.3
Poissons Ratio	0.34

Table 3 - Aluminium properties [21].

## 2.2 Aluminium alloy series

When the aluminium is combined with other metals, its own properties changes.

They are widely used in the transport industries (28%), like automotive, aerospace and so on, because its high strength to weight ratio allows to reduce the whole weight of the mechanical components without losing in strength and stability.

The aluminium alloys are grouped in seven different series depending on the composition. They are classified by four- digit number where the first indicates the principal alloying element, the second the impurities and the last two identify properly the alloy and the purity level. After these digits there could be a letter followed by a maximum of three-digit number which indicates the mechanical and/or heat treatment to which the alloy has been subjected. For example, F, H and O represent, respectively, the as- fabricated, strain-hardened, and annealed states; T3 means that the alloy was heat treated, cold worked, and then naturally aged to a substantially stable condition.

The principal properties of the aluminium alloys' series, summed in the Figure 17, are [3]:

1. *Series 1xxx*: they are composed by pure Aluminium (99%). The last 2 of the 4 digits indicate the minimum percentage of aluminium. For example, 1070 indicates aluminium purity of 99.70%. The second digit gives information about any modifications in impurity limits or alloying elements [3]. They have an excellent corrosion resistance and high thermal and electrical conductivity. They are used in chemical plant, heat exchangers, electrical conductor, food industries and so on.
2. *Series 2xxx*: they are used since 1930 to make structural element in the airplanes. The element combined with Al is the copper, Cu, even if it is possible to find also magnesium and manganese when the goal is having good mechanical properties and lightness as well.  
An example could be 2014 whose composition presents Cu (4-4.58%), Si (0.6-0.9%), Mn (0.4-1.2%) and Mg (0.5-0.9%) [3].  
Other examples of the most used alloys in this group are 2017, 2024 and 2011 [3].  
They require solution heat treatment to achieve optimum mechanical properties.  
They are more difficult to weld.
3. *Series 3xxx*: they are characterized by the addition of Manganese. The addition of 1% of it increase the total strength of the alloy of about 10-15% [3].  
The most used are 3105+3103 for roofing sheets and 3103 for vehicle panelling.
4. *Series 4xxx*: the principal element with Al is the silicon that gives a good resistance to wear and causes a lowered melting point. They are not-heat-treatable.
5. *Series 5xxx*: they are the alloys used in the Friction Stir Welding. Characterized by the combination between Al – Mg (Magnesium), they present high ductility, good weldability and the mechanical properties are enhanced by cold work. When the level of Mg exceeds 3% the stress corrosion resistance reduces [3].
6. *Series 6xxx*: the main elements present in the alloy are Al-Mg-Si. They show good formability, workability, weldability and good mechanical strength and corrosion resistance.

7. *Series 7xxx*: the main alloying element is Zn. The most important characteristic of this alloy is its mechanical strength and low weight. For this reason, they are widely used for frames in bike and motorbike.

A typical example is 7075 whose composition presents Zn (5-6%), Mg (2-3%) and Cu (1-2%) and whose tensile strength is about 580 MPa [3].

Aluminium Alloy Designation System (CEN)							
		Major alloying element	Atoms in solution	Work hardening	Precipitation hardening		
WROUGHT ALLOYS*) EN AW-	1XXX	None (min. 99.00% Al)		X		Non-heat treatable alloys	
	3XXX	Mn	X	X			
	4XXX	Si	X	X			
	5XXX	Mg	X	X			
	2XXX	Cu	X	(X)	X	Heat treatable alloys	
	6XXX	Mg + Si	X	(X)	X		
	7XXX	Zn	X	(X)	X		
	8XXX	Other	X	(X)	X		
	CASTING ALLOYS*) EN AB- EN AC- EN AM-	1XXX0	None (min. 99.00% Al)				*) letters preceding the alloy numbers have the following meaning EN = European Standard A = Aluminium B = Ingot C = Cast Alloy M = Master Alloy W = Wrought Alloy
		2XXX0	Cu				
4XXX0		Si					
5XXX0		Mg					
7XXX0		Zn					
8XXX0		Sn					
	9XXX0	Master Alloys					

Sources: according to EN 573; prEN 1780

<b>TALAT</b> Training in Aluminium Application Technologies	Aluminium Alloy Designation System	1501.03.01
--	------------------------------------	------------

Figure 17 - Aluminium Alloy Designation System [3].

The relationship between the mechanical properties and characteristics of the various alloys is showed in the Figure 18.

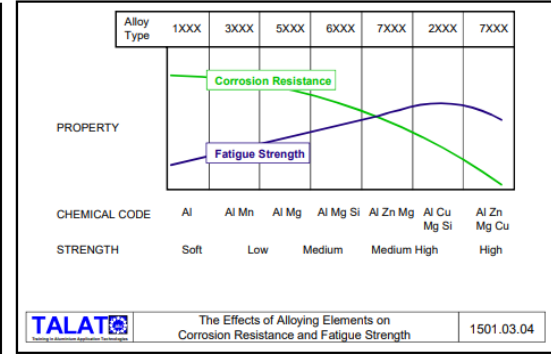
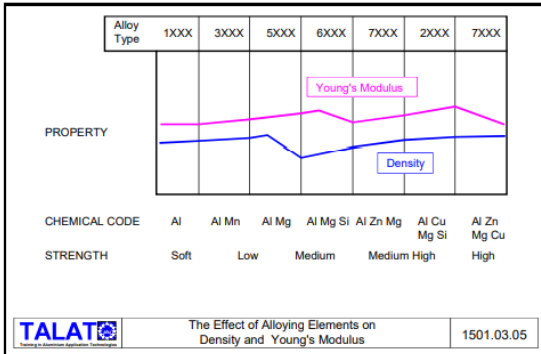
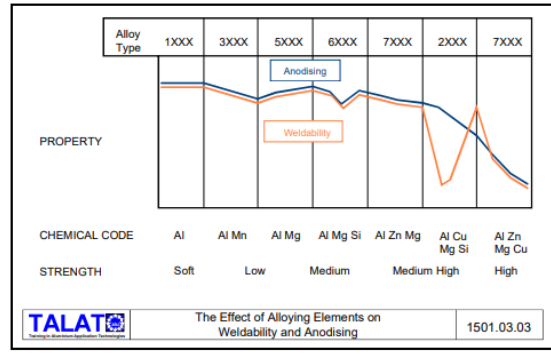
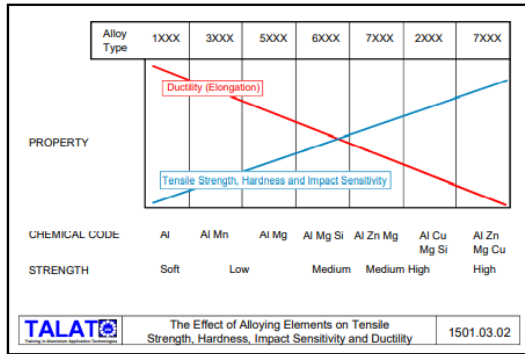


Figure 18 - Comparison between different groups of alloys [3].

### 3. Experimental procedure

The third chapter consists first in a better understanding of the main properties of the Friction Stir welding machine presents in “Eurodies” company and how it works.

Then, defined the materials to be welded, Aluminium Alloys series 5xxx with thickness of 1.5 mm and 2.5 mm, a deep research in literature, consulting books and scientific articles that fit nearly the working conditions, has been done.

All the knowledge acquired has been used to design different types of welding tools.

Furthermore, in order to well fit the dimensions of the clamping region of the tool holder, a tool adapter for all the welding tools has been designed.

Both welding tools and tool adapter have been verified against the static failure.

#### 3.1 STIRTEC Friction Stir Welding machine

The FSW 100 LAB is a machine that presents a vertical and orientable welding head so that the transport and the insertion is facilitated.

The rotation of the welding head is guaranteed by means of an electric drive system with servo-regulation.

The force developed during the welding process is known thanks to a load cell and can be electrically adjusted. Even the torque of the spindle is regulated electrically by current.

The welding is performed in only one direction, X, by means of the movement of the working table, since the head is maintained fixed along X direction and moves only in Z direction. The return stroke is free of external force.

The machine is surrounded by an aluminium and synthetic material cage in order to ensure the safety of the workers. They can approach the machine for the insertion of new components to be welded by means of a double revolving door that opens pressing a button.

The maximum processing loads sustained by the machine are 100kN of vertical force, 40 kN of transversal and lateral force while the maximum spindle torque is about 600 Nm.

Some of general data about the machine are reported in the Table 4:

Overall dimensions L x L x H	2812 x 1400 x 2953	mm
Weight including electrical cabinet	8500	kg
Weight excluding electrical cabinet	8350	kg

Table 4 - Overall machine dimensions.

Table 5 provides an overview of maximum value of force and torque when is performed a welding of Aluminium alloys with thickness 20 mm. However, all the data must be adapted of

any different working conditions because they depend also on the design and material of the FSW tool, on the program test and so on.

The maximum spindle rotational speed is about 1500 rpm and can be reached when materials with small thickness are going to be welded.

Materials	Materials' quality	Thickness	Torque	Downward force	Transversal force	Spindle rotational speed	Traverse speed
Aluminium	EN AW 2017A	20 mm	240 Nm	85 kN	18 kN	300 rpm	120 mm/min
Aluminium	EN AW 5083	20 mm	220 Nm	75 kN	11 kN	300 rpm	80 mm/min
Aluminium	EN AW 6082	20 mm	240 Nm	65 kN	16 kN	500 rpm	350 mm/min
Aluminium	EN AW 7020	20 mm	355 Nm	55 kN	3 kN	200 rpm	90 mm/min
Aluminium	EN AW 7075	20 mm	280 Nm	67 kN	13 kN	200 rpm	80 mm/min

*Table 5 - Working parameters.*

Some images of the STIRTEC Friction Stir Welding machine are here reported:

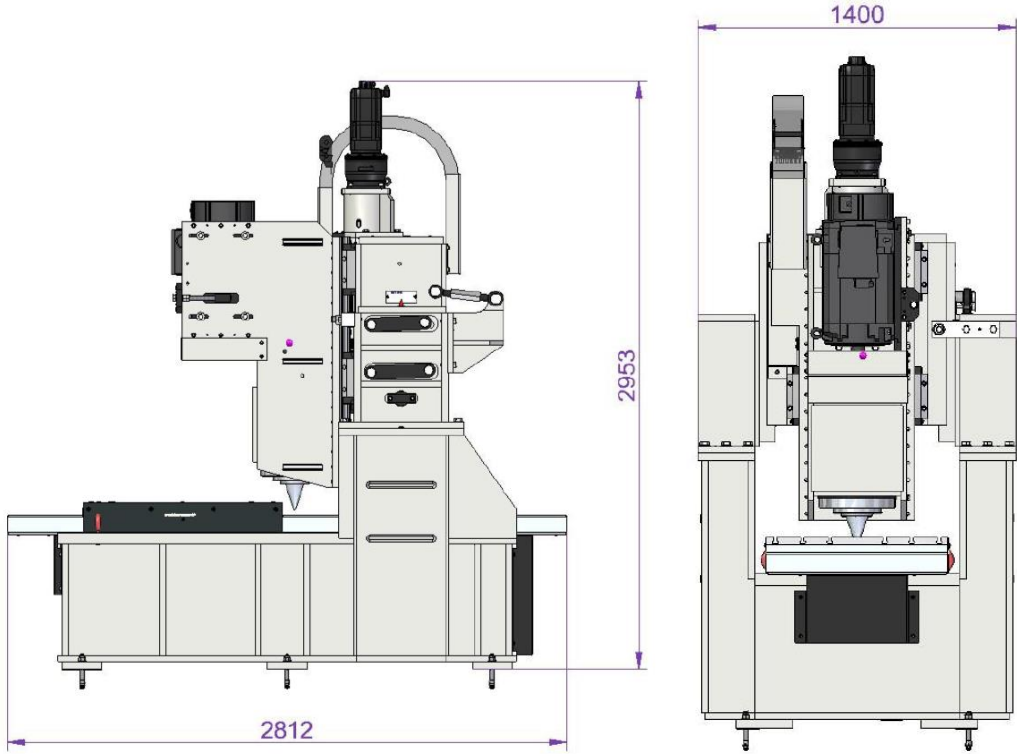


Figure 19 - STIRTEC Machine main dimensions.



Figure 20 - STIRTEC Friction Stir Welding Machine.

### 3.2 Tool adapter

Starting from the dimensions drawing of the tool holder, it is possible to see that the hole machined for clamping the welding tool is about 32 mm, Figure 21 and 22.

The complete Tool holder drawing is reported in the attachments.

Since the dimension of tool shoulders for welding Aluminium Alloys sheets are much lower than 32 mm, as will be described later in the following chapter, to avoid a strong change of diameter dimension that would lead to a local stress intensification, a tool adapter has been designed by using SolidWorks CAD.

Some other images, Figure 23 and 24, about the tool holder are reported.

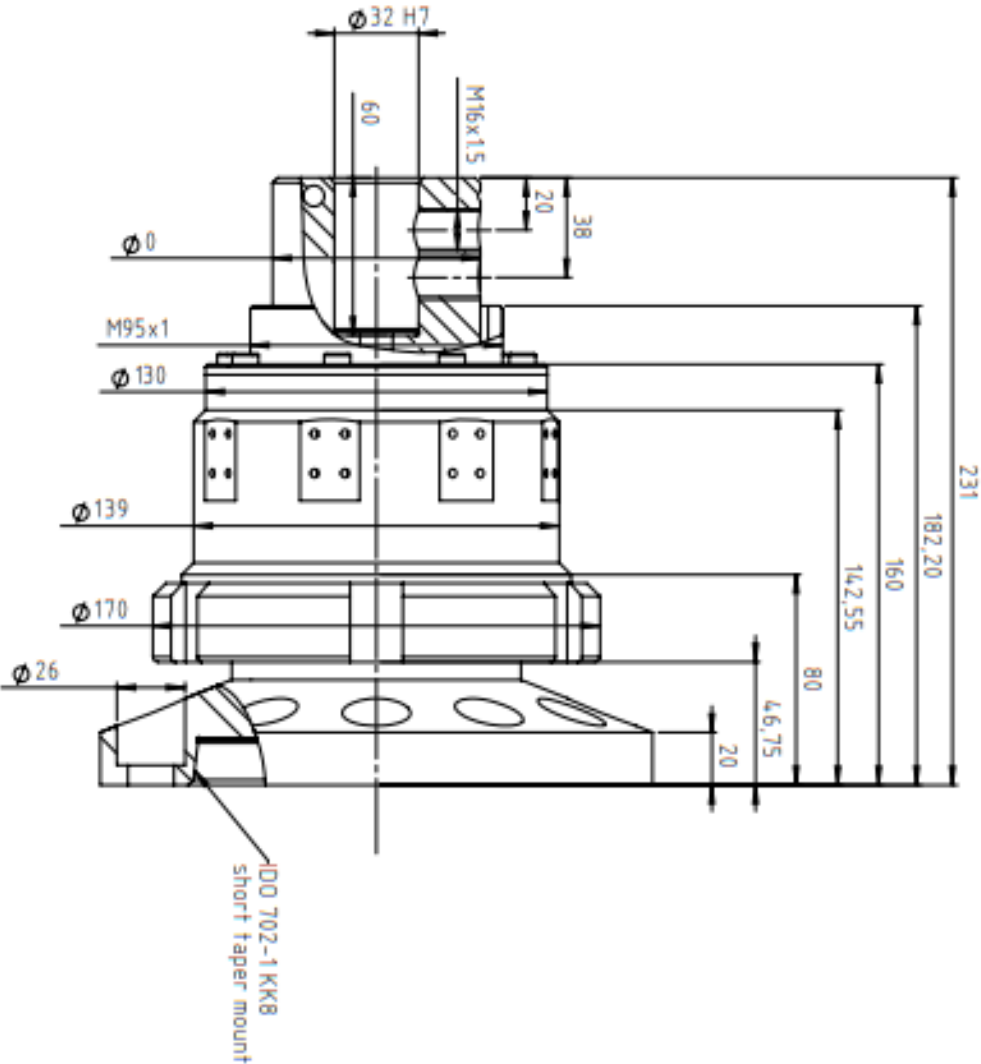
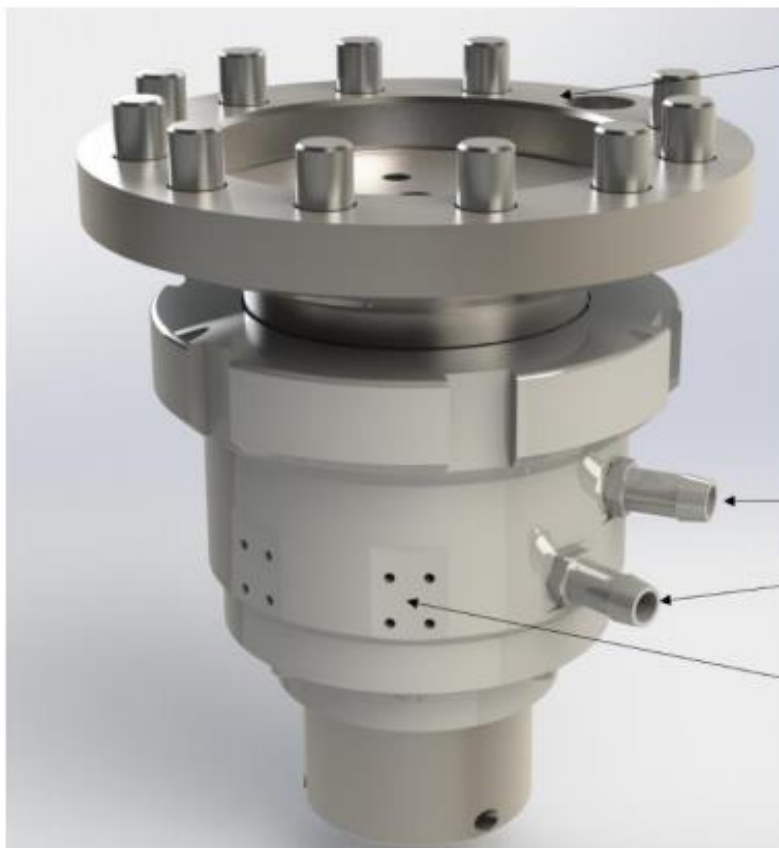


Figure 21 - STIRTEC tool holder dimensions.



Fixture for the welding tool  
( $\text{Ø}32\text{ H7}$ )

Figure 22 - STIRTEC Tool holder\_hole for fixture welding tool.



Mounting flange for spindle

Cooling water inlet

Cooling water return

Mounting surfaces for  
the torque support

Figure 23 - STIRTEC Tool Holder.

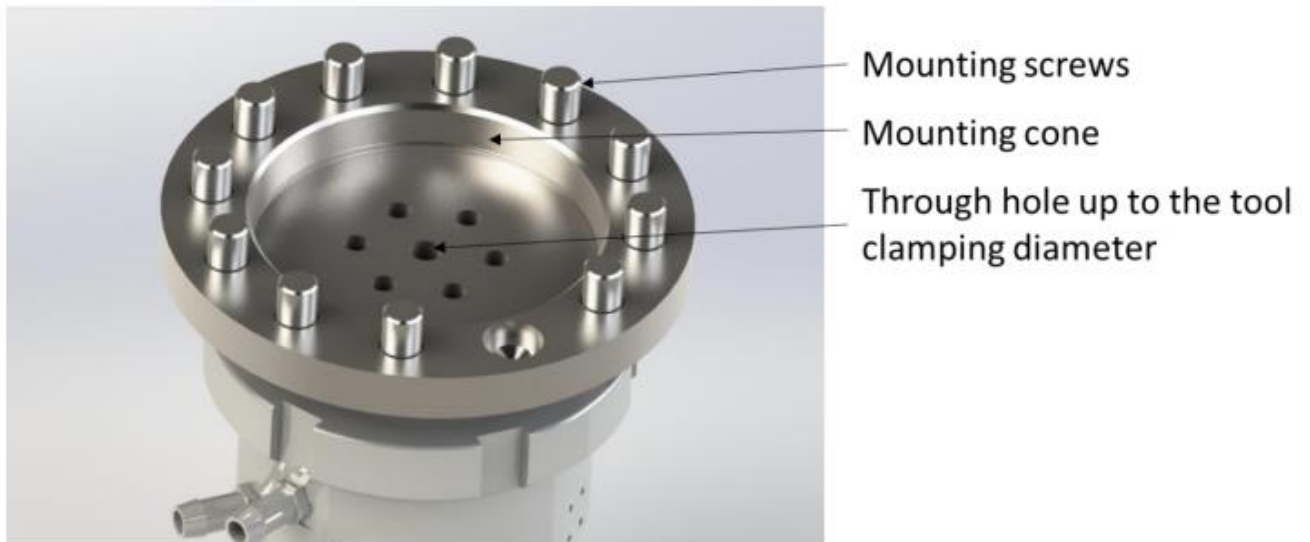


Figure 24 - STIRTEC Tool holder upper part.

The tool adapter, reported in Figure 25 and 26, is characterized by a total length of 90 mm where 60 mm are inside the tool holder and, obviously, presents a diameter of 32mm.

The connection between the tool holder and the tool adapter is guaranteed by means of two M16 studs that pass through the two holes present on the former and go in touch with a groove deep 3mm and large 19 mm designed on the latter, as reported in Figure 26.

The last part of the tool adapter is characterized by a length of 23 mm and an outer diameter of 36mm.

Furthermore, it has a hole of 16 mm of diameter and depth 20 mm to accommodate the different types of welding tools and four holes arranged two by two at 90° for M5 to carry out the clamping.

The connection between the tool adapter and the welding tool has been taught so that, at the beginning the welding tool fills the entire 20 mm of depth and is fixed by means the two upper threaded holes. Then, after a while, when the welding tool's pin has worn out, it could be re-machined from the shoulder and re-used, fixing it to the tool adapter by means of the bottom two threaded holes.

The empty space left by the welding tool will be filled by inserting a disk that will withstand the vertical forces produced in working conditions.

In this way the welding tool could be re-used more time gaining a saving of money, especially when its material's cost is high.

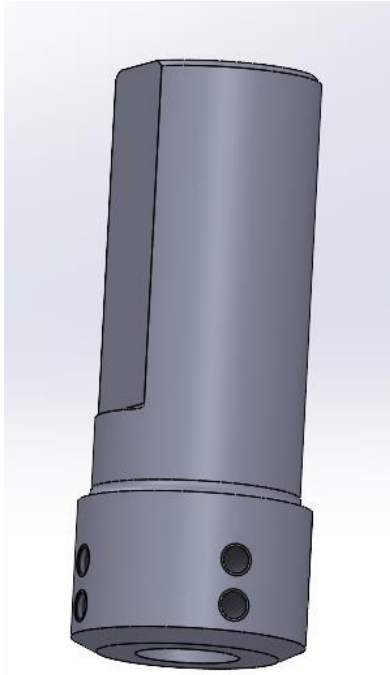


Figure 25 - Tool Adapter, 3D drawing.

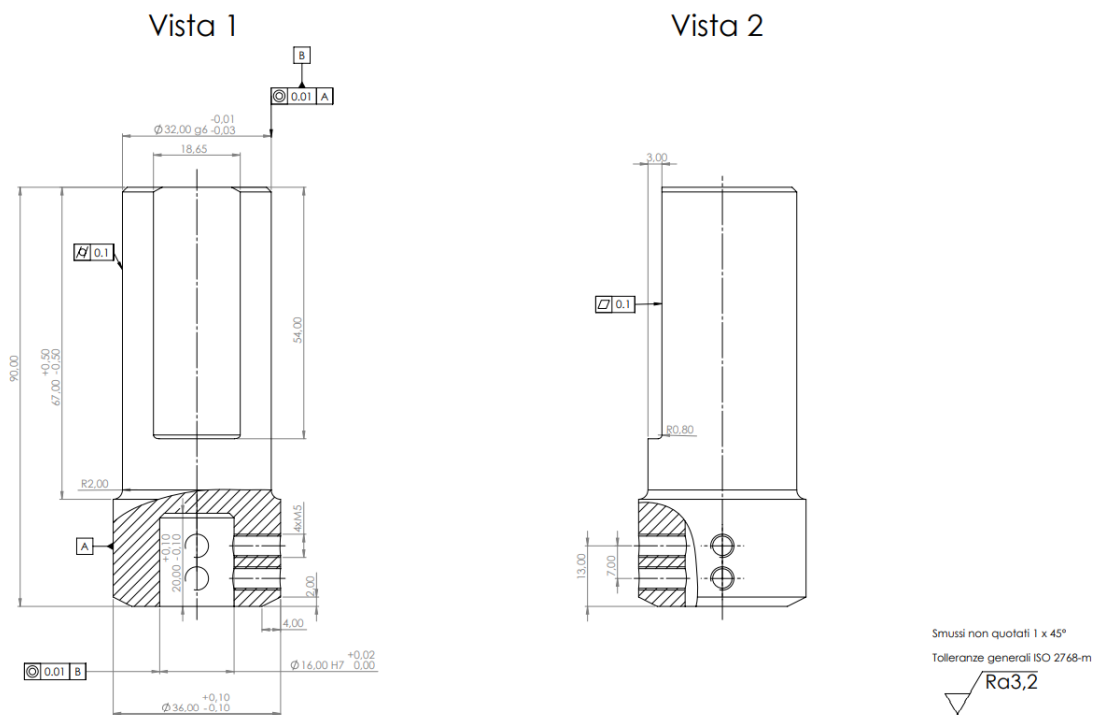


Figure 26 - Tool Adapter 2D Drawing.

### 3.2.1 Tool adapter design verification

The tool adapter, once designed, is subjected to a static verification in which the most critical sections must withstand the stresses coming from the action of the spindle's torque without overcoming the yield strength.

In some sections, in which a strong change of diameters is present, a stress concentration factor is taken into account.

A fatigue analysis is not performed since, in working conditions, the tool adapter is not subjected to any cyclic or variable loads.

First, in order to define the admissible stresses, a material must be chosen.

The material selected for the tool adapter is AISI H13 (ISO X40CrMoV5-1) whose properties are summed in the Table 6 below [22].

Properties	Value
Density	7.69e3 – 7.84e3 kg/m <sup>3</sup>
Yield strength	1000-1380 MPa
Ultimate tensile strength	1200-1590 MPa
Reduction of area	50.00 %
Young Modulus	215 GPa
Poisson ratio	0.27 – 0.30
Thermal expansion coefficient	10.2 – 10.7 $\mu$ strain/°C

Table 6 - H13, material properties.

Furthermore, considering a safety factor of 1.5 the normal allowable stress is considered to be :

$$\sigma_{adm} = \frac{\sigma_{yield}}{SF} = \frac{1000}{1.5} = 666.67 \text{ MPa}$$

And, consequently, using the Von Mises criterium, the shear allowable stress is:

$$\tau_{adm} = \frac{\sigma_{adm}}{\sqrt{3}} = \frac{666.67}{\sqrt{3}} = 384.67 \text{ MPa}$$

The sections analysed from the static point of view are the following highlighted in the drawing in Figure 27.

In each section the torque applied is:

$$M_t = 100000 \text{ N} * \text{mm}$$

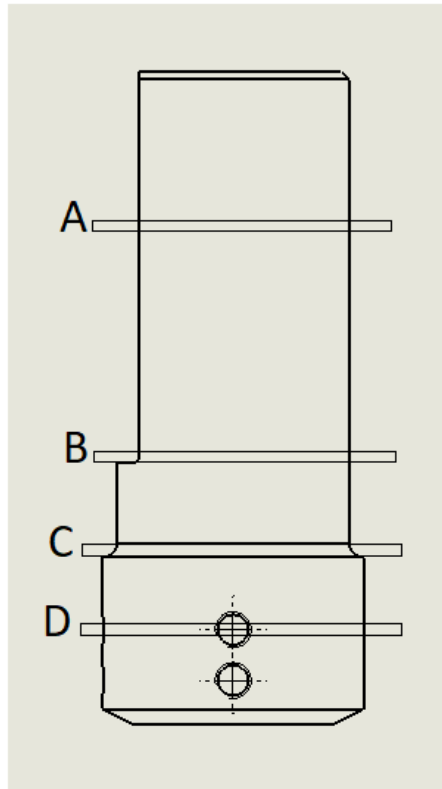


Figure 27 - Sections chosen for static analysis.

### 3.2.1.1 Static verification section A

The first section verified is the section A, reported in Figure 28.

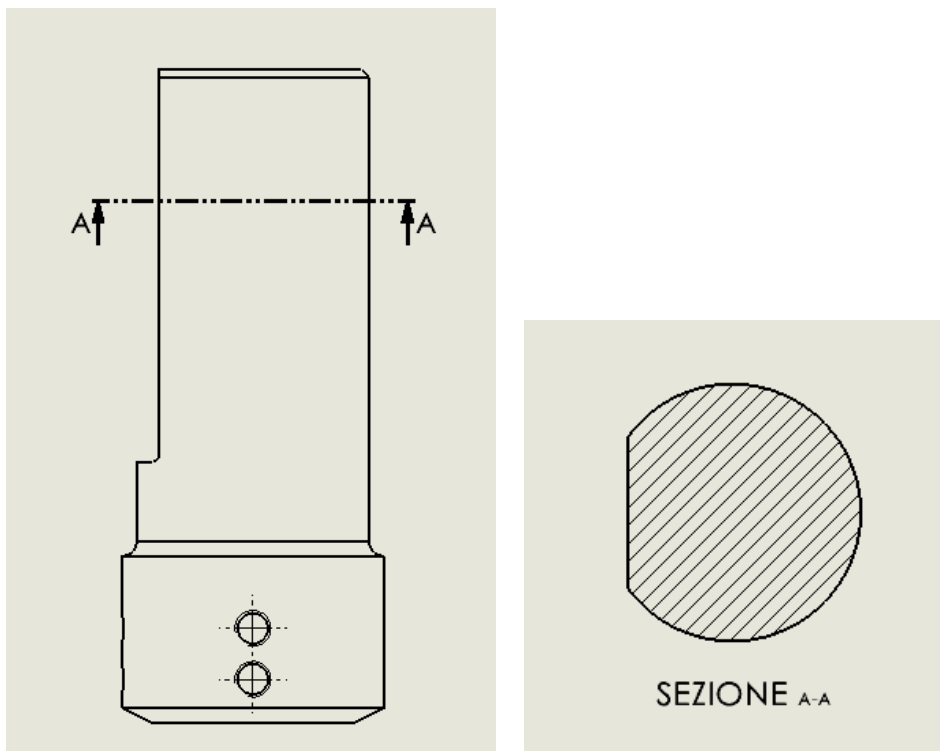


Figure 28 - Section A of the tool adapter.

The diameter of the section is considered equal to  $d=29$  mm. In fact, the groove present on the tool adapter is taken into account following a conservative approach, so considering the circular cross section with a diameter  $d$  that is smaller than the actual one.

The maximum shear stress acting on the section is:

$$\tau_{MAX,A} = \frac{16 * M_t}{\pi * d^3} = 20.9 MPa$$

Then, the comparison between the maximum shear stress due to torsion and the allowable shear stress is performed:

$$\tau_{MAX,A} < \tau_{adm}$$

The section A is able to withstand the tension due to the torque applied.

### 3.2.1.2 Static verification section B

The second section verified against static failure is the section B, reported in Figure 29.

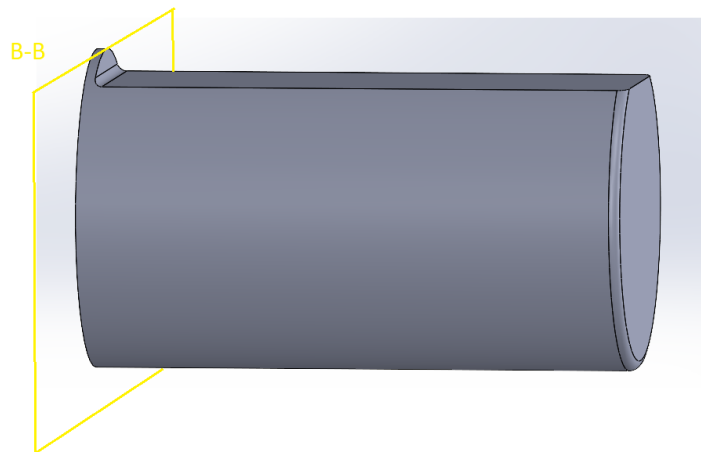
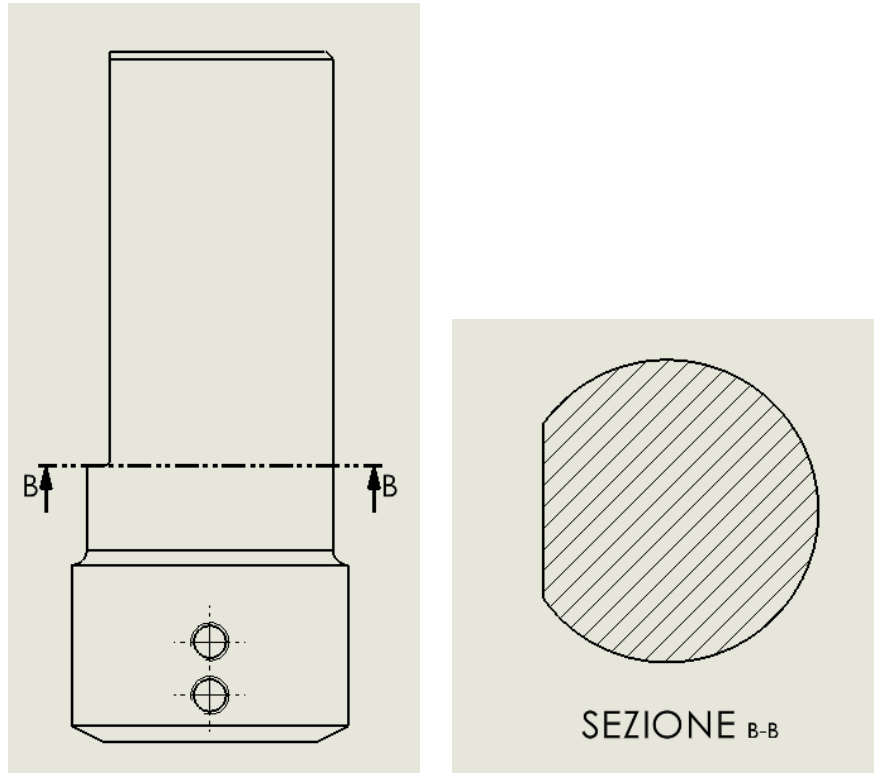


Figure 29 - Section B of the tool adapter.

The section B is characterized by the presence of notch that leads to a local increase of stress in that region. For this reason, a stress concentration factor  $K_t$  is computed in order to evaluate the maximum local stress, even if in the static analysis it has not so much influence.

The stress concentration factor depends only on the geometry and is determined by means the following graph, Figure 30. Even in this case, a conservative approach is pursuit since, in the studying case, the reduction of cross section's diameter does not take place all around the cylinder, as reported in the graph, but it is present only in upper part.

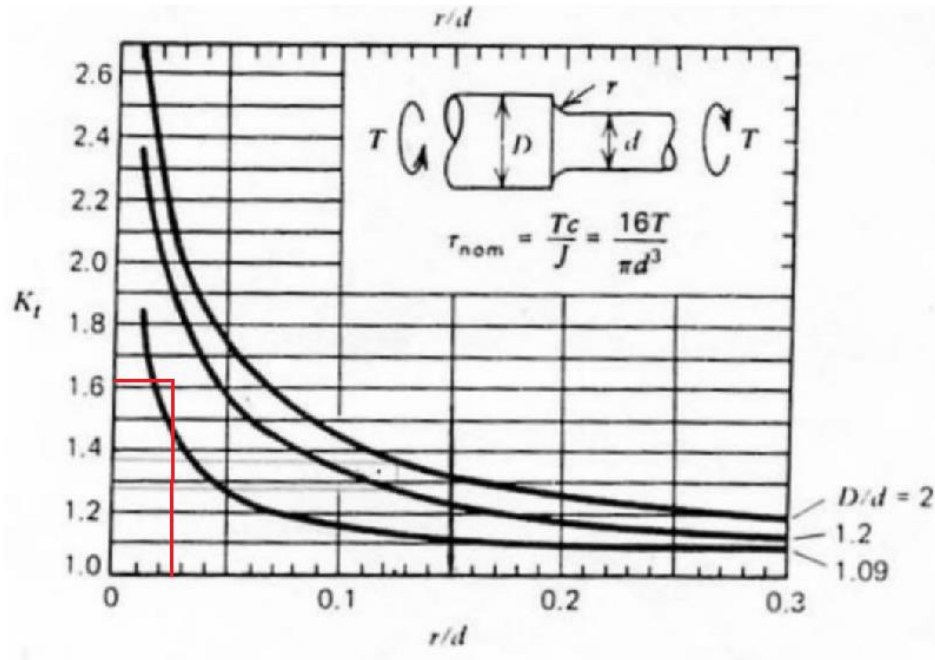


Figure 30 - Stress concentration factor  $K_t$  for shaft in torsion.

The data used to enter in the graph and determine the value of  $K_t$  are summed in the Table 7.

Major diameter	D	32 mm
Minor diameter	d	29 mm
Diameters ratio	D/d	1.103
Notch radius	r	0.8 mm
Ratio notch radius and minor diameter	r/d	0.027
Stress concentration factor	$K_t$	1.61

Table 7 - Data used for the computation of the stress concentration factor.

The maximum nominal value of the shear stress is:

$$\tau_{nom,B} = \frac{16 * M_t}{\pi * d^3} = 20.9 \text{ MPa}$$

The maximum shear stress considering its increment due to the presence of the notch is:

$$\tau_{MAX,B} = K_t * \tau_{nom,B} = 33.62 \text{ MPa}$$

Then, like what has been done for the section A, the comparison between the maximum shear stress due to torsion and the allowable shear stress is performed:

$$\tau_{MAX,B} < \tau_{adm}$$

The section B is able to withstand the tension due to the torque applied.

### 3.2.1.3 Static verification section C

The third section important to analyse is the section C, reported in Figure 31.

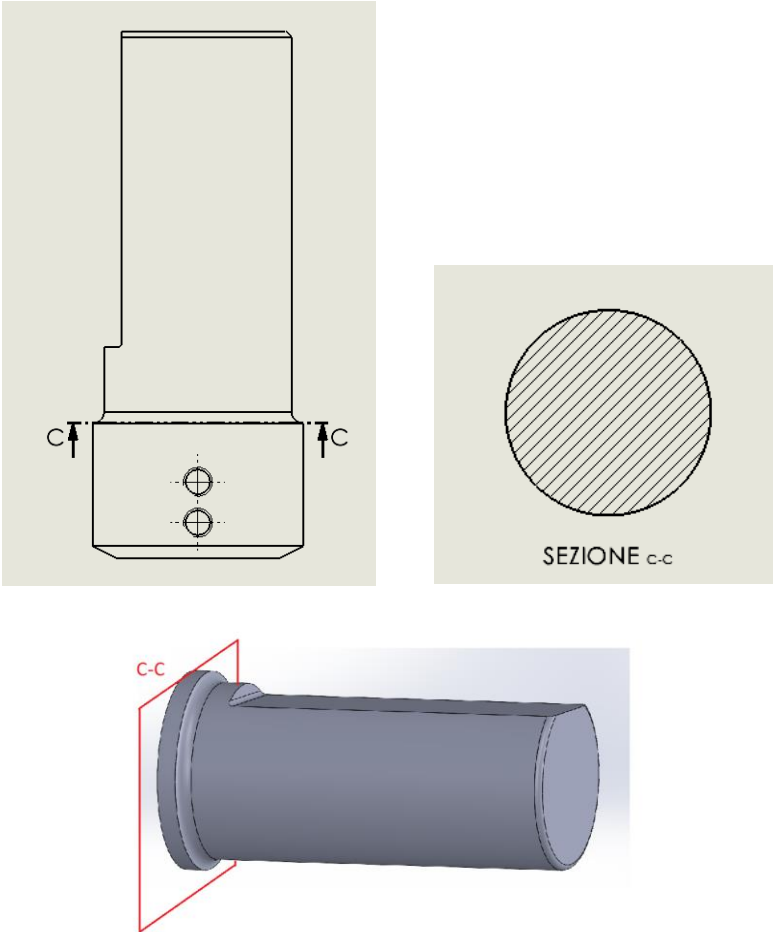


Figure 31 - Section C of the tool adapter.

Following the same passages done before for the section B:

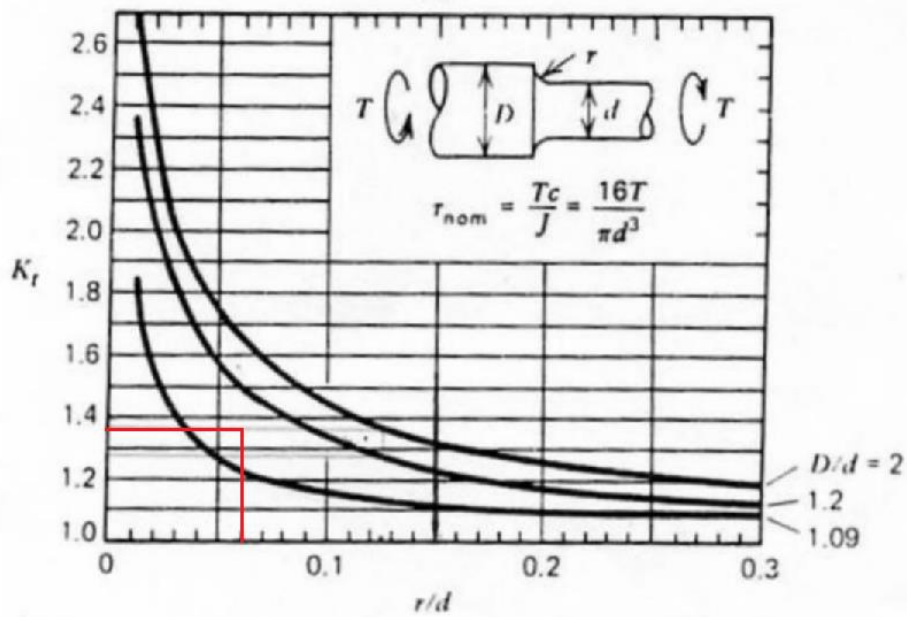


Figure 32 - Stress concentration factor  $K_t$  for shaft in torsion.

The data used for the computation of the stress concentration factor are summed in the Table 10 below.

Major diameter	D	36 mm
Minor diameter	d	32 mm
Diameters ratio	D/d	1.125
Notch radius	r	2 mm
Ratio notch radius and minor diameter	r/d	0.0625
Stress concentration factor	$K_t$	1.38

Table 8 - Data used for the computation of the stress concentration factor.

The maximum nominal value of the shear stress is:

$$\tau_{nom,C} = \frac{16 * M_t}{\pi * d^3} = 15.54 \text{ MPa}$$

The maximum shear stress considering its increment due to the presence of the notch is:

$$\tau_{MAX,C} = K_t * \tau_{nom,C} = 21.44 \text{ MPa}$$

The section C is able to withstand the tension due to the torque applied since the maximum shear stress due to torsion is lower than the allowable shear stress:

$$\tau_{MAX,C} < \tau_{adm}$$

### 3.2.1.4 Static verification section D

The last section that must withstand the stress coming from the torque's action is reported in Figure 33.

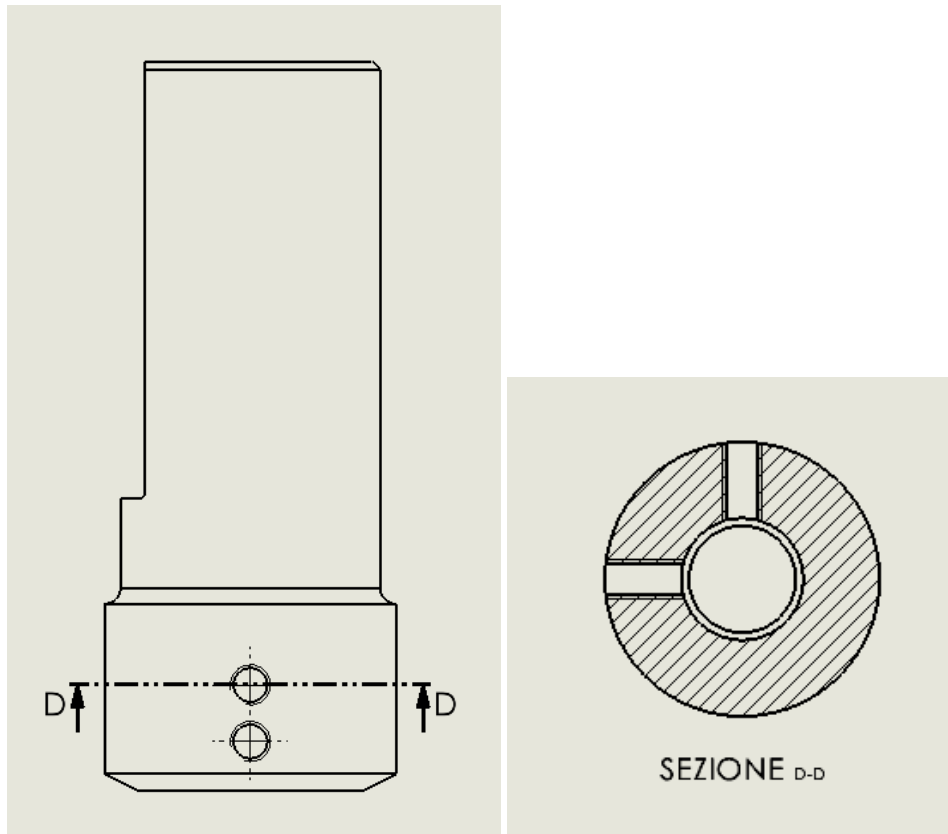


Figure 33 - Section D of the tool adapter.

The section D is characterized by a circular crown section with major diameter  $D=36$  mm and minor diameter  $d=16$  mm and two threaded holes placed at  $90^\circ$  for M5 studs.

So, the resistant area is the circular crown area minus the two rectangular areas with dimension  $b=4.20$  mm and  $h=10$  mm, so:

$$A = \pi * \frac{(D^4 - d^4)}{4} - 2 * b * h = 732.8 \text{ mm}^2$$

The polar moment of inertia:

$$I_p = \pi * \frac{(D^4 - d^4)}{32} - \left( \frac{h * b^3}{12} + A_r * l^2 \right) - \left( \frac{b * h^3}{12} + A_r * l^2 \right) = 143854.2 \text{ mm}^4$$

where  $A_r$  is the area of the rectangles and  $l = 13$  mm is the distance between the axis passes through the rectangle center of gravity with respect to which its moment of inertia is computed

and the axis passes through the centre of rotation.  
The Huygens-Steiner theorem is applied.

And finally, the maximum shear stress due to torsion is:

$$\tau_{MAX,D} = \frac{M_t}{I_p} * \frac{D}{2} = 12.51 \text{ MPa}$$

Even the last section is strong enough and is able to support the shear stress due to the action of the torque since:

$$\tau_{MAX,D} < \tau_{adm}$$

### 3.3 Analysis of tolerances

In mechanical production of components, it is almost impossible to achieve a perfect level of accuracy in dimensions and shape and when it is achieved the component's price is so high that it could not even enter in the market.

Machined workpieces always present deviations of size, form, orientation and location and for this reason, the dimensional and geometrical tolerances have been introduced so that a small error could be under control.

In this section the choice of the different geometric dimensioning and tolerancing used in the tool adapter drawing, reported here below in Figure 34, are explained.

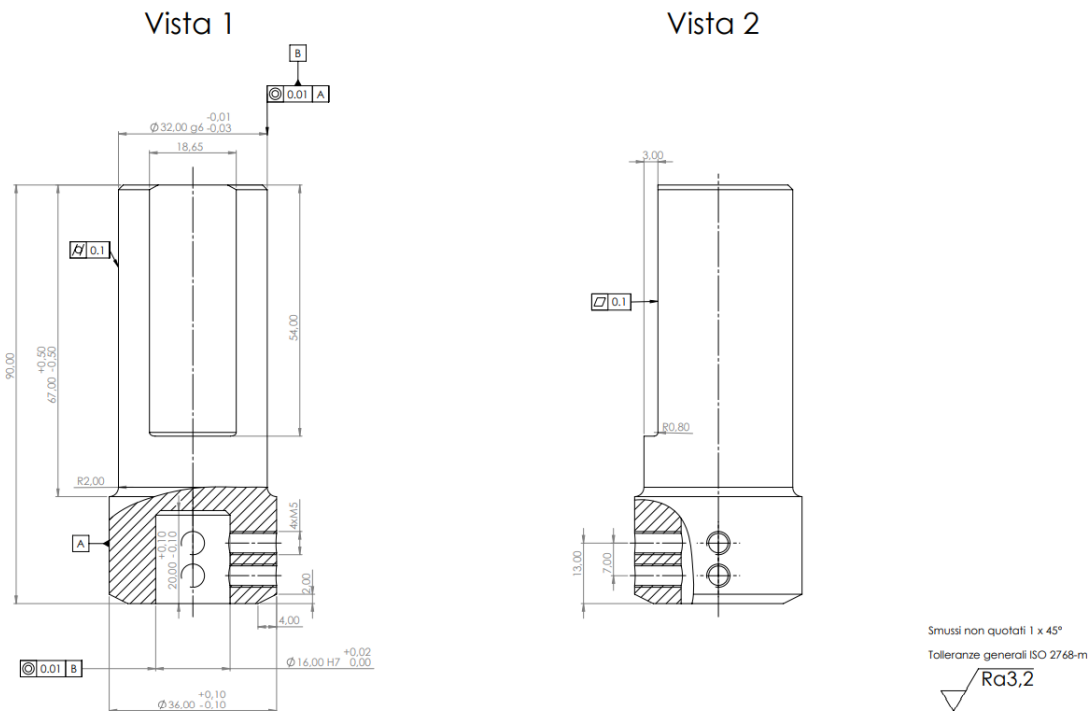


Figure 34 - Tool Adapter 2D Drawing.

Starting from the analysis of the tool holder's hole with 32 mm of diameter that needs to be matched with the tool adapter upper part, following the ISO (International Organization for Standardization) designation, it has a dimensional tolerance of H7.

The number, 7 in this case, gives the size range in which the component is still good, and, for a theoretically perfect hole of 32 mm, means that its maximum dimension acceptable is (32 + 0.03) mm, while its minimum dimension must be equal to 32mm.

The letter, uppercase for hole and lowercase for shaft, explains which type of joint shaft/hole should be with respect of their own application. It could range from clearance to interference fits.

So, the tolerance that should be put on the tool adapter's corresponding part, is strictly connected to H7.

The one chosen is g6 since it guarantees a slightly clearance both in idle and in working conditions. In working conditions a thermal expansion has been taken into account considering a thermal expansion coefficient of about  $\alpha = 10.7 \mu\text{strain}/^\circ\text{C}$  and a  $\Delta T = 100^\circ\text{C}$  for both Tool Holder and Tool Adapter.

All the computations are reported in the following Figure 35.

TOOL HOLDER				TOOL ADAPTER			
	32 mm	HOLE			32 mm	SHAFT	
material	H13			material	H13		
Tolleranza	H7			Tolleranza	g6		
Dmax	32,03	mm		Dmax	31,99	mm	
Dmin	32	mm		Dmin	31,97	mm	
Thermal expansion coefficient		$\alpha$	10,7 $\mu\text{strain}/^\circ\text{C}$	Thermal expansion coefficient		$\alpha$	10,7 $\mu\text{strain}/^\circ\text{C}$
$\Delta T$	100 $^\circ\text{C}$			$\Delta T$	100 $^\circ\text{C}$		
In work	-0,010	-0,060	= mm				
In idle	-0,010	-0,060	= mm				
	Max	Min					
	if POSITIVE means interference						
	if NEGATIVE means clearance						

Figure 35 - Tool Holder and Tool Adapter tolerances.

The main equations used to take out both the maximum and minimum interference value (negative for clearance) in working conditions are:

$$i_{max} = (D_{maxadapter} + \alpha * \Delta T * D_{maxadapter} * 10^{-6}) - (D_{minholder} + \alpha * \Delta T * D_{minholder} * 10^{-6})$$

$$= -0.01 \text{ mm}$$

$$i_{min} = (D_{minadapter} + \alpha * \Delta T * D_{minadapter} * 10^{-6}) - (D_{maxholder} + \alpha * \Delta T * D_{maxholder} * 10^{-6})$$

$$= -0.06 \text{ mm}$$

In idle condition it has been done just the difference between the diameters of the Tool holder and Tool adapter to get the two values of interference:

$$i_{max} = (D_{maxadapter}) - (D_{minholder}) = -0.01 \text{ mm}$$

$$i_{min} = (D_{minadapter}) - (D_{maxholder}) = -0.06 \text{ mm}$$

Furthermore, specific tolerances have been put on the bottom diameter of 36mm, on the 60mm length on the hole of 16 mm of length and on the groove depth.

The same analysis has been pursued for the connection between tool adapter and welding tool used for titanium welding. The computations are the same explained before and the results are here reported in Table 9.

TOOL ADAPTER				TOOL			
material	H13	16 mm	HOLE	material	W/Re	16 mm	SHAFT
Tolerance	H7			Tolerance	g6		
Dmax	16,02	mm		Dmax	15,99	mm	
Dmin	16	mm		Dmin	15,98	mm	
Thermal expansion coefficient	$\alpha$	10,7 $\mu$ strain/ $^{\circ}$ C		Thermal expansion coefficient	$\alpha$	4,6 $\mu$ strain/ $^{\circ}$ C	
$\Delta T$	600 $^{\circ}$ C			$\Delta T$	1000 $^{\circ}$ C		
In work	-0,039	-0,069	<	mm			
In idle	-0,010	-0,040	>	mm			
	Max	Min					
	if POSITIVE means interface						
	if NEGATIVE means clearance						

Table 9 - Tool Adapter - Welding Tool tolerances.

All dimensions must have a tolerance, but in order to avoid an overloaded drawing difficult to read, for all the features written in the 2D drawing that are not followed by tolerances, the ISO 2768, Figure 36, has been used to fix them as a general indication.

Dimensioni in mm

Classe di tolleranza		Scostamenti limite per campi di dimensioni fondamentali							
Designazione	Denominazione	da 0,5 <sup>1)</sup> fino a 3	oltre 3 fino a 6	oltre 6 fino a 30	oltre 30 fino a 120	oltre 120 fino a 400	oltre 400 fino a 1 000	oltre 1 000 fino a 2 000	oltre 2 000 fino a 4 000
f	fine	$\pm 0,05$	$\pm 0,05$	$\pm 0,1$	$\pm 0,15$	$\pm 0,2$	$\pm 0,3$	$\pm 0,5$	-
m	media	$\pm 0,1$	$\pm 0,1$	$\pm 0,2$	$\pm 0,3$	$\pm 0,5$	$\pm 0,8$	$\pm 1,2$	$\pm 2$
c	grossolana	$\pm 0,2$	$\pm 0,3$	$\pm 0,5$	$\pm 0,8$	$\pm 1,2$	$\pm 2$	$\pm 3$	$\pm 4$
v	molto grossolana	-	$\pm 0,5$	$\pm 1$	$\pm 1,5$	$\pm 2,5$	$\pm 4$	$\pm 6$	$\pm 8$

1) Per le dimensioni nominali minori di 0,5 mm, gli scostamenti devono essere indicati vicino alla/e dimensione/i nominale/i relativa/e.

Figure 36 - General tolerances ISO 2768 [34].

Regarding the geometrical tolerances the ISO 1101, ISO 5459 and ISO 10579 has been used.

Form tolerance defines the maximum acceptable value for the form deviation. According to ISO 1101, the tolerance's allowable zone is defined with a specific width, coming from the accuracy achievable, within all the points of the feature must be contained.

The shape tolerances indicated in the tool adapter drawing are:

- Cylindricity: the surface must be contained between two coaxial cylinders with a radial distance equal to the tolerance indication.  
It has been put on the cylindrical surface of the tool adapter that matches with the tool holder, so that any problems of connections between them is avoided.  
The cylindricity tolerance controls even the circularity, straightness and parallelism.
- Flatness: the surface must be contained between two parallel planes distant the tolerance indication.  
It has been located on the groove, so that the connection with the M16 screw, that guarantees the torque transmission has no problem of deviation and the two surfaces can match perfectly.
- Coaxiality: the actual axis shall be contained within a cylinder of diameter equal to the tolerance indication coaxial with the datum axis.  
It has been indicated with respect to precise reference planes or datum A, B that are determined following the production turning process.

Finally, an indication about a general roughness of  $3.2 \mu\text{m}$  has been indicated.

### 3.4 Case study 1: Lap Joint

The first case study is about designing a proper welding tool in order to realize a LAP joint between Aluminium Alloys sheets with 1.5 mm of thickness.

The definition of its own geometries and features comes from the analysis of some scientific papers that best fit the case study's working conditions and parameters.

For each document found, it has been evaluated the tool used, the configurations and features of the shoulder and the pin, the diameters and the lengths, and the results that the specific tool used gives in terms of surface finishing, micro and macro-structure and mechanical properties.

Among all the various articles, the one written by Emad Salari et al. [7] has been chosen as reference for the case study one.

It consists of a Friction Stir Welding of AA5456 Aluminium Alloy, with two different tempers T321 and O, and two different thickness of 5 mm and 2.5 mm, in lap joint as reported in the Figure 37 below:

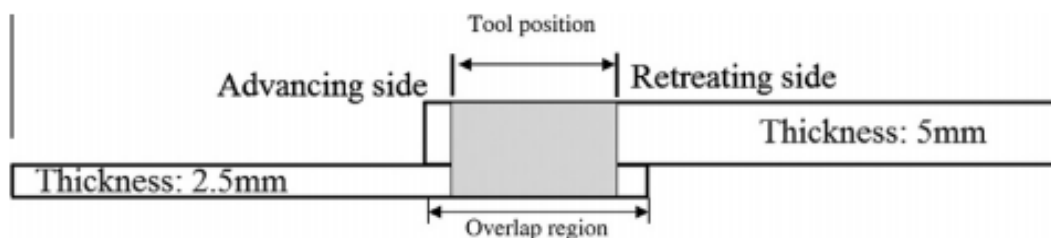


Figure 37 - Friction Stir LAP welding [7].

In the study, four different welding tools are used, all characterized by threads on their outer pin surface. Their schematic representation and main dimensions are reported in Figure 38.

Tools	Description of the pin	Big diameter of the pin (mm)	Small diameter of the pin (mm)	Pitch of the pin (mm)
T1	Conical screw thread pin	7	5	0.8
T2	Cylindrical-conical thread pin	7	5	0.8
T3	Stepped conical thread pin	7.5	4	0.8
T4	Neutral Flared-Triflute pin	7	5	0.8

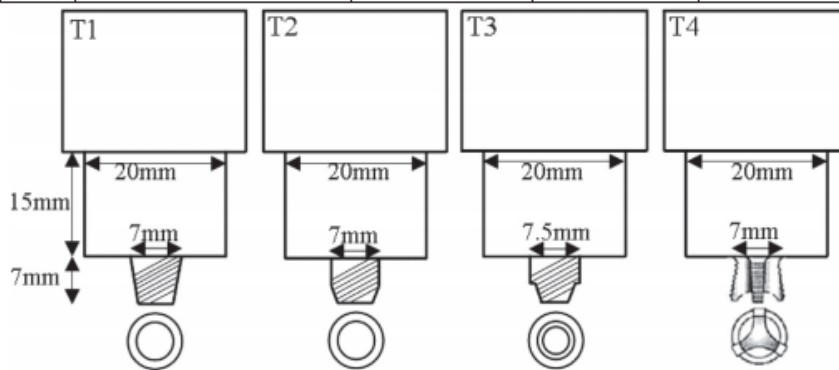


Figure 38 - Features and geometry of four welding tools [7].

The welding tool T3, consisting of a stepped conical thread pin is the one that gives the best results in terms of joint integrity and mechanical properties.

Actually, starting from the macro-structure point of view, T3 allows to keep low the height of the Hook defect and the plate effective thickness ET, Figure 39, because its geometrical features guarantee a better mixing of plasticized material.

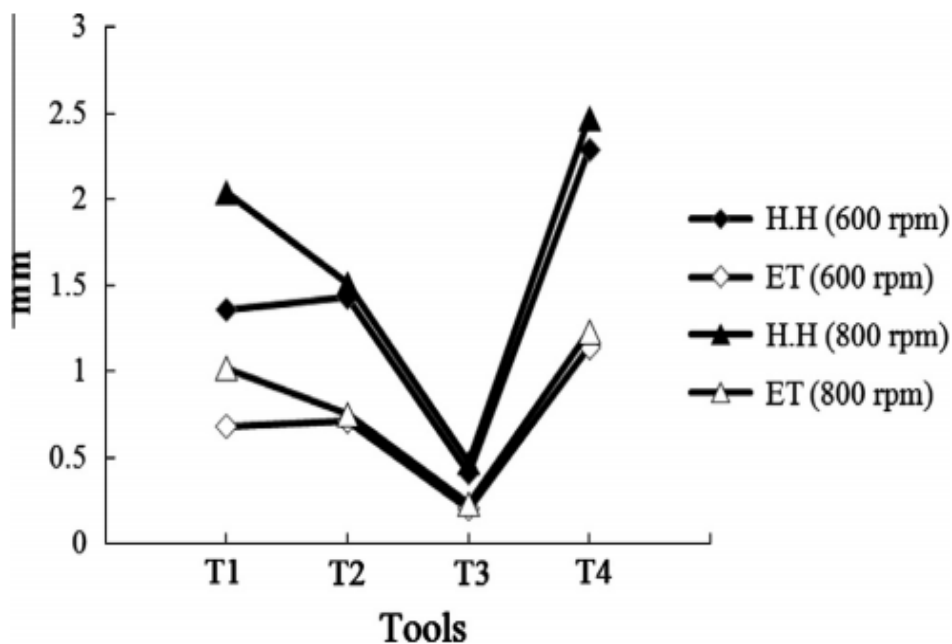


Figure 39 - Hooking height (HH) and lower plate effective thickness (ET) for the different tools [7].

Besides the hook height, even its slope is an important aspect to evaluate in order to get a good lap. As before the lower slope is obtained with tool T3, Figure 40.

When the tool T3 is used, the rotational spindle speed has no influence on hook height and slope and on ET.

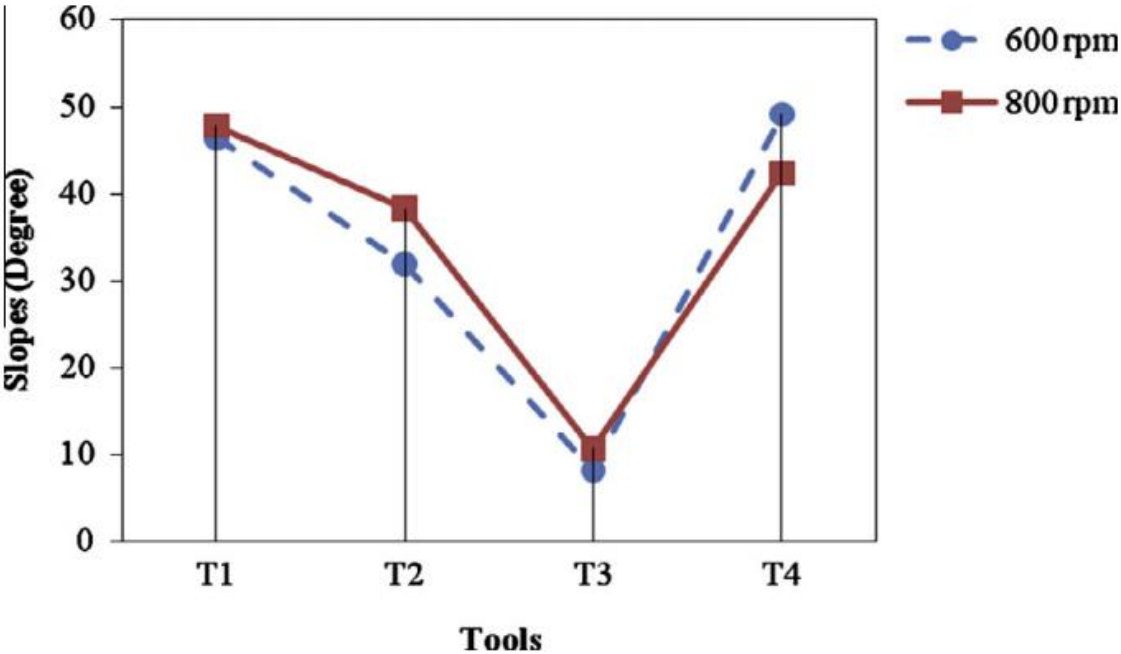


Figure 40 - Hook slope for the different tools [7].

Regarding the mechanical properties, the welded joint produced with tool T3 shows the best tensile properties compared to the other tools T1, T2 and T4, as it is demonstrated by the following Figure 41. The graph comes out after testing three different specimens for each condition.

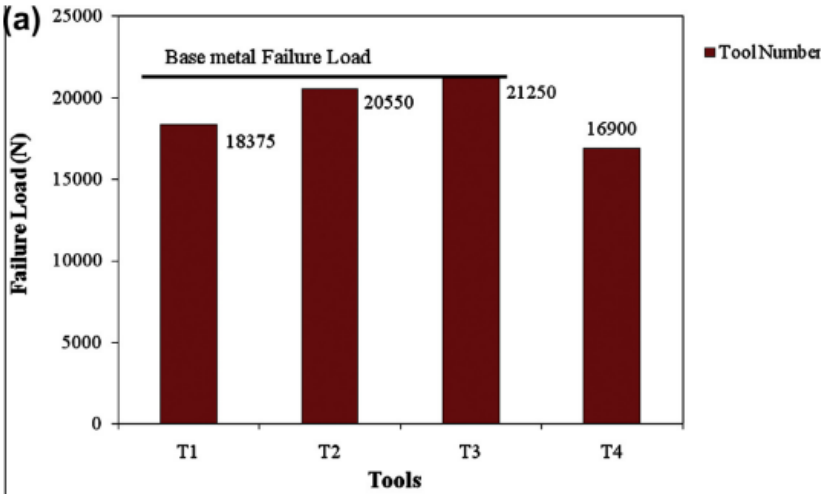


Figure 41 - Results of tensile test, 600 rpm rotational speed [7].

### 3.4.1 Tool Design: Suggested solution

Starting from the article explained before, the welding tool that proper fits the case study 1's working conditions and parameters is characterized by the same pin as the previous paper, stepped conical threaded pin, but all the dimensions must be arranged following what the literature suggests:

- The tool pin's length should be the 90% mm of the thickness of the workpiece (sum of thickness of the two pieces in case of Lap welding) [8].
- The shoulder to pin diameter ratio should range between 2:1 – 5:1 [8].
- The relation between plate thickness and shoulder diameter should be about 4 - 4,5 - 5 times bigger [9].

All welding tools' upper part must be the same because they all must match with the same single tool adapter described before.

So, as can be seen in the Figure 42, there are two grooves deep 1 mm and long 10.1 mm by means the connection with the tool adapter is performed thanks to the M5 studs.

Then a cylindrical part long 23 mm with a diameter of 16 mm and a final conical region long 7 mm up to the shoulder diameter.

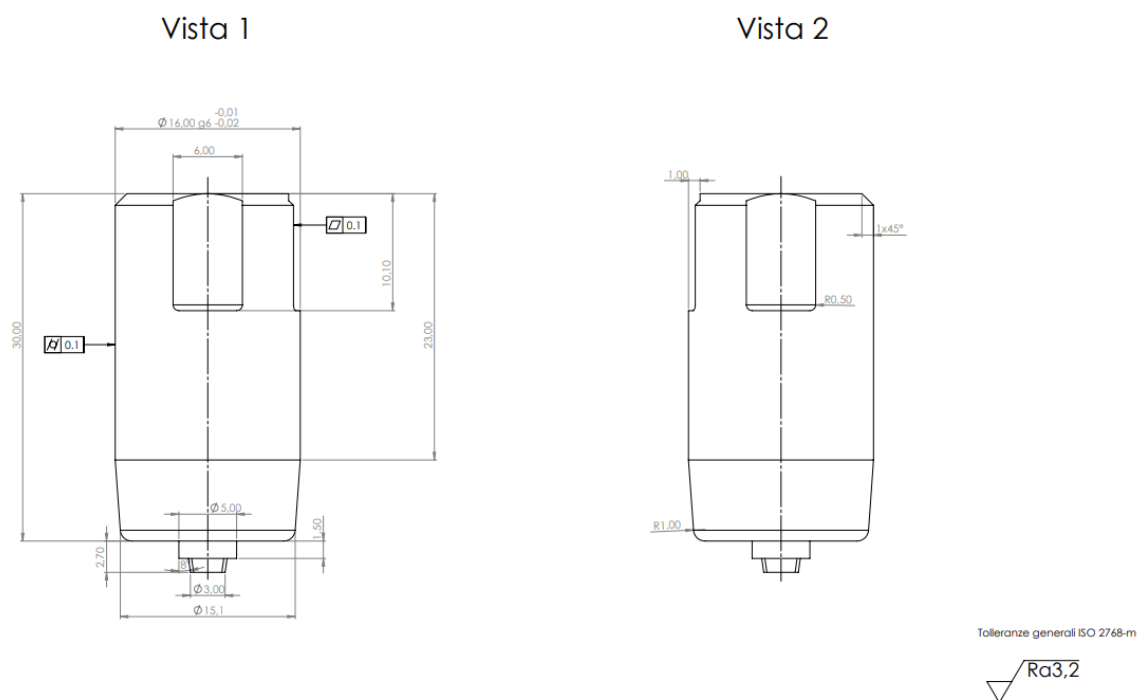


Figure 42 - Lap joint Welding Tool's 2D drawing.

The dimensions of pin and shoulder are computed as described here below.

The shoulder diameter is the five times the total thickness (1.5mm + 1.5 mm) and so it is equal

to 15 mm.

In the drawing is reported 15.1 mm as shoulder diameter because of the presence of junction R1.

The conical pin's diameter, the bottom part, is equal to the shoulder diameter divided by 5, while its total length is the 90% of the total thickness (3mm).

The other dimensions are reported in the 2D drawing.

Regarding the form and size tolerances, the approach used for the tool adapter is here repeated.

In Figure 43 is reported the Welding Tool's 3D Drawing done with CAD "SolidWorks".

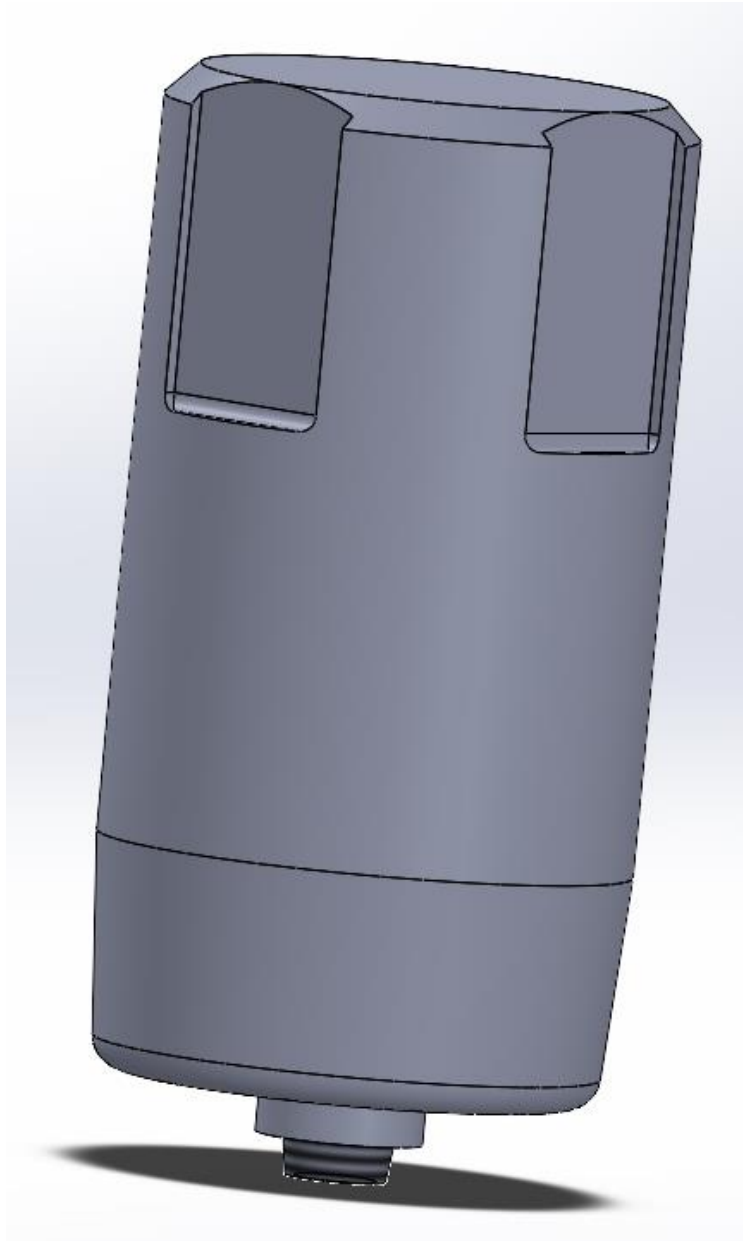


*Figure 43 - Lap joint Welding Tool's 3D drawing.*

### 3.5 Case Study 2: Butt Joint

The second case study consists of developing the proper tool to perform the butt joint of Aluminium alloys sheets with thickness 1.5 mm and 2.5mm. As did before, the analysis starts from a deep research in literature. For butt joint two welding tools, characterized by different features have been designed.

The reference article for designing the first type of butt joint welding tool is the one written by A. Scialpi et al. [6] in which the effect of different shoulder geometries on microstructural and mechanical properties have been evaluated welding 6082 T6 aluminium alloy with thickness 1.5mm.

The welding process is performed with 1810 rpm rotating tool speed and 460 mm/min traverse speed.

The three different shoulder geometries studied present scroll and fillet the first, cavity and fillet the second and only fillet the third one as reported in the Figure 44.

All the three tools are characterized by the same non-threaded pin with a 1.7 mm diameter and 1.2mm height.

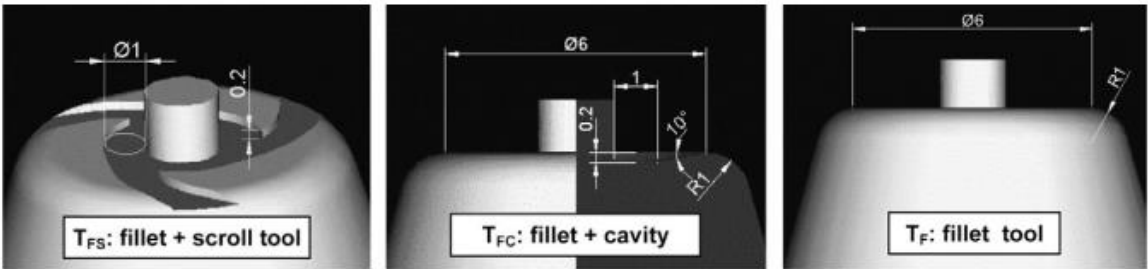


Figure 44 - Different tool shoulder geometries. Dimension in mm [6].

Among the various studies performed in the article, here are just reported some of them. Starting from the surface finishing, the tool with fillet and cavity gives the best quality results: the welding line surface appears very smooth and with very little flash, Figure 45.

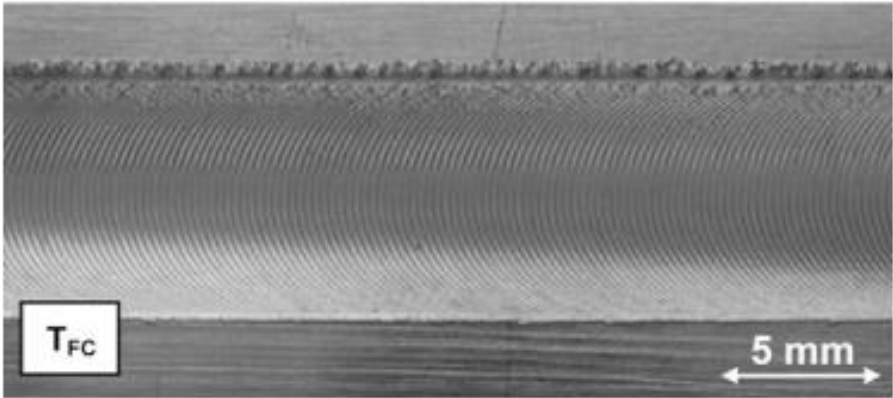


Figure 45 - Welding surface by Tool T<sub>FC</sub> [6].

Then, analysing the grain growth, as it is known, it depends on the amount of heat that reaches the different zones because the temperature is leading factor in the grain growth.

A higher heat input causes addition grain growth.

The heat produced is directly proportional also to the amount of shoulder’s surface in contact with the specimens: the higher the contact surface, the higher the heat produced and so the higher grain growth, Figure 46, and lower mechanical properties. In fact, in the nugget zone the highest harden is shown when the grain size is the smallest, so when tool  $T_{FC}$  is used, Figure 47.

Tool	Nominal contact surface (mm <sup>2</sup> )	Average grain size (μm)
$T_{FS}$	15.6	3.5
$T_{FC}$	13.4	2.8
$T_F$	29.8	3.9

Figure 46 - Nominal contact surfaces between shoulder and specimens [6].

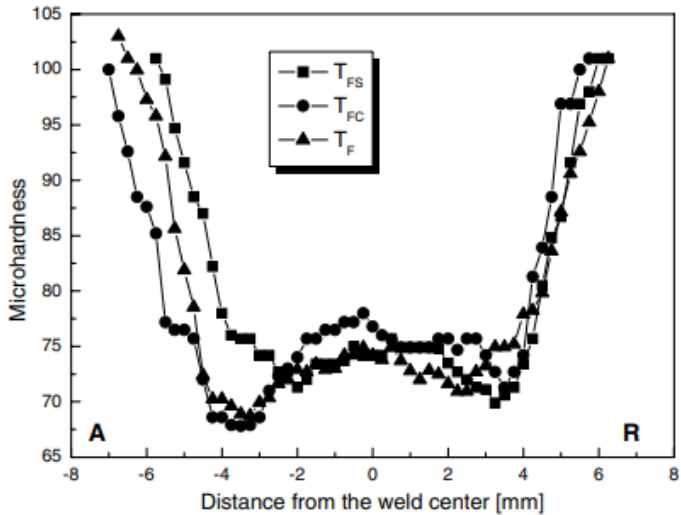


Figure 47 - Horizontal microhardness. "A" means advancing side, "R" retreating side [6].

### 3.5.1 Tool Design: Suggested solution

The first type of tool used for butt joint, whose zoom of the final region is reported in Figure 48, is the same used in article [6] and so, characterized by a shoulder with fillet and a cavity with an angle of  $10^\circ$  and a simple cylindrical pin. The dimensions vary depending on the thickness of the aluminium alloys sheets that is going to be welded. The theoretical dimensions, computed following the previous explained literature suggestions, are summed in the Table 10 below.

Tool for butt joint dimensions _ type 1		
Thickness	1.5 mm	2.5 mm
Shoulder diameter	6 mm	10 mm
Pin diameter	1.7 mm	3.7 mm
Pin Length	1.2 mm	2.2 mm

Table 10 - Dimensions of tool 1 for butt joint.

With respect to the theoretical dimensions, the shoulder diameter of the butt joint welding tool used to weld Aluminium Alloy with 1.5mm of thickness, is slightly bigger, 6.6mm, because of the presence of R0.8 and the conical region.

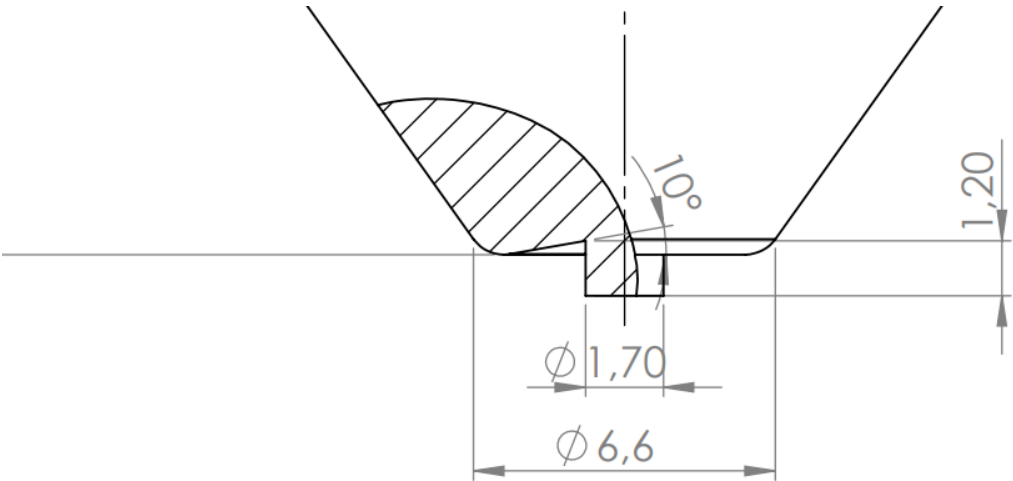


Figure 48 - Focus on shoulder and pin features.

The next figures 49 and 50 show the 3D drawing done with CAD “SolidWorks” and a detailed 2D drawing with dimensions and tolerances.

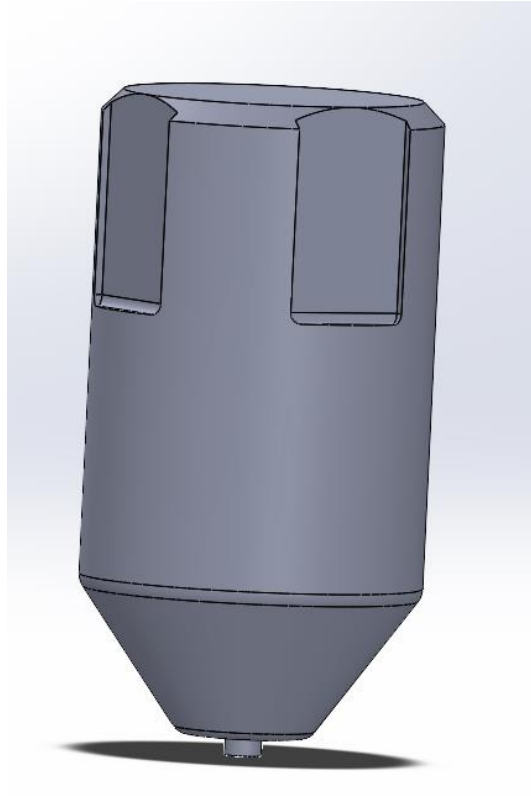


Figure 49 - Butt joint Welding tool's 3D drawing.

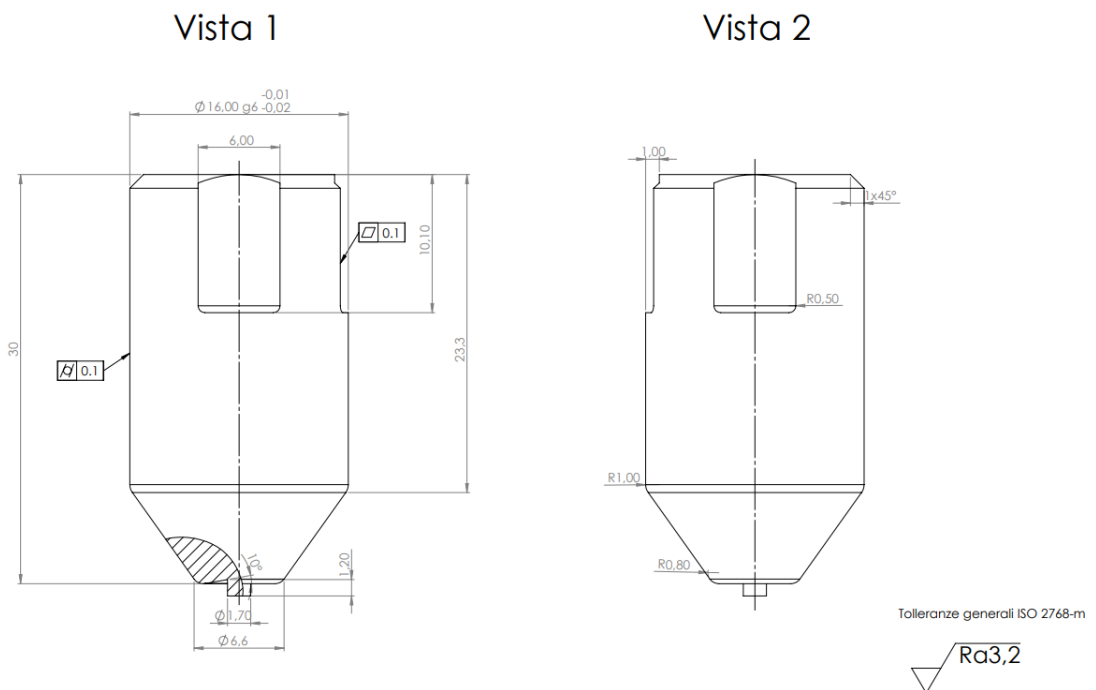


Figure 50 - Butt joint welding Tool's 2D drawing.

### 3.6 Case Study 3: Butt Joint

The case study 3 presents another possible tool design for Friction Stir Welding Butt joint. H.M. Anil Kumar et al. [9] wrote an article in which they studied how the tool parameters such as shoulder diameter, tool offset (distance from the weld center) and tool tilt angle affect the tensile properties (ultimate tensile strength, yield strength and % elongation). The friction stir welding process is done on aluminium 5083-H111 and 6082-T6 alloys with 4mm of thickness. The three different tools used, reported in Figure 51, are characterized by shoulder diameter of 16, 18,20 mm and scroll and a taper square pin with length of 3.4 mm and width of 3mm and 5 mm on the top and bottom surface respectively.



Figure 51 - Three different tools used [9].

The main results important to report here are about the tensile properties. From the analysis conducted in the paper [9] comes out that the tool that presents the best tensile properties, as seen in Figure 52, is the one with shoulder's diameter of 18 mm. This is due to the proper occurrence of dynamic recrystallization and the grain growth.

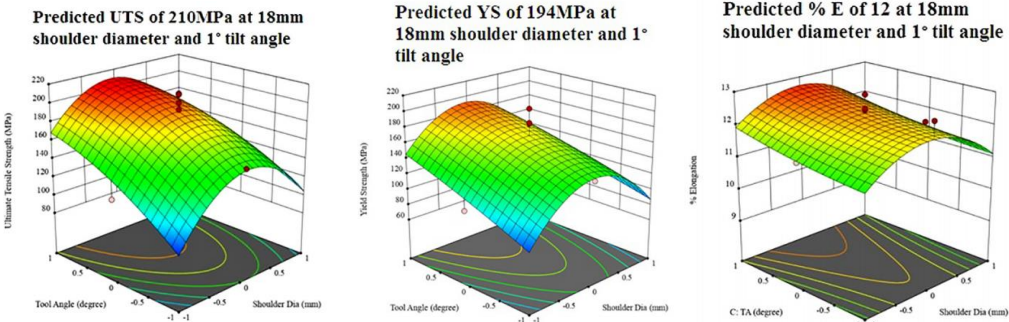


Figure 52 - Tensile properties with tool with shoulder diameter 18 mm [9].

### 3.6.1 Tool Design: Suggested solution

The article [9] gives the right suggestion to design another tool that allows to get good mechanical properties when butt joint is realized.

So, using the same features of the article, adding a spiral to achieve a better material flowing and rearranging the dimensions, the tool presents a spiral scroll shoulder and a tapered squared pin, whose detailed drawing is reported in the Figure 54, and the dimensions reported in Table 11.

Tool for butt joint dimensions type 2		
Thickness	1.5 mm	2.5 mm
Shoulder diameter	7.5 mm	12.5 mm
Pin major square length side	2 mm	3 mm
Pin minor square length side	1 mm	2 mm
Pin length	1.2 mm	2.2 mm

Table 11 - Dimensions of tool 2 for butt joint.

In the following, the Figures about Butt welding Tool used to weld Aluminium Alloy with 1.5 mm of thickness are reported.

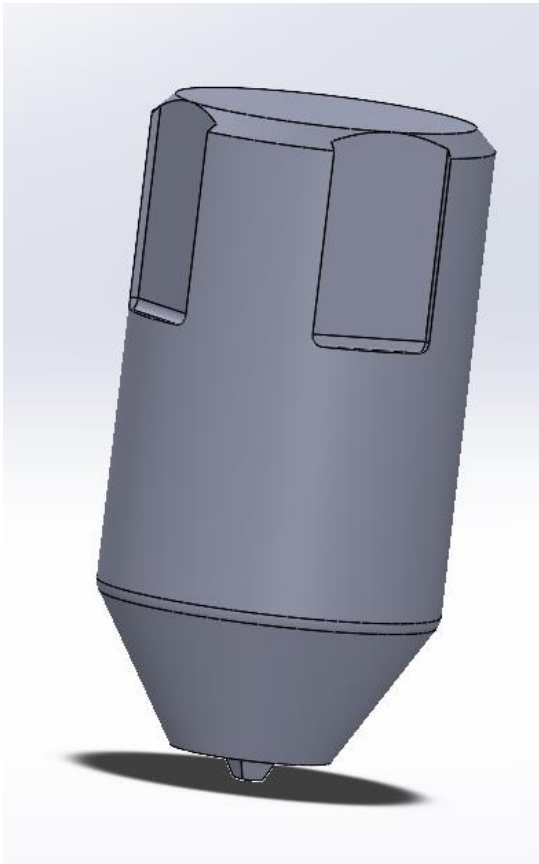
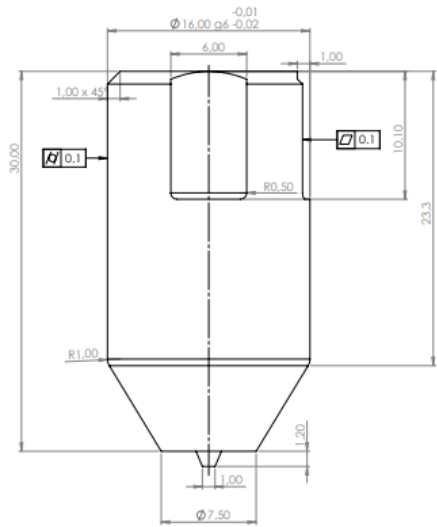


Figure 53 - Butt joint Welding tool's 3D drawing.

### Vista 1



Tolleranze generali ISO 2768-m  
 $\nabla Ra3,2$

### Vista 2

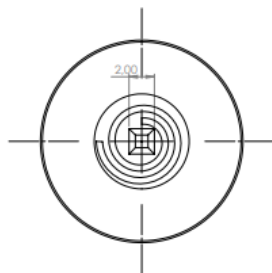


Figure 54 - Butt joint Welding Tool's 2D drawing.

The scroll is an important feature that could be adopted for the shoulder.

It consists of spiral groove cut starting from the shoulder diameter up to the pin one.

It enhances the vertical flow of the material and allows to use zero tilt, so a vertical tool without any inclinations.

Spiral channel increases the plastic deformation and the heat produced because of a higher contact surface.

The spiral groove adopted for the tool of Case Study 3 is 0.25 mm deep and is 1.6 mm far from the centre, as could be seen in Figure 55. It is characterized by a path of 1mm and 1.75 revolutions in order to cover all the shoulder region.

The reference article for building the proper scroll feature for Case Study 3's welding tool is the one written by Krishna Kishore Mugada et al. [18].

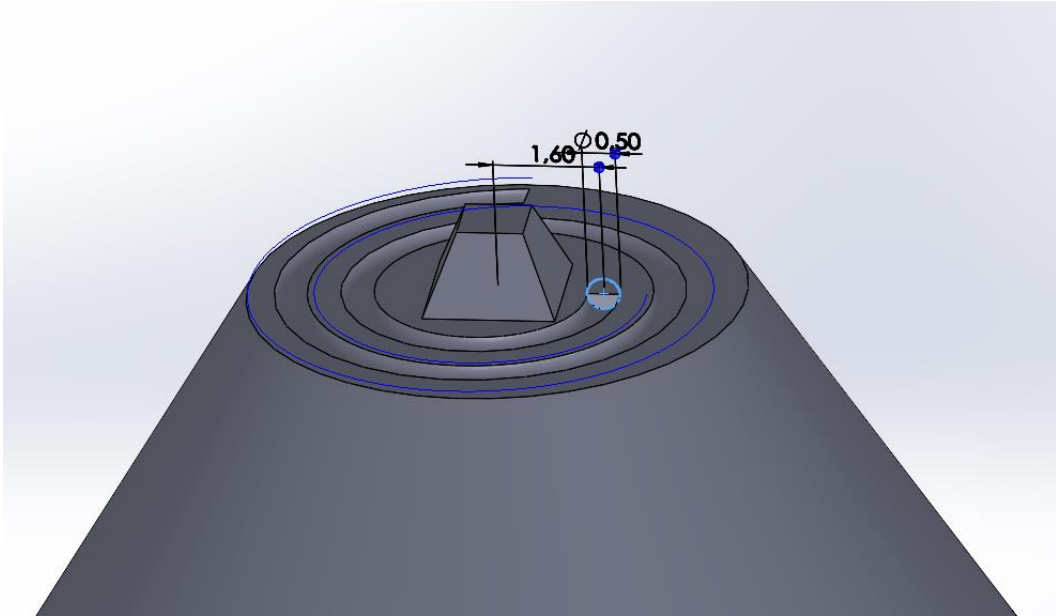


Figure 55 - Spiral channel for Tool Case Study 3

### 3.7 Static analysis of welding tool

The same procedure done for the tool adapter is repeated even for the welding tool. Since all the welding tools present the same upper part, the static analysis performed on section A and B is the same for all the cases study, while for section C has been chosen the worst condition, the one present in butt joint, Case study 2, Figure 56.

The sections analysed are depicted in the Figure 56.

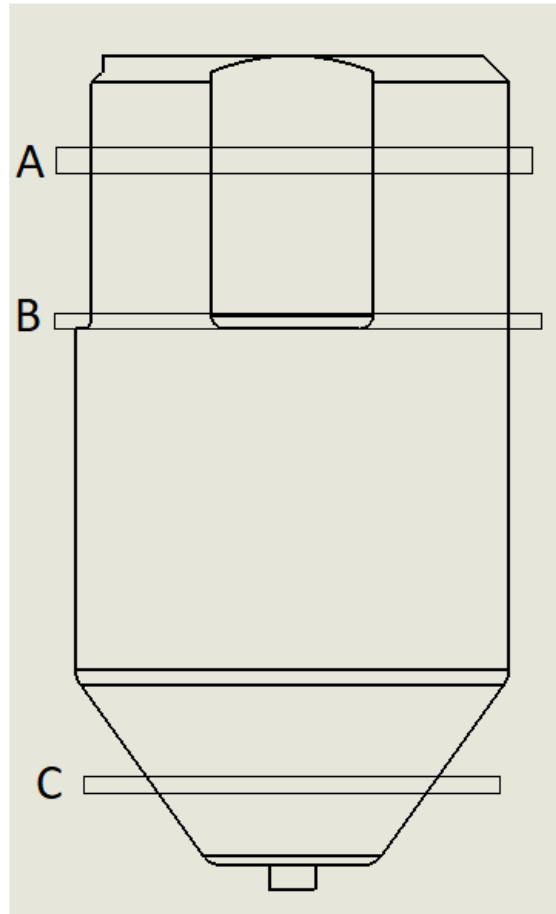


Figure 56 - Sections chosen for static analysis.

The material chosen for the welding tool is the same used for the Tool Adapter, H13 and its properties are summed in the Table 6. The allowable stresses are, as before:

$$\sigma_{adm} = \frac{\sigma_{yield}}{SF} = \frac{1000}{1.5} = 666.67 \text{ MPa}$$

And, consequently, using the Von Mises criterium, the shear allowable stress is:

$$\tau_{adm} = \frac{\sigma_{adm}}{\sqrt{3}} = \frac{666.67}{\sqrt{3}} = 384.67 \text{ MPa}$$

In each section the torque applied is:

$$M_t = 100000 \text{ N} * \text{mm}$$

### 3.7.1 Welding Tool-Section A

The first section decided to be evaluated from a static point of view is reported in Figure 57.

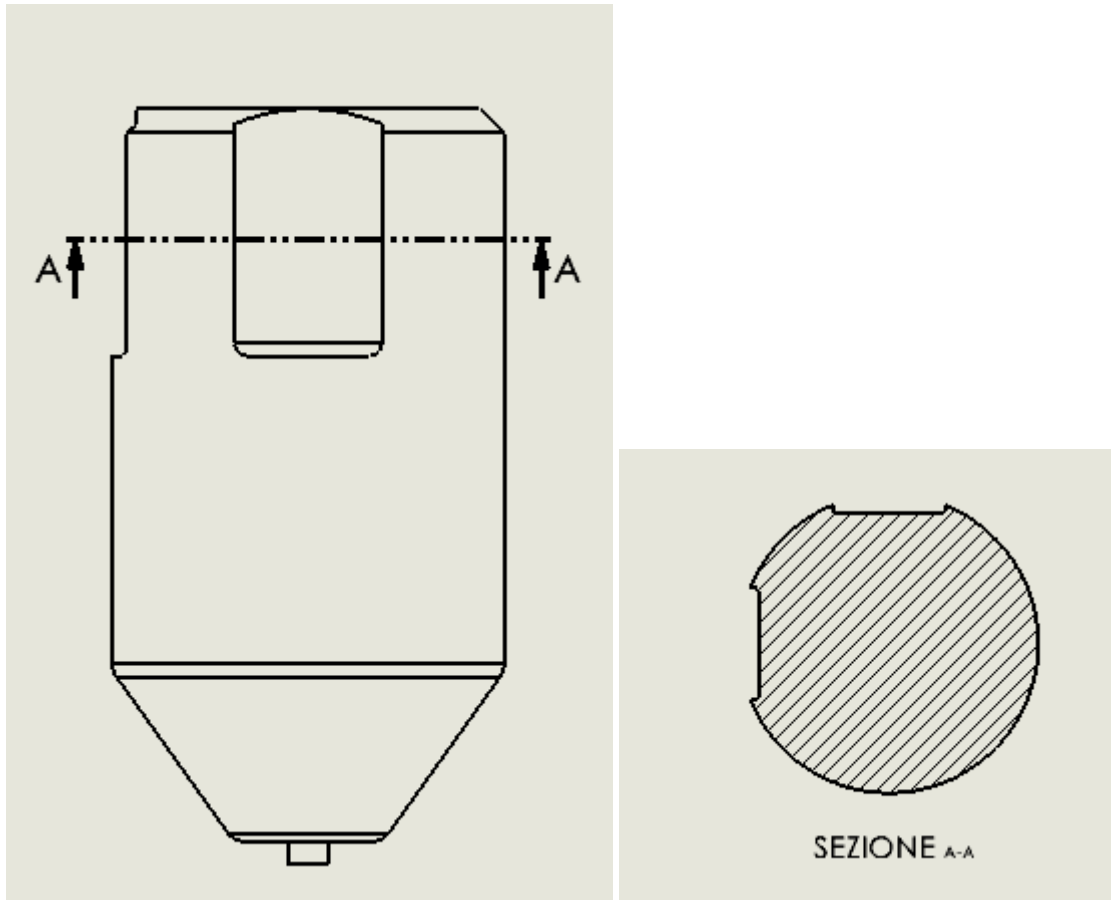


Figure 57 - Section A of the welding tool.

The diameter of the cross section chosen is  $d=14$  mm. In fact, following a conservative approach like before, the circular cross section considered with a diameter  $d$  is smaller than the actual one and in this way the presence of the two grooves is taken into account.

The maximum shear stress acting on the section is:

$$\tau_{MAX,A} = \frac{16 * M_t}{\pi * d^3} = 185.6 \text{ MPa}$$

Then, the comparison between the maximum shear stress due to torsion and the allowable shear stress is performed:

$$\tau_{MAX,A} < \tau_{adm}$$

The section A of the welding tool is able to withstand the stress due to the torque applied.

### 3.7.2 Welding Tool-Section B:

The section B is reported in Figure 58.

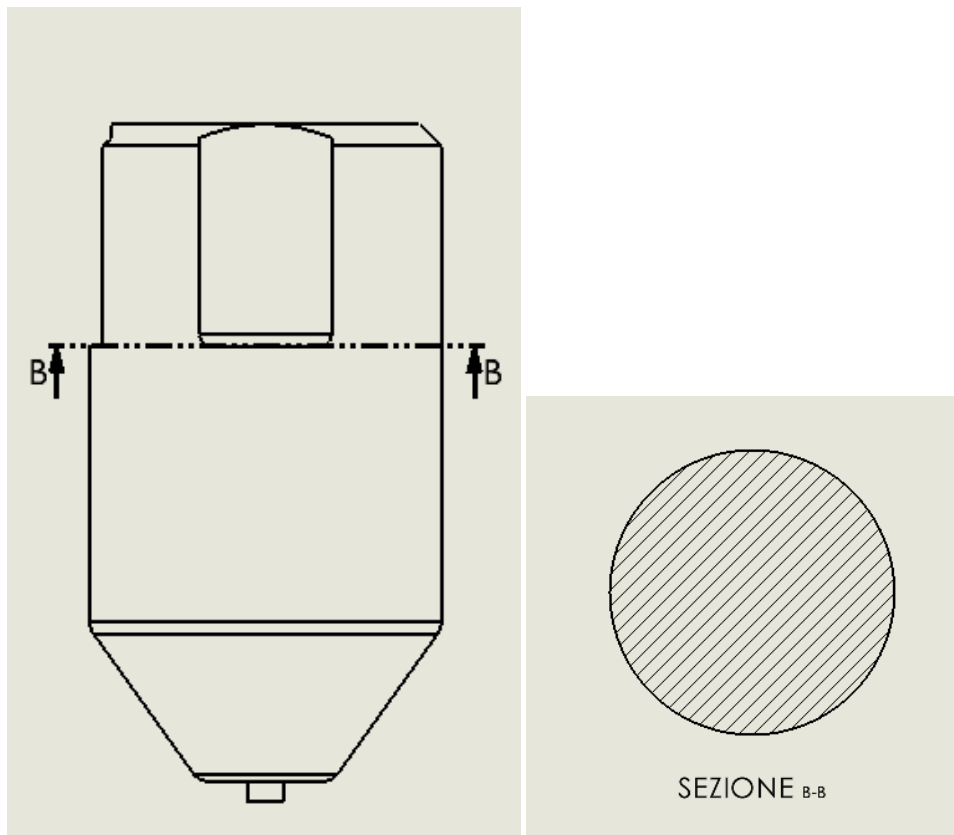


*Figure 58 - Section B for welding tool.*

The section B is characterized by the presence of two notches. Obviously, they lead to a local increase of stress that must be taken into account. For this reason, a stress concentration factor  $K_t$  is computed in order to evaluate the maximum local stress, even if, as wrote before, in the static analysis it has not so much influence.

The stress concentration factor depends only on the geometry and is determined by means the following graph, Figure 59. Even in this case, a conservative approach is pursuit since the reduction of cross section is not present all around the cylinder.

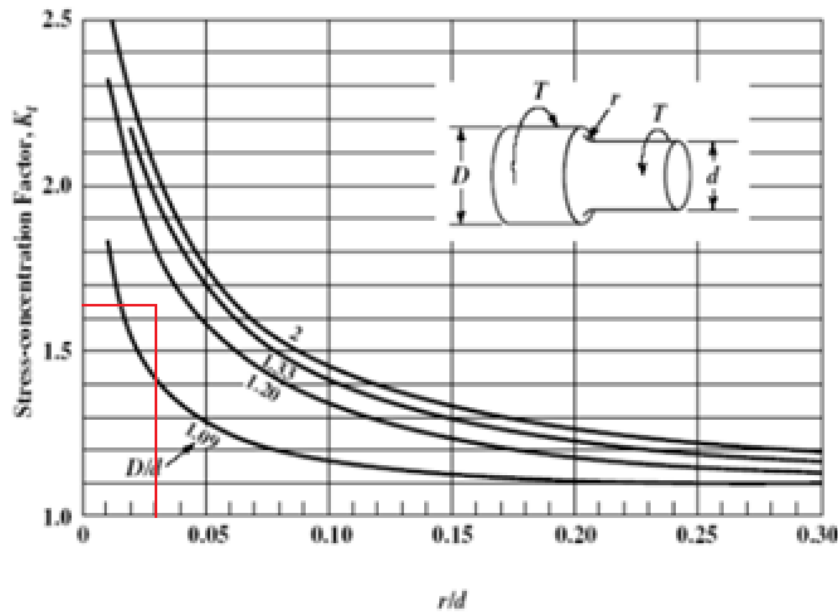


Figure 59 - Stress concentration factor  $K_t$  for shaft in torsion.

The data used to enter in the graph and determine the value of  $K_t$  are summed in the Table 12.

Major diameter	D	16 mm
Minor diameter	d	14 mm
Diameters ratio	D/d	1.14
Notch radius	r	0.5 mm
Ratio notch radius and minor diameter	r/d	0.03
Stress concentration factor	$K_t$	1.63

Table 12 - Data used for the computation of the stress concentration factor.

The maximum nominal value of the shear stress is:

$$\tau_{nom,B} = \frac{16 * M_t}{\pi * d^3} = 185.6 \text{ MPa}$$

The maximum shear stress considering its increment due to the presence of the notch is:

$$\tau_{MAX,B} = K_t * \tau_{nom,B} = 302.5 \text{ MPa}$$

Then, like what has been done for the section A, the comparison between the maximum shear stress due to torsion and the allowable shear stress is performed:

$$\tau_{MAX,B} < \tau_{adm}$$

The section B is able to withstand the tension due to the torque applied.

### 3.7.3 Welding Tool Section C

The section C, Figure 60, has been chosen in the middle part of the conical region where the torque is supposed to not be influenced by the working conditions.

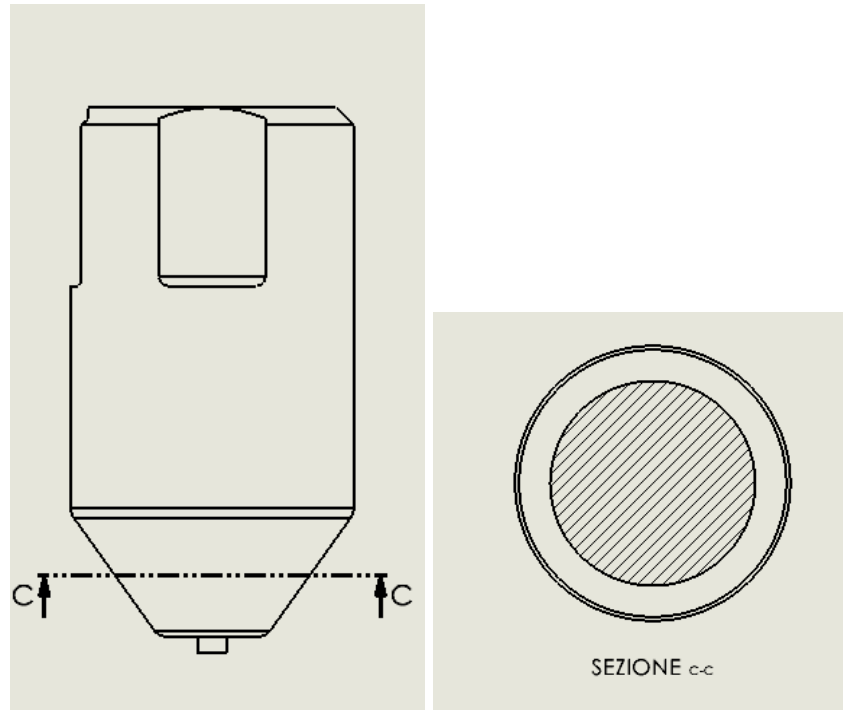


Figure 60 - Section C of the welding tool.

The section C is characterized by a circular cross section with diameter  $d=13$  mm.

The maximum shear stress produced by the action of the torque is:

$$\tau_{MAX,C} = \frac{16 * M_t}{\pi * d^3} = 231.81 \text{ MPa}$$

Even the last section is strong enough and is able to support the shear stress due to the action of the torque since:

$$\tau_{MAX,C} < \tau_{adm}$$

### 3.8 Deflection deformation of Welding Tool

The further analysis needed to be performed and verified is about the deflection deformation of the welding tool due to the force acting on the tip of it because of the motion of the working table where the pieces are fixed.

Considering the welding tool as a cantilever beam, so fixed at one end and free at the other, where the load is applied, the computation procedure starts imposing the maximum deflection allowable,  $f$ . It is defined, in case of welding tool used for butt joint of sheets with 1.5mm thickness, Case Study 1, as half of the diameter of the pin. So:

$$f = \frac{D_{pin}}{2} = \frac{1,7 \text{ mm}}{2} = 0,85 \text{ mm}$$

In this way it is possible to compute what will be the maximum allowable force acting in the process.

There are two main considerations important to underline. The first one is about which diameter consider in the computation since the welding tool presents even a conical region. The perfect way to proceed is integrating considering this change of diameter in the section modulus. However, in order to perform a simpler computation, a conservative approach has been adopted considering the smallest diameter, the shoulder one. The smaller is the diameter considered, the lower is the allowable force.

The second consideration is where to put the hinge for the computation of the deflection. The first hinge is put where the first hole for M5 is located. The total length from that point to the tip of the tool is  $l_1 = 23\text{mm}$ . Then the same computation is repeated considering a length of  $l_2 = 16 \text{ mm}$ , taking into account the second hinge.

The force  $F_1$  and  $F_2$  for the two hinges, considering the Young modulus equal to  $215000 \text{ N/mm}^2$ , the section moment of inertia  $J = \pi * \frac{D_{shoulder}^4}{64} = 63.617 \text{ mm}^4$  are:

$$F_1 = \frac{3 * f * E * J}{l_1^3} = 2866.62 \text{ N} \quad F_2 = \frac{3 * f * E * J}{l_2^3} = 8515.17 \text{ N}$$

### 3.9 Verification of M16 x 1,5 stud

The resistance class of the stud is 8.8. This means that the yield strength and the rupture strength are respectively:

$$R_{p0.2} = 640 \text{ MPa} \quad R_m = 800 \text{ MPa}$$

The nominal resistance circular section of this stud is  $A=167 \text{ mm}^2$ .

Considering the torque applied,  $M_t = 100000 \text{ N}\cdot\text{mm}$  and the radius of the adapter,  $r_{\text{adapter}}=16 \text{ mm}$ , it is possible to compute the force applied on the adapter:

$$F_{\text{adapter}} = \frac{M_t}{r_{\text{adapter}}} = 6250 \text{ N}$$

Now, in order to compute the shear stress applied on the stud, the Jourawsky formula for a circular section is used:

$$\tau_{\text{max}} = \frac{F_{\text{adapter}} * S}{J * b} = F_{\text{adapter}} * \frac{D^3}{12} * \frac{64}{\pi * D^4} * \frac{1}{D} = \frac{4}{3} * \frac{F_{\text{adapter}}}{A} = 49.9 \text{ MPa}$$

Where S is the static moment, J the moment of inertia and b is the length of the section that in the circular section is equal to the diameter.

Since the yield shear stress equal  $\tau_s = \frac{\sigma_s}{\sqrt{3}} = 369.28 \text{ MPa}$  is higher than the maximum shear stress acting of the stud's section, there is no problem of failure.

### 3.10 Verification of M5 stud

The same passages done before are repeated on M5 stud to verify if there could be any problem of failure due to the action of the shear stress.

The resistance class chosen for the stud is 10.9. This means that the yield strength and the rupture strength are respectively:

$$R_{p0.2} = 900 \text{ MPa} \quad R_m = 1000 \text{ MPa}$$

Considering the same torque applied before, and the tool radius,  $r_{\text{tool}}=10 \text{ mm}$ , the force acting on the tool and so on the two studs that connect the tool adapter and the welding tool is:

$$F_{\text{tool}} = \frac{M_t}{r_{\text{tool}} * 2} = 5000 \text{ N}$$

Then, the shear stress is computed, using the same formula for M16 stud:

$$\tau_{\text{stud}} = \frac{4}{3} * \frac{F_{\text{tool}}}{A_{\text{stud}}} = 469.483 \text{ MPa}$$

Where the nominal section area is equal to  $A=14.2 \text{ mm}^2$ .

Even in this case, the stud can withstand the shear stress acting on its own section since:

$$\tau_{stud} < \tau_s = 519.3 \text{ MPa}$$

## 4. Turning operation: overview

Turning operation is performed by means of a NC and CNC machine tool, like the lathe machine.

The operations performed on the lathe consists of having the workpiece fixed on a spindle by means of three or more contact points and lead to rotate on an axis, while a specific tool useful for the upgoing operation, rigidly held and supported in a tool post, cuts its unwanted material producing small chips and getting the right shape and dimensions, Figure 61.

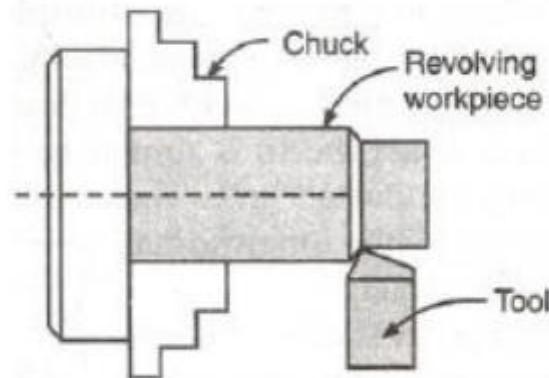


*Figure 61 - Turning operation [25].*

The main movements during turning operation are the rotary motion of the pieces going to be machined and the straight movement along the rotational axis of the cutting tool.

Numerical control NC is a method of automatically operating a manufacturing machine in which all the operations are driven by letters, numbers and special characters inserted in a part program. The last one is then translated into electrical signals that allow all the machine's motions.

The most recent machines have a computer on board (CNC machines) and can reach very high level of performance and greater accuracy and efficiency.

The CNC machine allows to overcome the human error, producing pieces with very little variation and making the productivity very high.

## 4.1 Lathe machine structure

The structure of a CNC machine must satisfy some requirements: deformation must not exceed the limits of load acting in machine structure, structure should ensure working stress, the connection between all the machine's components should present a high degree of accuracy. In order to ensure them, the machine should have a great stiffness since the higher the stiffness, the higher the accuracy. It depends on many aspects such as the material used, type of spindle, type of slideways and so on.

Furthermore, the dimensional accuracy of the part machined is ensured by the machine damping that should be good enough in order to reduce or delete vibrations inside the structure.

The machine tool structure, whose schematic drawing is reported in Figure 62, consists of five majors' parts [24]:

1. Headstock: It is located on the left side and it is made up of cast iron. Inside the headstock there are all the mechanisms needed to start and stop the machine, like motor, drive system, pulleys, back gears and so on.
2. Tailstock: It is located on the opposite side with respect to the headstock. It also consists of sub parts like tailstock spindle, lock wheel and so on. Its purpose is to support the other end of the workpiece.
3. Bed: It consists of two of four feet. It is fabricated using cast iron (mainly in the past) welded steel, polymetric concrete or a combination of them.
4. Carriage: It is between the headstock and the tailstock. It can slide along the bed by means of sliding friction slideways, anti-friction slideways or pressurized slideways allowing the cutting tool to cut away the material as it moves.
5. Feed mechanism: Servo drive mechanism in a CNC machine consisting of command feeder, a command controller and a feedback mechanism in a close loop system.

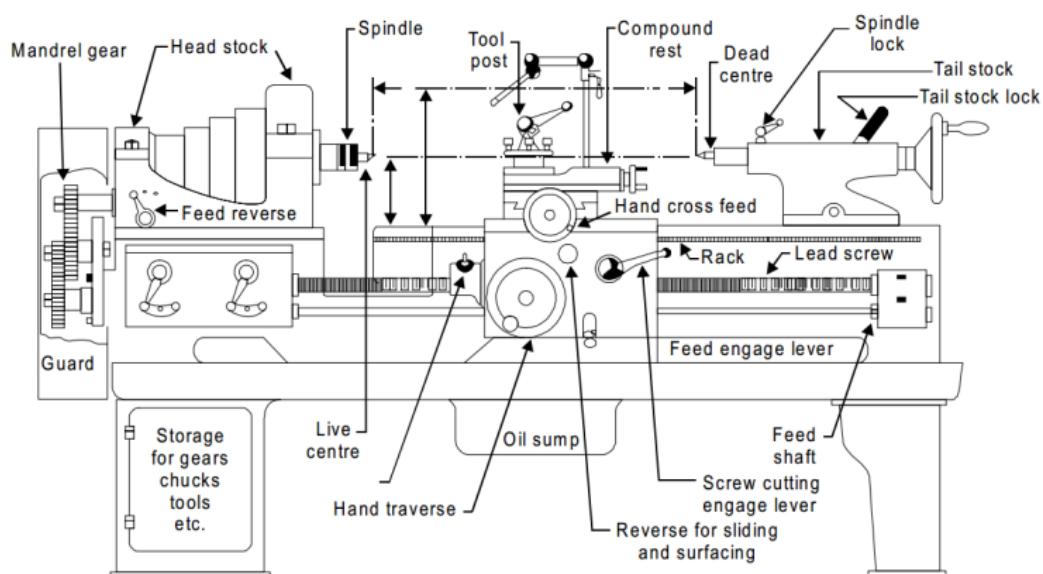


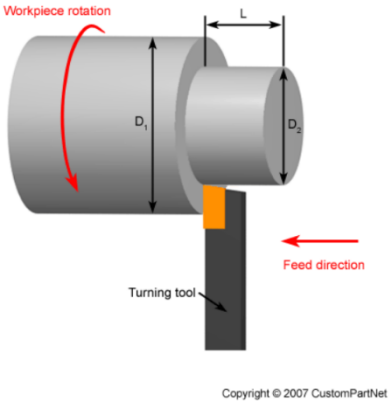
Figure 62 - Lathe machine [24].

The machine tool should withstand the static load (weight of the different machine's parts), thermal load (deformation coming from a thermal stress), and the dynamic load that could be produced by forced vibrations from environment or other parts of the machine and by self-excitation from the interaction between the cutting process and the structure of the machine tool.

## 4.2 Operations

The lathe machine allows to perform a large variety of operations that could be classified as external or internal. For each of them a proper cutting tool should be used. Here below some of them are briefly described.

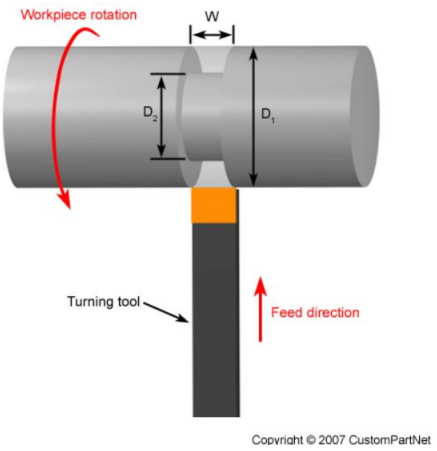
- Turning



A turning tool moves axially while the workpieces is rotating. Multiple passes are made until the right diameter has been obtained.

Figure 63 - Turning operation [27].

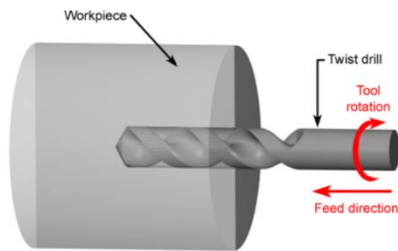
- Grooving



The tool moves radially while the workpiece rotates. A groove with the same width of the tool is machined.

Figure 64 - Grooving operation [27].

- Drilling



The workpiece is fixed and still, while the tool rotates and moves axially creating a hole with a diameter equal to that of it.

Copyright © 2007 CustomPartNet

Figure 65 - Drilling operation [27].

## 4.3 Cutting parameters

### 4.3.1 Cutting speed and depth of cut

The cutting speed has a big influence on tool life that greatly affects the manufacturing costs. The Taylor's equation relates the cutting speed and the tool life:

$$V * T^n = C$$

Where T represents the tool life in minutes, V is the cutting speed in m/min, C and n are constant values that depend on the tool material and the workpiece.

Tool material	n	C (m/min)
<b>High speed steel</b>		
Non-steel work	0.125	120
Steel work	0.125	70
<b>Cemented carbide</b>		
Non-steel work	0.25	900
Steel work	0.25	500
<b>Ceramic</b>		
Steel work	0.6	3000

Figure 66 - Constant values for Taylor's equation [26].

Even the depth of cut influences the tool life, and they are related by the following equation [26]:

$$V_c * T^n * X * d^x * f^y = C$$

Where  $V_c$  is the cutting speed,  $T$  is the tool life,  $d$  is the depth of cut,  $f$  is the feed rate,  $x$  and  $y$  are determined experimentally.

A high depth of cut leads to high vibrations, and on the other hand, a low depth of cut leads to a surface hardening.

The other parameters, divided in Machine Parameters and Job Parameters are summed in the following Table 13:

Machine Parameters	Job Parameters
Feed rate	Length of cut
Rigidity of Machine	Cutting tool materials
Machine/spindle power	Tool geometry
Spindle speed	Depth of cut
	Coolant
	Cutting speed

Table 13 - Cutting parameters.

The cutting speed has influence on roughness grade, the amount on material removed, the temperature of the cutting tool that reduces its hardness and so on.

After determining the cutting speed, the next step consists of determine the rotational spindle speed by means of the following equation or using graphs:

$$n = \frac{1000 * V_c}{\pi * D}$$

Pardeel Kumar et al. [30] studied the influence of five input parameters such as Cutting speed ( $V_c$ ), Feed rate ( $f$ ), Depth of cut ( $ap$ ), Nose radius (NR) and work piece Hardness (H) to minimize the surface roughness, using the Response Surface Methodology (RSM), in a dry turning with CNC lathe of 5000 rpm.

The material machined is AISI H13, the same material used to produce the tool adapter and the various welding tools, in the form of round bars with 50mm of diameter and 150mm of length, while the cutting tool used is polycrystalline cubic boron nitride (PCBN) because of its ability to maintain a workable cutting edge at elevated temperature, good thermal resistance and high coefficient of thermal conductivity.

As it is possible to see on the Figure 67 below, the best surface roughness is achieved when it is used the lowest feed rate and the highest cutting speed. Depth of cut as almost no influence in the surface roughness.

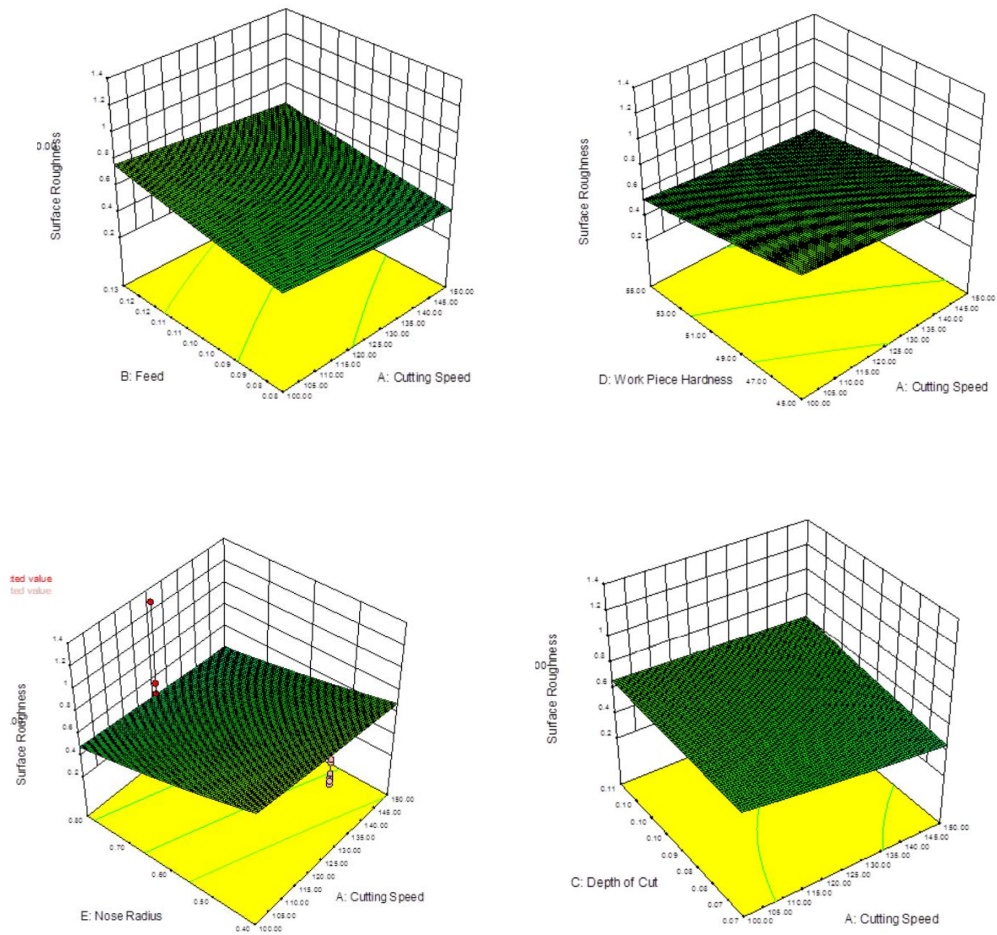


Figure 67 - Effect of cutting speed, feed rate, depth of cut, nose radius and work piece hardness on the surface roughness [30].

Table 14 shows the optimal values of cutting parameters to get the best surface roughness (Ra):

Parameters	Goal	Optimum conditions					Surface Roughness	lower	upper	Desirability
		v (m/min)	f (mm/rev)	ap (mm)	NR (mm)	W/P Hardness				
Ra	Minimum	150.00	0.08	0.07	0.8	45	0.230378	0.18	1.91	0.965

Table 14 - Optimization parameters [30].

# 4.4 Cutting Tools

Cutting tool is used to remove material from the workpieces through shear deformation. In turning operation, it is typically a single-point cutting tool, Figure 68:

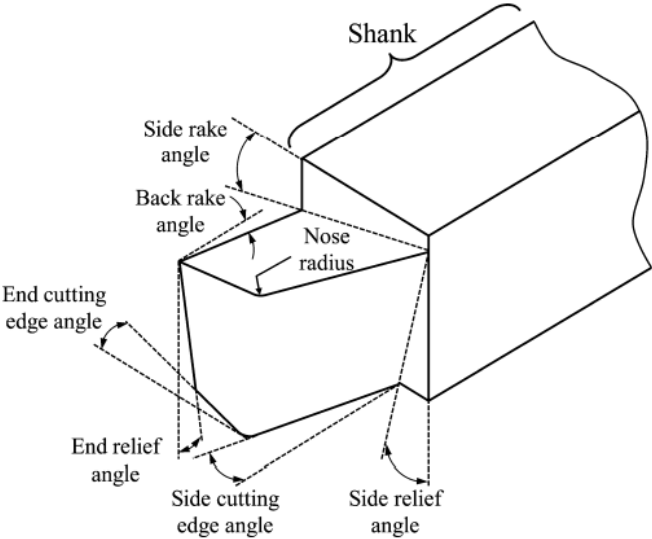


Figure 68 - Single point cutting tool [31].

It could be a single piece of metal or can present at the end side of a rectangular tool shank an insert that could be a square, triangle, diamond shaped piece and with different nose radius. [27].

Some examples of them are reported in the Figure 69, where it is possible to see inserts that differ one to the other by nose radius and shape depending on the type of operations needed to be performed.

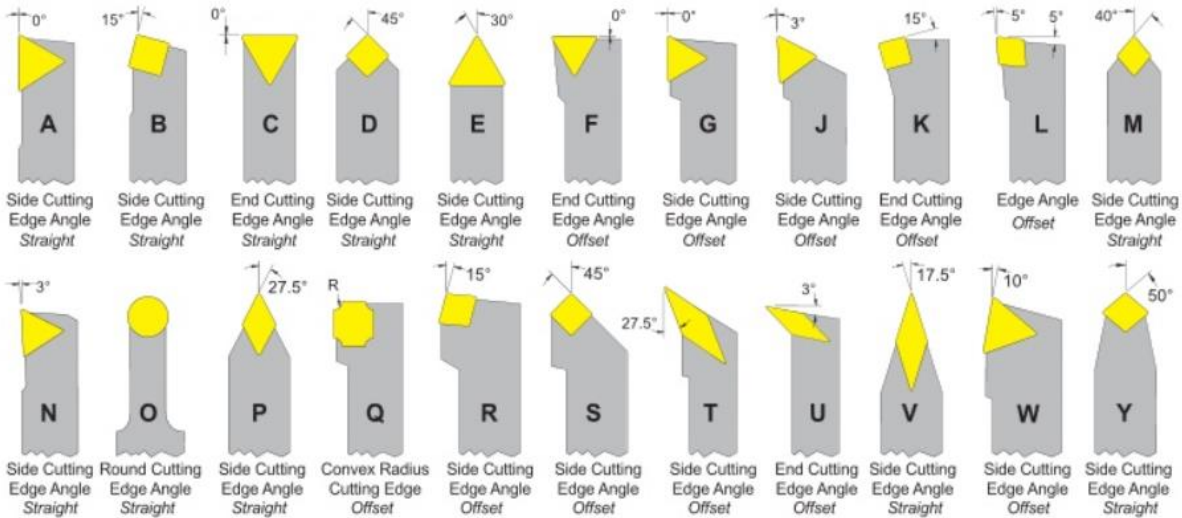


Figure 69 - Different types of insert [33].

It must be made of material harder than the material which is going to be cut and the tool must be able to withstand the heat generated in the cutting process.

Furthermore, also the geometry of the tool is very important, in fact it should have clearance angles designed so that only the cutting edge is in contact with the workpiece.

The selection of a specific tool is driven by the following information [26]:

1. The starting and finished part shape.
2. The work-pieces hardness.
3. The material's tensile strength.
4. The material's abrasiveness.
5. The type of chip generated.
6. The working holding setup.
7. The power and speed capacity of the machine tool.

The ideal cutting tool should present the following properties [26]:

1. Harder material than the piece that is going to be machined.
2. Higher temperature stability.
3. Resistant to wear and thermal shock.
4. Impact resistant.

The main tools used in turning operations are summed in the following Figure 70.

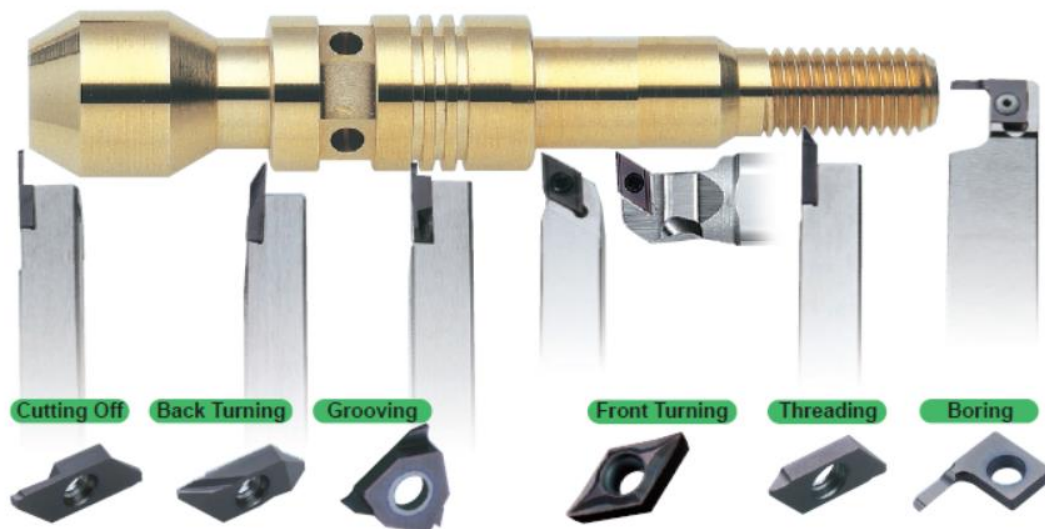


Figure 70 - Different types of Turning tools' insert [32].

## 4.4.1 Cutting tool's materials

The cutting tools material depends on many factors such as the material workpiece, cost and tool life.

The most important properties that a material used for cutting tool must show are hardness, toughness, cold hardness, high thermal conductivity, low friction coefficient and resistant to wear.

Among all possible materials that could be used for producing the tool, the most important and used are here summed [27]:

1. High-speed steel (HSS)
2. Carbide.
3. Carbon steel
4. Cobalt high-speed steel
5. Ceramics.

In order to increase the tool life and to improve tool's performance, sometimes they are coated with thin layers of tungsten carbide, WC, that increases the wear resistance, but reduces tool strength, or titanium carbide, TiC, titanium nitride, TiN, aluminium oxide,  $Al_2O_3$ .

Tungsten carbide tools are commonly used to machine steel.

The graph reported in the following Figure 71 show the relation between hardness and toughness of the various materials that could be used for the cutting tools.

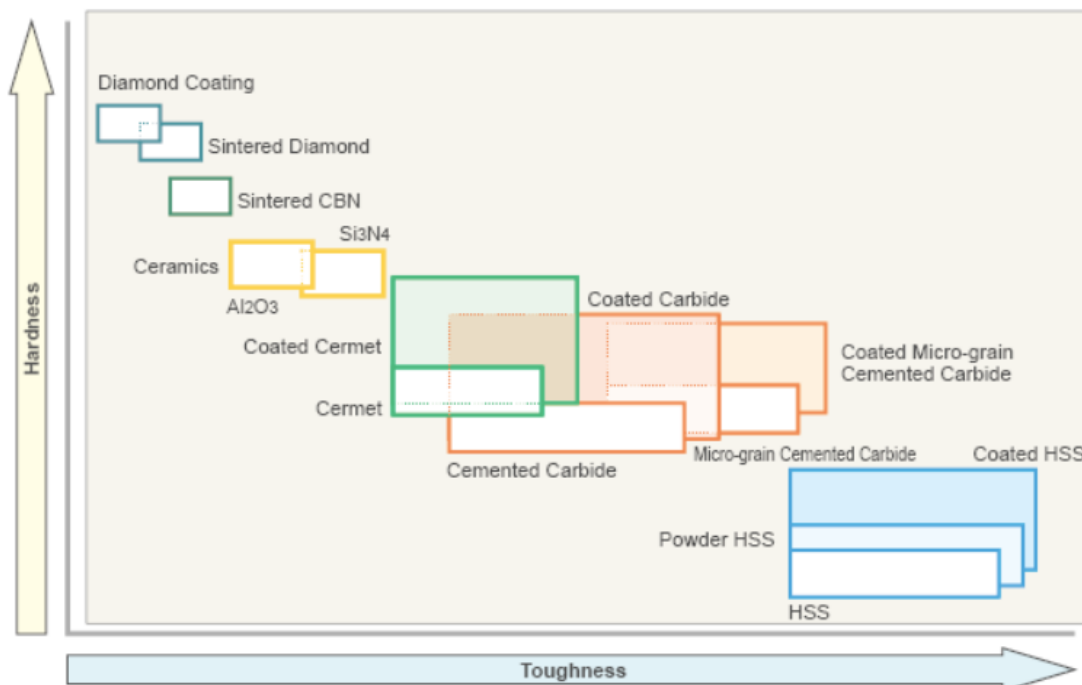


Figure 71 - Relation between hardness and toughness of the main materials used for cutting tools [28].

The hardness versus temperature graph for different cutting tools' materials is reported in Figure 72.

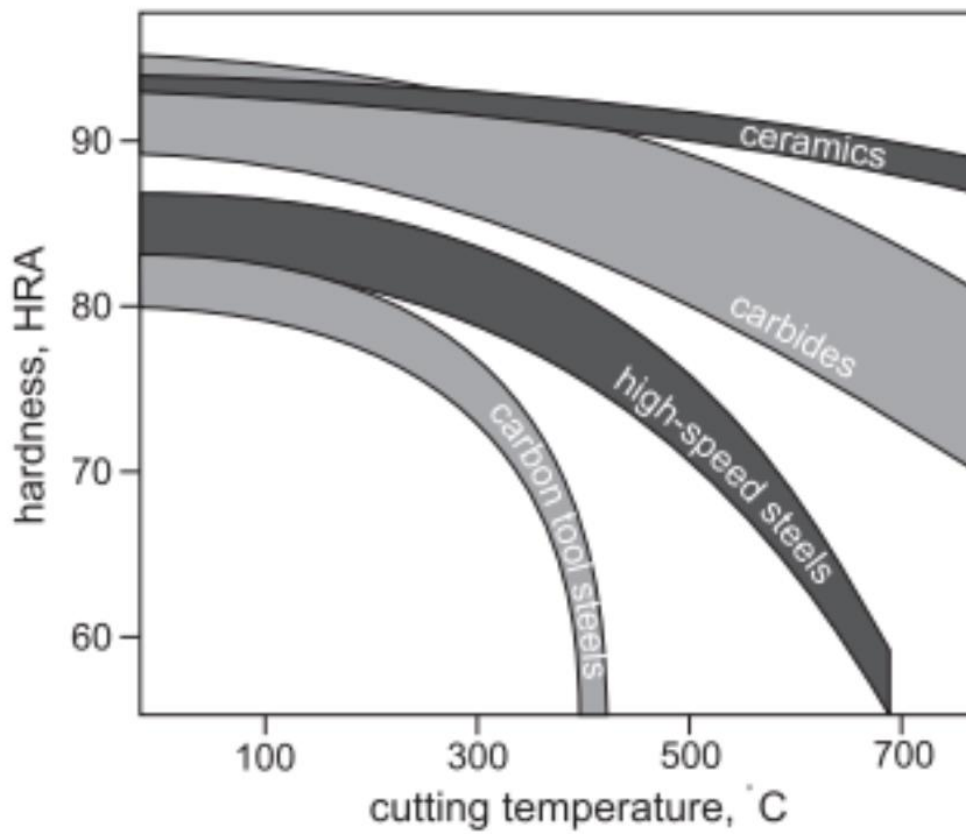


Figure 72 - Hardness vs Temperature graph for different cutting tools' materials [29].

## 5. Milling operation: overview

The milling operation is performed in the production of the Tool Adapter when the groove and the four holes for M5 stud have to be machined.

For this reason, a brief explanation of the milling operation and its main tools used is important to report.

Milling is a process in which a specific rotating cutting tool removes materials from a workpiece, that is fixed on a working table able to move, giving to it the wanted shape.

As described for the turning operation, the desired workpiece is obtained after a series of operations that start with roughing, in which a high amount of material is removed and end with the finishing one, where the level of accuracy required is achieved.

During working process a coolant should be used because the heating of both cutters and material machined could lead to damage and distortions.

### 5.1 Milling machine

The milling machine could be vertical or horizontal with them own characteristics, as can be seen in the Figure 73 below. The main difference between them is the machine spindle orientation.

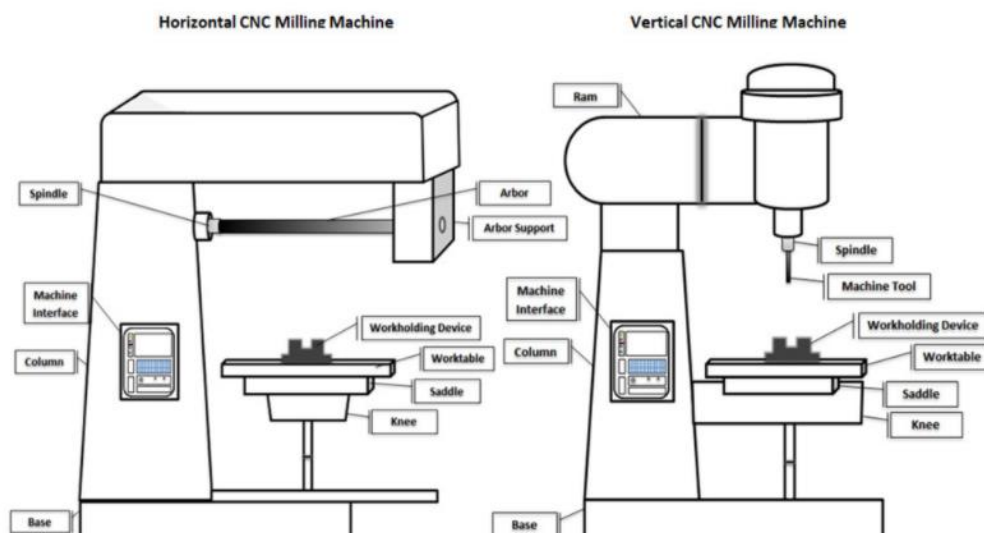


Figure 73 - Horizontal and Vertical Milling machine [35].

The main components shared by both are [35]:

- Machine interface: it allows the operator to set and evaluate all the parameters that must be set to work properly the components.

- Column: it supports the working load and avoids the collapse of the machine.
- Knee: it could adjust the Z-axis position required for the milling operations and sustains the saddle and the worktable.
- Saddle: it allows a horizontal movement of the worktable.
- Worktable: it presents a clamping system to fix properly the workpiece.
- Spindle: it is arranged on a horizontal or vertical axis depending on the type of milling machine. It holds the cutting tool forcing it to rotate. It is driven by an electric motor presents in the column.
- Arbor: it is a shaft inserted into the spindle in which tools for horizontal milling operations could be mounted on. It guarantees additional stability.

## 5.2 Operations

The milling machine allows to make different types of operations depending on what shape the component need to get.

Some of them are here reported and briefly described.

- Plain Milling: It is performed to realize a flat surface. In this operation, also known as slab milling, the axis of the cutting tool is parallel to the machined plain surface. The depth of the cut and its accuracy is regulated by moving the worktable or by selecting a specific tool.

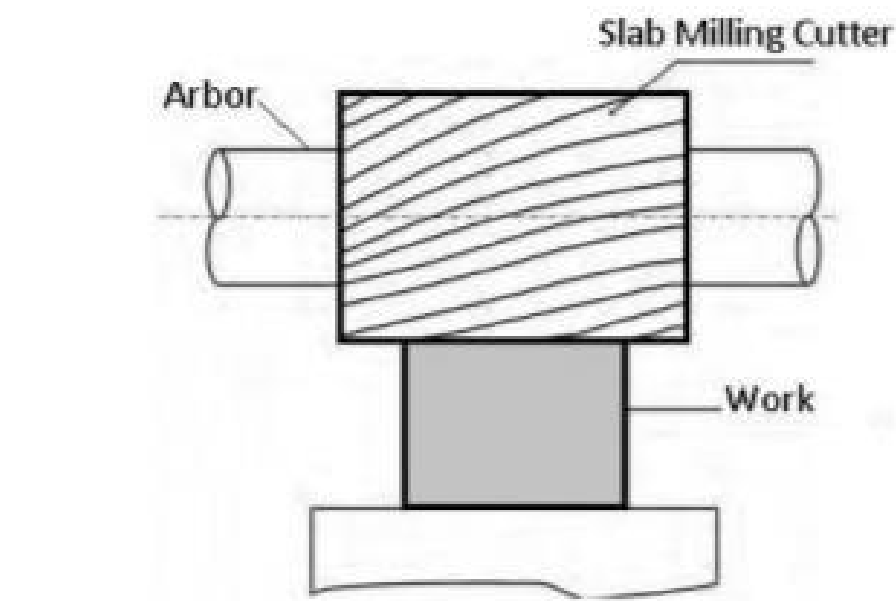


Figure 74 - Plain Milling Operation [36].

- Face Milling: The axis of the tool is perpendicular to the workpiece going to be machined. The tool used, called face milling cutter, in this operation presents teeth on both periphery and tool face [35].

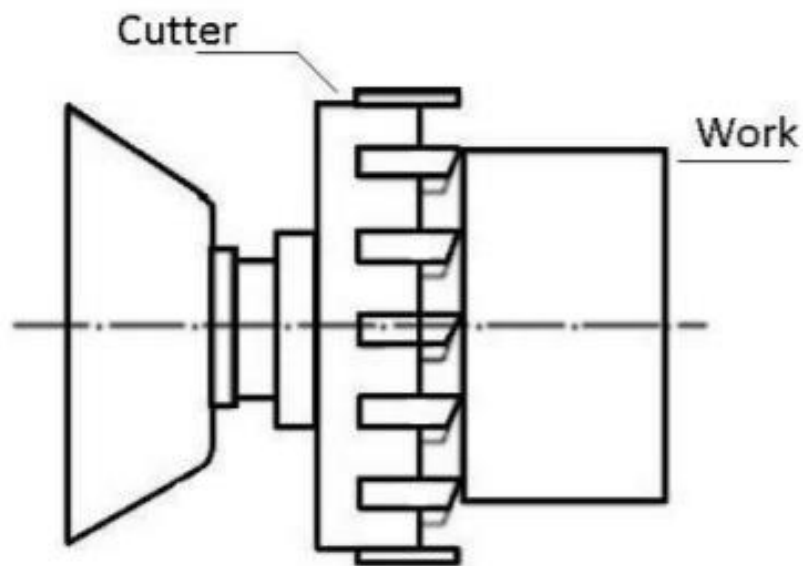


Figure 75 - Face Milling Operation [36].

- Straddle Milling: This operation consists of having two cutters placed on the arbor so that, simultaneously, can machine two sides of a single workpiece.

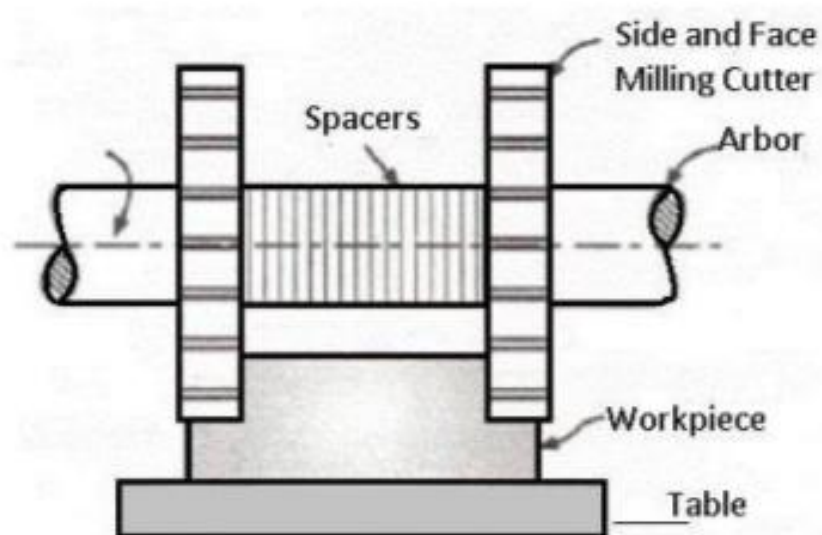


Figure 76 - Straddle Milling Operation [36].

- Angular Milling: This operation allows to produce grooves, whose angle depends on the type of contour of the angular cutter used.

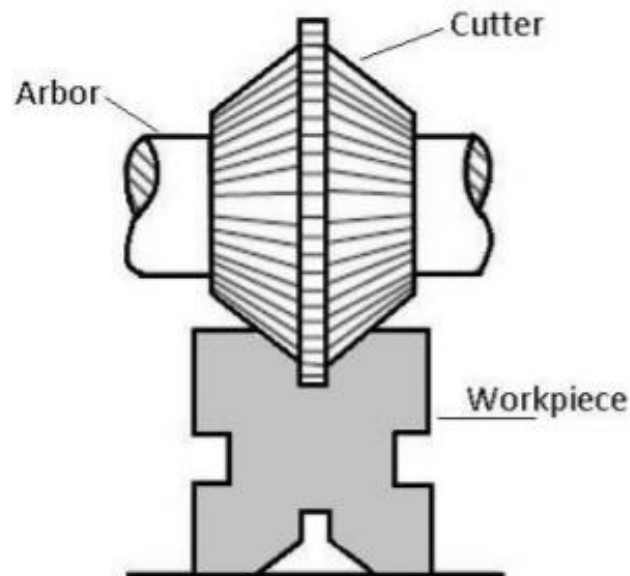


Figure 77 - Angular Milling [36].

Other operations could be: Form milling, Profile milling, End milling, Saw Milling and so on.

## 5.3 Milling parameters

The main parameters needed to be set in order to get a well machined workpiece are [37]:

1. The rotational spindle speed,  $n$  [rpm].
2. Diameter of the tool,  $D_c$  [mm].
3. Cutting speed,  $v_c$  [m/min].

$$v_c = \frac{\pi * D_c * n}{1000}$$

Higher the cutting speed, higher the amount of products realized (productivity) and better the surface finishing.

Its value depends on the type of workpiece's material and it could be chosen from tables, like the one reported here below.

Material to be machined	High speed steel	Cemented carbide	ISO Grades
Unalloyed steel C<0.8%	16 - 24	120 - 690	P
Low-alloy steel	14 - 20	90 - 450	P
High-alloy steel	12 - 18	65 - 335	P
Stainless Steel	Not suitable	45 - 300	M
Cast Iron	14 - 20	85 - 600	K
Non-ferrous metals	50 - 180	1000 - 1300	N
Heat Resistant Material	Not suitable	220 - 1300	S
Hardened Material	Not suitable	40 - 80	H

Figure 78 - Suggested Cutting speed [m/min] used in milling operations [40].

4. Feed speed,  $v_f$  [mm/min].

$$v_f = f_f * n$$

5. Feed per blade/tooth,  $f_z$  [mm/tooth].

$$f_z = \frac{f_f}{z}$$

It has consequences in the chip thickness and determines the surface finishing.

6. Feed per revolution,  $f_r$  [mm/rev].

7. Width and depth of cut [mm].

The steps required to be performed for determining the right machining parameters start with the analysis of the workpiece material, then, depending on it, and on which type of machining operation is going to be done (roughing, shaping, or finishing), the milling cutter is selected. After that, the selection of the cutting speed,  $v_c$  and of the feed per blade,  $f_z$ , by means of catalogue, and the machine parameters  $n$  and  $v_f$  are set. Finally, depending on the machining efficiency the width and depth of cut are determined.

## 5.4 Milling Tools

The milling tools are characterized by different cutters depending on which type of operation it is going to be done and which shape and size the component should get.

The materials of the milling tools are similar to the ones use for turning tools like High-speed steel, cemented carbides, carbon steel, ceramics and so on.

They should present hot hardness and wear resistance.

The most used tools that here will be reported are [38]:

- End Mill Tool: during the cutting process the end mill tool works both with the end and the sides of the cutters, so they can cut axially and laterally.

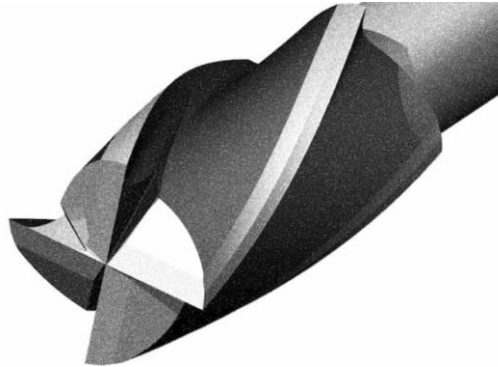


*Figure 79 - End Mill Tool [38].*

- Slab Mill: their most use is in roughing operation, so when large amount of material is going to be removed.



*Figure 80 - Slab Mill Tool [39].*

- Roughing end mill: it is similar to end mill tool. By the way, the only difference complies with the presence of jagged teeth that allows to have a cutting process faster and less accurate that results in a rough surface finishing.



*Figure 81 - Roughing End Mill Tool [38].*

- Thread mill: it is used to produce tapped holes. The creation of a finer and accurate thread depends on the type of cutter used.



*Figure 82 - Thread Mill Tool [38].*

Other examples of cutting tools used to get workpiece with different shape in milling operations are summed in the following Figure.



Figure 83 - Types of Milling Cutters [39].

## 6. G-code

The Tool Adapter is produced by means the CNC lathe machine.

The sequence of various operations is briefly described and showed with some images writing the G-Code using the “CNCSimulator” software.

The program done is inserted in the attachments.

The lathe machine decodes the code composed of numbers and letters and performs the necessary operations.

The main G-code functions are:

- G00: Fast traverse. It is used when the motion of the tool could be fast, and no precisions are required. G00 is written when the tool approaches from its tool magazine to the workpieces, or when no the cutting is performing.
- G01: Linear feed traverse. The command is used when a linear cutting is done. It could be straight or inclined.  
In the same line a feed rate (F) indication needs to be written.
- G02-G03: Arc interpolation clockwise- Arc interpolation counter clockwise. Both commands are used to perform an arc or radius cutting. R can be used to define the radius.
- M3-M4: Spindle starts clockwise – Spindle starts counter clockwise. The command allows the spindle to rotate. It needs to be followed by an S and a number that indicates the spindle rotational speed.
- M5: Spindle Stop.
- M6: Execute tool change. This command permits the tool to return to its station and perform the tool exchange.

- M8-M9: Coolant on- Coolant off.
- M30: Program end.

All the others G-code commands are summed in the Figure 84 reported below.

G Code	Function	G Code	Function
G00	Positioning at rapid travel;	G58	Set Datum;
G01	Linear interpolation using a feed rate;	G59	Set Datum;
G02	Circular interpolation clockwise;	G70	Finish cycle (Lathe);
G03	Circular interpolation, counterclockwise;	G71	Rough turning cycle (Lathe);
G04	Dwell	G72	Rough facing cycle (Lathe);
G17	Select X-Y plane;	G73	Chip break drilling cycle;
G18	Select Z-X plane;	G74	Left hand tapping (Mill);
G19	Select Z-Y plane;	G74	Face grooving cycle;
G20	Imperial units;	G75	OD groove pecking cycle (Lathe);
G21	Metric units;	G76	Boring cycle (Mill);
G27	Reference return check;	G76	Screw cutting cycle (Lathe);
G28	Automatic return through reference point;	G80	Cancel cycles;
G29	Move to a location through reference point;	G81	Drill cycle;
G31	Skip function;	G82	Drill cycle with dwell;
G32	Thread cutting operation on a Lathe;	G83	Peck drilling cycle;
G33	Thread cutting operation on a Mill;	G84	Tapping cycle;
G40	Cancel cutter compensation;	G85	Bore in, bore out;
G41	Cutter compensation left;	G86	Bore in, rapid out;
G42	Cutter compensation right;	G87	Back boring cycle;
G43	Tool length compensation;	G90	Absolute programming;
G44	Tool length compensation;	G91	Incremental programming;
G50	Set coordinate system (Mill);	G92	Reposition origin point (Mill);
G50	Maximum RPM (Lathe);	G92	Screw thread cutting cycle (Lathe);
G52	Local coordinate system setting;	G94	Per minute feed;
G53	Machine coordinate system setting;	G95	Per revolution feed;
G54	Set Datum;	G96	Constant surface speed (Lathe);
G55	Set Datum;	G97	Constant surface speed cancel;
G56	Set Datum;	G98	Feed per minute (Lathe);
G57	Set Datum;	G99	Feed per revolution (Lathe);

GCodeTutor.com

Figure 84 - G-code commands [41].

The turning operations starts with a cylinder of 40 x 90 mm. Fixed it on the spindle and forced to rotate, a tool cuts for a length of 67 mm getting a reduction in diameter from 40mm to 32mm.

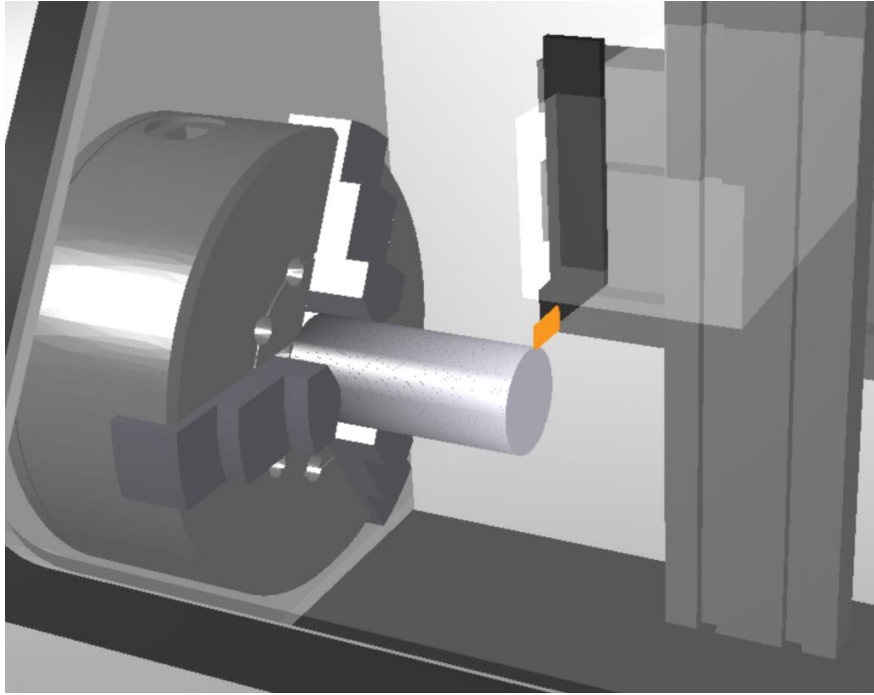


*Figure 85 - Starting workpiece: Cylinder with 90 mm of length and 40 mm of diameter.*

Then, a finishing operation is performed.

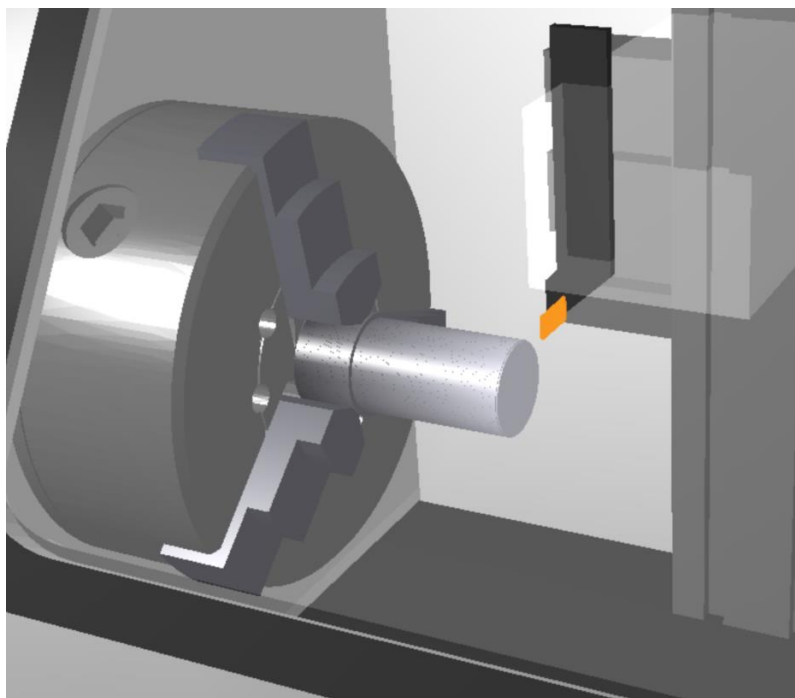


*Figure 86 - Cylinder after first turning operation.*

After that, the prefabricated workpiece is rotated, and the spindle is started again.

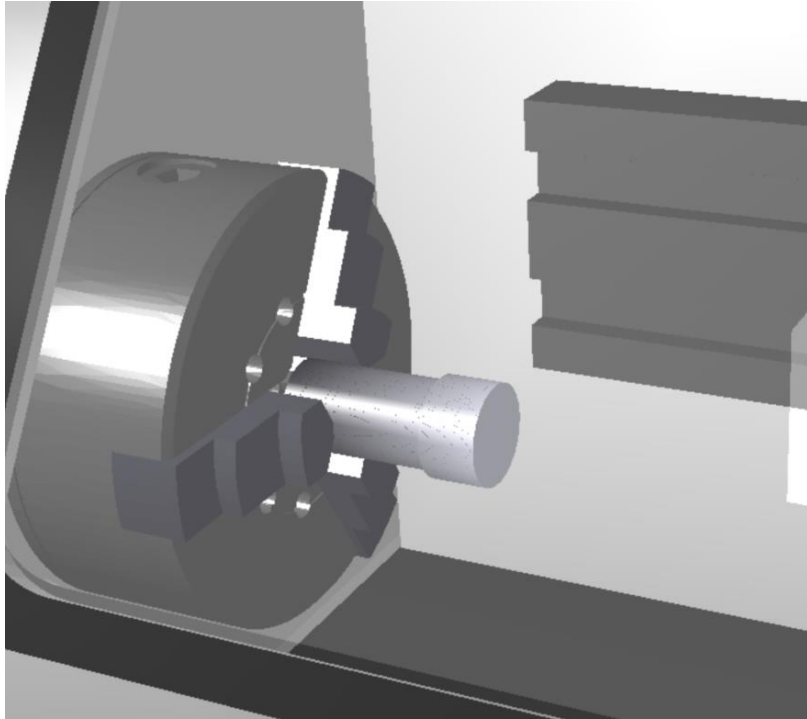


*Figure 87 - Starting cylinder workpiece for machining the bottom part.*

From this configuration, a diameter of 36mm is obtained and, after tool changing, a hole of 20 mm of length and 16 mm of diameter is obtained.

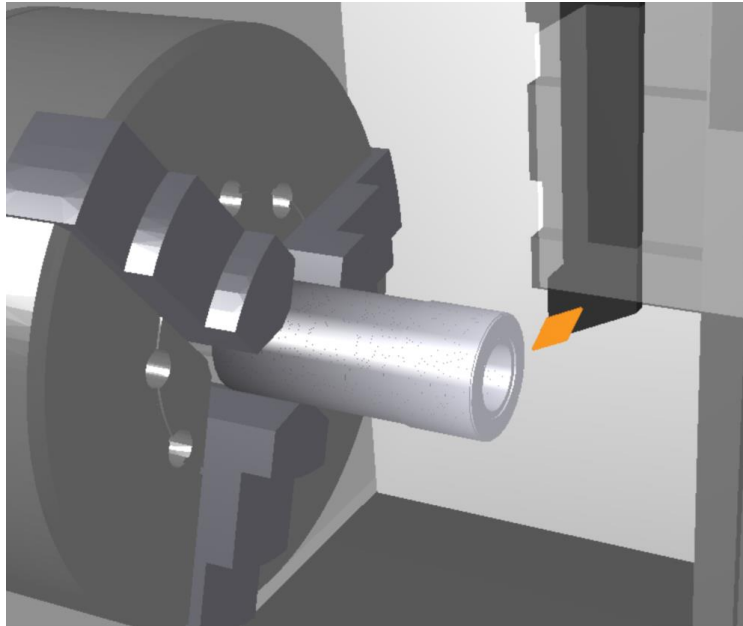


*Figure 88 - Hole machining.*

The machining of the groove and of the four holes for M5 studs can be performed with a lathe machine, maintaining the spindle fixed and forcing the rotation of the tool, or with the milling machine, fixing the workpiece properly at the working table and using an End Mill milling tool

to machine the groove and a thread mill cutter to obtain the M5 hole .

## 7. Conclusion

Friction Stir Welding is considered a green technology since it offers numerous environmental advantages compared to other joining methods as written by Sevel P et al. [43]. In fact, it is known that the energy consumption of Friction Stir Welding is 30-40% less than the common fusion welding processes (TIG, MIG, MAG). The energy consumption depends on the size of the equipment used, on the workpieces thickness and on whether single-pass or multi pass welding is used [43]. FSW is always single pass, giving consequently energy savings.

Furthermore, it has a low environmental impact because there is no use of filler material and shielding gasses. The non-use of consumable materials allows to overcome any problems related to composition compatibility.

Moreover, in Friction Stir Welding, since the materials do not reach the melting temperature but only a 75% of it, there are no problems related to the solidification phase such as distortion, residual stresses, gas inclusion, hot cracking, segregation and so on.

Because of all these positive aspects, FSW's application is growing up continuously.

Friction Stir Welding technique is going to be adopted by more and more companies, from the automotive to the naval or aerospace sector due to the optimal mechanical results that comes out analysing the components and because of its environmental friendliness, goal that the entire world wants to achieve in any field.

In particular, in the aerospace applications the principal advantages of friction stir welding adoption are [44]:

- Design and manufacturing: Weight saving (elimination of the use of fasteners), higher reliability of the joint (joint shows higher strength and improved fatigue performance), environmental demands (less energy used and reduced waste).
- In operation: Reduction of fuel consumption (by weight saving), reduction of maintenance costs (by easier testing) and so on.

The future of Friction Stir Welding is for sure bright. In fact, as could be read in the article written by TWI [42], FSW is going to be used more by business and industry around the world. Here the main examples are reported.

- *Space launch Vehicles*: Boeing USA's Delta II and Delta IV rockets, the Space X Falcon 9, NASA's new Orion spacecraft & Space Launch System (SLS).
- *Train*: Japanese manufacturers Hitachi, KHI and Nippon Sharyo recently adopted FSW.
- *Motor Vehicles*: FWS is used mostly by Audi, Ford, Mazda and Tesla.
- *Apple iMac*: Apple used FSW to join the front and back of the case components since the conventional welding techniques would not work with the new design.

The thesis work has been done during the Internship with "Eurodies", company located in Rivoli (TO), and in collaboration with the J-Tech Lab of Polytechnic of Turin.

During the internship, a tool adapter, useful to accommodate welding tools with a maximum shoulder's diameter of 15 mm, has been designed and produced.

It could be used to weld both aluminium alloys and titanium alloys with small thickness (1mm/2mm).

The connection between the tool adapter and the welding tool has been thought so that, at the beginning the welding tool fills the entire 20 mm of depth and is fixed by means the two upper threaded holes. Then, after a while, when the welding tool's pin has worn out, it could be re-machined from the shoulder and re-used, fixing it to the tool adapter by means of the bottom two threaded holes. The empty space left will be filled by a disk that will withstand the vertical forces produced in working conditions.

This solution is important to adopt specially when the material of the welding tool is very expensive. In fact, when titanium alloys are going to be welded, the material chosen for the welding tool is tungsten rhenium, that is a very expensive one.

After designing and verifying statically the tool adapter, three various welding tools have been created, one for lap joint of aluminium alloys with 1.5mm of thickness and two tools able to create butt joint.

All these components, currently in production, have been designed in order to perform future experimental activities and with the aim of making wider the application field of this technology.



## 2. Tool adapter, 2D drawing

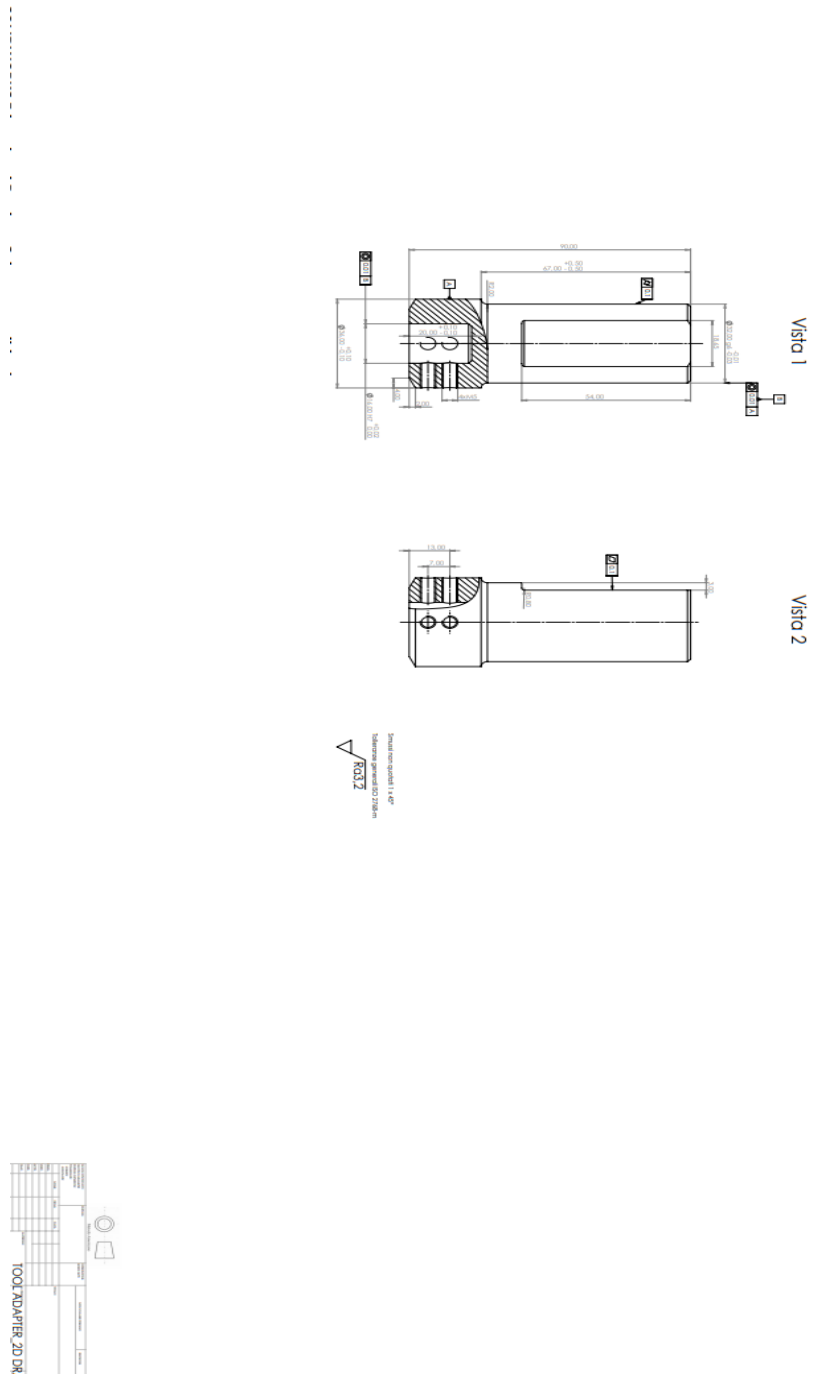


Figure 90 - Attachment 2: Tool Adapter.







# Bibliography and Sitography

- [1] R.S. Mishra, Z.Y. Mab, “Materials Science and Engineering”, R 50 1-78, *Friction stir welding and processing*, August 2005.
- [2] Daniela Lohwasser, Zhan Chen, *Friction stir welding: from basics to applications*, 2010.
- [3] Ron Cobden, Alean, Bandury, *Aluminium: Physical Properties, Characteristics and Alloys*, EAA, 1994.
- [4] Toralf Cock, Skanaluminium, Oslo. *Aluminium, A Light Metal, a brief introduction to aluminium*, EAA, 1999.
- [5] William D. Callister, Jr., David G. Rethwisch, *Materials Science and Engineering*, USA, 2007.
- [6] A. Scialpi, L.A.C. De Filippis, P. Cavaliere, *Influence of shoulder geometry on microstructure and mechanical properties of friction stir welded 6082 aluminium alloy*, “Materials and Design” 28 (2007) 1124–1129.
- [7] Emad Salari, Mohammad Jahazi, Alireza Khodabandeh, Hadi Ghasemi-Nanesa, *Influence of tool geometry and rotational speed on mechanical properties and defect formation in friction stir lap welded 5456 aluminum alloy sheets*, “Materials and Design” 58 (2014) 381-389.
- [8] H.H. Jadav, V. Badheka, Daulat Kumar Sharma et al., *Effect of pin diameter and different cooling media on friction stir welding of dissimilar Al-Mg alloys*, “Material Today: Proceedings”, September 2020.
- [9] H.M. Anil Kumar, V. Venkata Ramana, *Influence of tool parameters on the tensile properties of friction stir welded aluminium 5083 and 6082 alloys*, “Materials Today: Proceedings” 27 (2020) 951-957.
- [10] Mandeep Kaur, Taljeet Singh, Kuldeep Singh, 2016. *Comparison between Friction stir welding & Fusion welding of Aluminium Alloys based on mechanical properties & microstructure: A Review*, Special Issue on International Journal of Recent Advances in Engineering & Technology (IJRAET) V-4 I-2 For National Conference on Recent Innovations in Science, Technology & Management (NCRISTM) ISSN (Online): 2347-2812, Gurgaon Institute of Technology and Management, Gurgaon 26th to 27th February 2016.
- [11] <https://megastir.com/friction-stir-welding-vs-traditional-welding/> . Consulted on 15/01/2021.
- [12] <https://www.industriaitaliana.it/friction-stir-welding-la-nuova-frontiera-della-saldatura-per-atrito/> Consulted on 13/01/2021.
- [13] <https://www.credenceresearch.com/report/friction-stir-welding-market>
- [14] D. Jacquina e G. Guillemot, *A review of microstructural changes occurring during FSW in aluminium alloys and their modelling*, “Journal of Material Processing Technology”, vol. 288, 2020.
- [15] M. Mahoney, R.S. Mishra, T. Nelson, J. Flintoff, R. Islamgaliev, Y. Hovansky, in: K.V. Jata, M.W. Mahoney, R.S. Mishra, S.L. Semiatin, D.P. Field (Eds.), *Friction Stir Welding and Processing*, TMS, Warrendale, PA, USA, 2001, p. 183.
- [16] Egoitz Aldanondo, Javier Vivas, Pedro Álvarez and Iñaki Hurtado, *Effect of Tool Geometry and Welding Parameters on Friction Stir Welded Lap Joint Formation with AA2099-T83 and AA2060-T8E30 Aluminium Alloys*, “Metals” 2020, 10, 872.
- [17] Saumil Joshi, Dr. Sadanand Namjoshi, Dr. Deepak Paliwal, *Effect of Tool Geometry on Friction Stir Welded 6061 Aluminum Alloy*, “Materials Today: Proceedings” 24 (2020) 738-745.

- [18] Krishna Kishore Mugada, Kumar Adepu, *Influence of tool shoulder end features on friction stir weld characteristics of Al-Mg-Si alloy*, “The International Journal of Advanced Manufacturing Technology”, 2018.
- [19] W.M. Thomas, E.D. Nicholas, S.D. Smith, in: S.K. Das, J.G. Kaufman, T.J. Lienert (Eds.), *Aluminum 2001— Proceedings of the TMS 2001 Aluminum Automotive and Joining Sessions*, TMS, 2001.
- [20] M H Jacobs, *Introduction to Aluminium as an Engineering Material*, EAA, 1999.
- [21] <https://www.azom.com/article.aspx?ArticleID=2863>. Consulted on 10/01/2021
- [22] <http://www.astmsteel.com/product/h13-tool-steel-x40crmov5-1-skd61-hot-work-steel/>. Consulted on 15/12/2020
- [23] <https://www.twi-global.com/technical-knowledge/faqs/faq-can-friction-stir-welding-be-used-to-make-lap-joints>. Consulted on 18/01/2021.
- [24] Zia Sialvi, *Lathe machine and it's mechanism, 1.1 introduction*, “Mechanics and Mechanical Engineering”, June 2020.
- [25] Sachin Chaturvedi, *Introduction to machine and machine tools, Basic of Mechanical Engineering*, April 2015.
- [26] Osama Khayal, *Literature review on lathe machine*, 16 August 2019.
- [27] <https://www.custompartnet.com/wu/turning#:~:text=The%20tooling%20that%20is%20required,triangle%2C%20or%20diamond%20shaped%20piece>. Consulted on 24/01/2021
- [28] [http://www.mitsubishicarbide.com/en/technical\\_information/tec\\_other\\_data/tec\\_other\\_data\\_top/tec\\_other\\_data\\_technical/tec\\_cutting\\_tool\\_materials](http://www.mitsubishicarbide.com/en/technical_information/tec_other_data/tec_other_data_top/tec_other_data_technical/tec_cutting_tool_materials). Consulted on 26/01/2021.
- [29] s.W.M.A.I. Senevirathne, *Effect of air and chilled emulsion minimum quantity lubrication (ACEMQL) in machining hard to cut metals*, July 2015.
- [30] Pardeep Kumar, Suresh Dhiman, Aman Agarwal, *Optimizing surface roughness during hard turning of AISI H13 steel using PCBN cutting tools*, “International Journal of Engineering Research & Technology (IJERT) NCAEM Conference Proceedings”, 2013.
- [31] Irving Paul Girsang, Jaspreet Singh Dhupia, *Machine Tools for Machining*, DOI: 10.1007/978-1-4471-4670-4\_4, September 2015.
- [32] [http://www.mitsubishicarbide.com/en/technical\\_information/tec\\_turning\\_tools/small\\_tool\\_s/tec\\_small\\_tools\\_guide/tec\\_small\\_tools\\_outline](http://www.mitsubishicarbide.com/en/technical_information/tec_turning_tools/small_tool_s/tec_small_tools_guide/tec_small_tools_outline). Consulted on 26/01/2021.
- [33] <http://mechanicstips.blogspot.com/2016/04/turning-tool-holder-system.html?epik=dj0yJnU9eHlxVmNIMEppb0NUMnc3eVAtenkxWVg3TWtWRjhnV3UmC0D0wJm49ZWhaYkhGRXdBdDZyUGFrd1pfMFZxZyZ0PUFBQUFBR0FSRlhN>. Consulted on 26/01/2021.
- [34] <https://newsroom.enginsoft.com/tolleranze-dimensionali-e-tolleranze-geometriche-esempio-applicativo>.
- [35] <https://www.thomasnet.com/articles/custom-manufacturing-fabricating/understanding-cnc-milling/>. Consulted on 29/01/2021.
- [36] Milling Machine Operations. Article available online: <http://www.jnkvv.org/PDF/0705202010111965201748.pdf>. Consulted on 29/01/2021.
- [37] <https://technologicalprocess.com/milling-machining-parameters/>. Consulted on 29/01/2021.
- [38] <https://fractory.com/milling-cutters-and-tools/>. Consulted on 29/01/2021.
- [39] <https://madhavuniversity.edu.in/types-of-milling-cutters.html>. Consulted on 30/01/2021.
- [40] <https://makingthat.wordpress.com/06-milling/>. Consulted on 30/01/2021.
- [41] <https://gcodetutor.com/cnc-machine-training/cnc-g-codes.html>. Consulted on 29/01/2021.
- [42] <https://www.twi-global.com/media-and-events/press-releases/2017-09-friction-stir-welding-joining-the-future-of-industry>. Consulted on 25/03/2021.
- [43] Sevel P, Jaiganesh V, *An detailed examination on the future prospects of friction stir*

*welding – a green technology*. February, 2014.

[44] Viliam Sinka, *The present and future prospects of friction stir welding in aeronautics*, July, 2014.

